AIR INJECTION STUDIES FOR ENHANCED OIL RECOVERY

BY

TAJUDEEN KOLAWOLE BELLO

DEPARTMENT OF CHEMICAL ENGINEERING
AHMADU BELLO UNIVERSITY,
ZARIA, NIGERIA

DECEMBER, 2016

AIR INJECTION STUDIES FOR ENHANCED OIL RECOVERY

BY

Tajudeen Kolawole BELLO
B. Eng Chemical (ABU) 2003
M.Sc Chemical Engineering (ABU) 2008
PhD/Eng/15277/07-08

A THESIS SUBMITTED TO THE SCHOOL OF POSTGRADUATE STUDIES, AHMADU BELLO UNIVERSITY, ZARIA

IN PARTIAL FULFILLMENT OF THE REQUIRMENTS FOR THE AWARD OF A DOCTORATE DEGREE IN CHEMICAL ENGINEERING

DEPARTMENT OF CHEMICAL ENGINEERING,
FACULTY OF ENGINEERING,
AHMADU BELLO UNIVERSITY,
ZARIA, NIGERIA

DECEMBER, 2016

Declaration

I declare that the work in this thesis entitled "A**ir Injection Studies for Enhanced Oil Recovery**" has been carried out by me in the Department of Chemical Engineering, Ahmadu Bello University, Zaria. The information derived from the literature has been duly acknowledged in the text and a list of references provided. No part of this thesis was presented for another degree or diploma in this or any other institution.

_____	_____	_____
Name of Student	Signature	Date

Certification

This Thesis entitled AIR INJECTION STUDIES FOR ENHANCED OIL RECOVERY by Tajudeen Kolawole Bello meets the regulations governing the award of the degree of PhD Chemical Engineering of the Ahmadu Bello University, and is approved for its contribution to knowledge and literary presentation.

Prof. I. A. Mohammed-Dabo Chairman, Supervisory Committee	_____ (Signature)	_____ Date
Dr. S. M. Waziri Member, Supervisory Committee	_____ (Signature)	_____ Date
Dr. P. C. Okonkwo Member, Supervisory Committee	_____ (Signature)	_____ Date
Dr. S. M. Waziri Head of Department	_____ (Signature)	_____ Date
Prof. K. Bala Dean, School of Postgraduate Studies	_____ (Signature)	_____ Date

Acknowledgements

I would never have been able to finish my thesis without the guidance of my supervisory committee, support from my family and help from friends.

I would like to express my deepest gratitude to the Chairman of my supervisory committee Prof. Ibrahim Ali Mohammed-Dabo for his excellent guidance, patience, understanding and provision of excellent atmosphere for the completion of my research work. I would like to thank members of the supervisory committe, Dr. S. M. Waziri and Dr P C Okonkwo for their encouragement and contribution towards achieving my goals. I would like to thank Dr. Abduljelil Iliyas, Dr. Faisal Khan, Dr. Kelly Hawboldt, Dr. David Grant and Dr. Lesley James who were helpful at some point during my experimental procedures in the thermal and mineral equipment laboratory at Memorial University of Newfoundland, Canada.

I would like to thank Dr. M. T. Isa for his encouragement and expert advice during the compilation of my thesis and also Dr. B. Mukhtar for his corrections and contributions during my presentations.

I would also like to thank my parents and siblings. They were always supporting me and encouraging me with their best wishes. It would have been a lonely life without my wife, Muinat and my son, Abduljabbar. They are always there giving me the strength to go on.

Finally, I would like to say a big thank you to the Petroleum Technology Development Fund (PTDF), Ahmadu Bello University Zaria, Nigeria and Memorial University of Newfoundland, Canada for their scholarships and study fellowships to the completion of my programme.

Dedication

This thesis is dedicated to my wife (Muinat) and son (Abduljabbar).

Abstract

Conventionally, air injection has been used for recovery of heavy crude oil in the production field, but studies have shown that depletion of light crude oil in the reservoir leads to abandonment of such wells. Hence, this work studied the kinetics and combustion of light crude oil in-situ the reservoir to understand their potentials for high-pressure air injection (HPAI) enhanced oil recovery (EOR). Advanced thermo-kinetic simulation and Pressure-Volume-Temperature tools (AKTS and PVTsim) were coupled with non-isothermal Differential Scanning Calorimetry (DSC) measurements and Accelerating Rate Calorimeter (ARC) for the studies. The combustion and kinetics of three (3) light crude oils obtained from Offshore of Newfoundland, Canada were precisely described by the methods. It was observed that the crude with the lowest API of 30.214 had the lowest enthalpy change of 10.9 J/g and the highest onset oxidation temperature of 220 ^{o}C, while the crude with the highest API gravity of 46.963 had the highest enthalpy of 24.6 J/g and the lowest onset oxidation temperature of 140 ^{o}C. Effect of 10% water saturation of one of the crude samples (Sample A) was studied and it was observed that there was increase in the onset oxidation temperature by 40 ^{o}C and lowering of the enthalpy change by 9 J/g. These findings provided evidence that the versatile Differential Scanning Calorimetry thermograms when coupled with kinetic simulation technique can yield reliable results with respect to oil recovery with high correlation coefficient ($r > 0.9$). This reliable information such as onset, peak and endset temperatures with their respective heat flow patterns, could then be used to provide precise thermo-kinetic parameters. Kinetic triplets such as activation energy, pre-exponential and the reaction model necessary for reservoir screening in an air injection EOR process can also be accurately determined. Mine tailings containing high pyrrhotite content were

then used as catalyst to study its effect on the onset oxidation temperature of the crude oils using ARC. An amount of 20% tailings in crude oil lowered the average onset oxidation temperature from 148 ^{o}C to 116 ^{o}C. It also had the widest oxidation temperature range of 63 ^{o}C between the onset and endset temperature, as well as the highest pressure drop of 2.4 bar, which signifies high conversion in the crude oil oxidation reaction as well as production of miscible flue gas which favoured enhanced oil recovery process. Products of air combustion products in-situ was studied as an injectant in a light oil Nigerian reservoir using a simulated slim tube experiment and was observed than flue gas products from air oxidation at high temperature and pressure favoured enhanced oil recovery.

TABLE OF CONTENT

Page

Cover Page ……I
Fly Page……II
Title Page……..III
Declaration…… ...IV
Certification…….....V
Acknowledgement…… ..VI
Dedication……...VII
Abstract…….. ... VIII
Table of Content…….....X
List of Figures……XIII
List of Tables.…….....XV
List of Plate……XVI
List of Appendices…….....XVII
Abbreviation, Definitions, Glossary and Symbols ……..…XVIII
1.0 **INTRODUCTION** ……..…….....1
1.1 Preamble……..1
1.2 Problem statement…….....……2
1.3 Justification of research……...……3
1.4 Aims and Objectives of Research……...……4
1.5 Scope of Research …….....…….....4

2.0 **LITERATURE RVIEW**…….....6
2.1 Oil Recovery Processes…….…….....6
2.1.1 Water drive reservoir……...……..…….....7
2.1.2 Gas cap drive reservoir……..…….....7
2.1.3 Solution gas reservoir ……..…….....8
2.2 Enhanced Oil Recovery (EOR) concept...……..9
2.3 Enhanced Oil recovery (EOR) Methods……12
2.3.1 Hot water injection ……..……..12
2.3.2 Steam injection (Huff and Puff).....…….....13
2.4 Air Injection for Enhanced Oil recovery (EOR)...……14
2.4.1 In-situ combustion ……15
2.4.2 Light oil air injection……16
2.5 Kinetics of Thermal EOR 16
2.5.1 Combustion reaction of crude oil 17
2.5.2 Oxidation of sulphur containing crude oils……..……18
2.5.3 Oxidation of mercaptans……20

2.5.4 Oxidation of aliphatic/cyclic suphides……20
2.5.5 Air injection for reservoir oxidation……21
2.5.6 Amount of Air Required for EOR…….....21
2.6 Arrhenius Studies of EOR Kinetics 22
2.6.1 Arrhenius studies of EOR kinetics using O_2 consumption bases…….....23
2.7 Kinetics of Iso-Conversional Methods 25
2.7.1 Differential (Friedmans's) 25
2.7.2 Ozawa-Flynn-Wall analysis 31
2.7.3 ASTM E698.....32
2.8 Non Thermal Methods.....32
2.8.1 Vaporising gas drive 35
2.8.2 Condensing gas drive 36
2.8.3 Immiscible gas drive 37
2.9 Reservoir Fluid Studies and Experiment……..38
2.9.1 Primary Tests……...39
2.9.1.1 Specific gravity tests…….39
2.9.1.2 Gas-oil ratio tests…….40
2.9.2 Routine hydrocarbon oil routine tests ……...41
2.9.2.1 Compositional analysis od reservoir fluids……41
2.9.2.2 Constant composition expansion……41
2.9.2.3 Differential Liberation tests……43
2.9.2.4 Separator tests……44
2.9.2.5 Constant volume depletion tests (CVD).……45
2.9.3 Special Laboratory PVT tests……47
2.9.3.1 Slim tube experiment……47
2.9.3.2 Swelling tests……49
3.0 **MATERIALS AND METHODS**……50
3.1 Material and Equipment……50
3.1.1 Materials and utilities……51
3.1.2 Equipment……52
3.1.3 Experimental Procedure ……52
3.1.4 Viscosity determination ……53
3.1.5 Specific heat capacity determination……53
3.1.6 Differential Scanning Calorimetry (DSC) tests ……54
3.1.7 Accelerating rate Calorimeter (ARC) tests……54
3.1.8 Mine tailings preparation……57
3.1.9 Mineral liberation analyser (MLA) for mine tailings studies……59
3.1.10 PVTSim19 and Design Expert software simulation for oil recovery analysis……60

4.0 **RESULTS AND DISCUSSION**..……61
4.1 Properties of crude oil……...…….…....61
4.2 Thermal behaviours of Crude Oils using DSC……..……...62
4.3 Thermal Kinetics of DSC Thermograms of Crude Oils..…….….....63
4.4 The use of Mine Tailings as catalysts in crude oil oxidation reaction……...….....76
4.5 Effect of Reservoir Conditions on Oil Recovery on Nigerian Oils……..….……...87
5.0 **CONCLUSIONS AND RECOMMENDATIONS**.……..…….....91
5.1 Conclusions…….……..91
5.2 Recommendations…….…...92
REFERENCES……..…….…….....93
APPENDICES……...…….....105

List of Figures

Page

CHAPTER 2

Figure 2.1 Reservoir classification based on drive mechanism……..8
Figure 2.2 Classification of Enhanced Oil Recovery (EOR)……11
Figure 2.3 Steam or Hot water injection……...13
Figure 2.4 Air Injection Route in thermal EOR Process ……...14
Figure 2.5 An air injection process diagram…….……..……15
Figure 2.6 Relationship of the reaction progress α vs time for reaction models.....26
Figure 2.7 Schematic representation of miscible displacement……...34
Figure 2.8 Ternary diagram illustrating miscible drives…….……...……..35
Figure 2.9 Vaporising gas drives……..36
Figure 2.10 Condensing gas drive……37
Figure 2.11 Immiscible gas drive…….38
Figure 2.12 Schematic diagram illustrating method for determining Gas to Oil ration……...41
Figure 2.13 Schematic diagram of a constant composition expansion experiment ……43
Figure 2.14 Schematic diagram of a Differential liberation experiment……...…...44
Figure 2.15 Schematic diagram of a three-stage separator experiment ……..45
Figure 2.16 Schematic representation of a constant volume depletion test ……46
Figure 2.17 Schematic diagram of a slim tube apparatus……48
Figure 2.18 Schematic representation of swelling test……50

CHAPTER 3

Figure 3.1 The Algorithm Logic of Heat-Wait-Seek Operation in ARC…….…….....54

CHAPTER 4

Figure 4.1 DSC thermograms of crude oil samples at 10K/min ……...…….62
Figure 4.2 Reaction Progress as a function of Temperature for Sample A…….....64
Figure 4.3 Reaction Progress as a Function of Temperature for Sample B……...….....64
Figure 4.4 Reaction Progress as a Function of Temperature for Sample C……...…….....65
Figure 4.5 Reaction Progress as a Function of Temperature for Sample A*……...65
Figure 4.6 Reaction rate for Sample A at different ramp rates. ……...…….……...67
Figure 4.7 Reaction rate for Sample B at different ramp rates. …….....……68
Figure 4.8 Reaction rate for Sample C at different ramp rates. ……...…….……68
Figure 4.9 Reaction rate for Sample A* at different ramp rates. ……..……69
Figure 4.10 Apparent Activation Energy of Sample A based on ASTM-E698…….……...70
Figure 4.11 Apparent Activation Energy of Sample B based on ASTM-E698…….……71
Figure 4.12 Apparent Activation Energy of Sample C based on ASTM-E698……..…….....71
Figure 4.13 Apparent Activation Energy of Sample A* based on ASTM-E698…...…….……...72
Figure 4.14 Activation energy and pre-exponential factor as a function of reaction progress for Sample A……...…….....……..……73

Figure 4.15 Activation energy and pre-exponential factor as a function of reaction progress for Sample B…….....73
Figure 4.16 Activation energy and pre-exponential factor as a function of reaction progress for Sample C……74
Figure 4.17 Activation energy and pre-exponential factor as a function of reaction progress for Sample A*……74
Figure 4.18 Comparison of experimental DSC thermograms with n^{th} order model prediction for sample A……75
Figure 4.19 Sulphide associated Mineral sites in Nigeria ……..……..78
Figure 4.20 DSC thermograms of varying amount of tailings in crude oil…….....…….80
Figure 4.21 Temperature / Pressure profile of crude oil without tailings…..…….…….....81
Figure 4.22 Temperature / Pressure profile of crude oil with 5% tailings……...…….....81
Figure 4.23 Temperature / Pressure profile of crude oil with 10% tailings…….....82
Figure 4.24 Temperature / Pressure profile of crude oil with 20% tailings…….....82
Figure 4.25 Temperature / Pressure profile of crude oil with 30% tailings…….....83
Figure 4.26 Temperature / Pressure profile of crude oil with 40% tailings……...……...83
Figure 4.27 Effect of amount of tailings on Onset temperature, Oxidation range and End set temperature during oxidation reaction of crude oils……..……84
Figure 4.28 Theoretical effect of tailings on onset temperature and oxidation reaction based on Reservoir conditions……...86
Figure 4.29 Effect of reservoir temperature and sulphur content on Oil Recovery……..88
Figure 4.30 Effect of CO2 content and Sulphur content on Oil Recovery……..……..…….89
Figure 4.31 Effect of CO2 content and reservoir temperature on Oil Recovery……..….....90

APPENDICES

Figure B.1: Box plot of the summary of ARC data on 20% tailings with oil……..107
Figure F.1: Tuned Z-factor as a function of pressure in the differential depletion experiment...128
Figure F.2: Tuned Relative volume as a function of pressure in constant mass expansion experiment…….128
Figure F.3: Tuned Oil density as a function of pressure in differential depletion experiment ……...…….129

List of Tables

Page

CHAPTER 2

Table 2.1 Reservoir drive mechanisms for oil production ……8
Table 2.2 Wide variety of reaction models f(α) 28

CHAPTER 3

Table 3.1 List of material and utilities used in the enhanced oil recovery study.....51
Table 3.2 List of equipment used in the enhanced oil recovery study.....52

CHAPTER 4

Table 4.1 Property of the crude oil samples…….…....61
Table 4.2 Summary of petro-physical and thermodynamic properties of the four (4) crude oil samples that showed clear/consistent peaks……...76
Table 4.3 Mineral and Chemical Constituents of the Tailings…….....77
Table 4.4 Summary of the Temperature-Pressure Data Obtained from an Accelerating Rate Calorimeter test including standard deviation……...……..85

APPENDICES

Table B.1: Summary of ARC's reproducibility tests…….107
Table C.1: Paraffins, Napthenes and Aromatics content of the Nigerian reservoir fluid.....109
Table C.2: Isothermal constant mass expansion of the Nigerian crude…….....110
Table C.3: Isothermal differential vaporization test of the crude……...110
Table C.4: First isothermal swelling tests of the crude…….……..…111
Table D.1: Properties of characterized crude oil using SRK Equation of State……..112
Table D.2: Interaction Parameters [kij(-)] of components of modelled crude…….119
Table D.3: Interaction Parameters [kij A (-)]of components of the modelled crude……...112
Table D.4: Interaction Parameters of crude oil components based on The Huron and Vidal Mixing Rule g/R (K)…....……..…..123
Table D.5: Interaction Parameters kij A (-) of the crude oil components……..……..……124
Table E.1: Properties of Characterized oil in 3 Pseudo components……126
Table E.2: Interaction parameters of Pseudo-components……....……....127
Table E.3: Interaction parameters of Pseudo-components [kij (-)]……..……....127
Table E.4: Interaction Parameters of pseudo-components based on The Huron and Vidal Mixing Rule HV g/R (K)…….....…….....127
Table E.5: Interaction parameters of Pseudo-components Mixing Rule kij A (-)……127
Table G.1: General regression results of tuned oil properties……...……130
Table H.1: Recovery response of design of experimental run…….……132
Table H.2: ANOVA analysis of oil recovery data using response surface cubic model (Aliased)……..133

Table H.3: Desirability table on Optimised reservoir conditions for improved oil recovery……..……..135
Table H.4: Final Equation in Terms of Actual Factors……..…135

List of Plates

Pages

CHAPTER 3

Plate 3.1 DSC system by Mettler Telodo with gas controller GC 2000…….....54
Plate 3.2 The Rotary Micro Riffler ……..…….....56
Plate 3.3 Tailing Samples in round mould prepared for Mineral Liberation Analysis.....57
Plate 3.4 The FEI Mineral Liberation Analyzer (MLA)……..…….....58

APPENDICES

Plate A.1: Backscatter image of tailings used …….....106

LIST OF APPENDICES

Pages

Appendix A: Mineral Liberation Analysis……106
Appendix B: Data from Accelerating Rate calorimeter (ARC)……107
Appendix C: Property of Nigerian Crude Oil……109
Appendix D: Characterisation of modelled crude using Soave-Redlich-Kwong (SRK) Equation of State……112
Appendix E: Characterisation of modelled crude to 3 pseudo-components……126
Appendix F: Equation of State (EOS) tuning of PVT tests……128
Appendix G: Regression results of oil characterisation……130
Appendix H: Design of Experiment for oil recovery……132

Abbreviations, Definitions, Glossary and Symbols

Abbreviations

ARC – Accelerating rate calorimeter

DSC – Differential scanning calorimetry

PVT – Pressure- Volume- Temperature

DOE – Design of experiment

EOR – Enhanced oil recovery

LTO – Low temperature oxidation

HTO – High temperature oxidation

SRK - Soave - Redlich – Kwong

EOS - Equation of state

s.g – Specific Gravity

Symbols

A = Pre-exponential factor

c = Critical point

Cp = Specific heat capacity

E = Activation Energy

f (α) = Reaction model

f = Final

i = Initial

n = Reaction order

R = Molar gas constant

Sat = Saturation

T = Temperature

t = Time

v = Darcy velocity

V = Volume

α = Reaction progress or conversion

β = Heating rate

CHAPTER ONE

1.0 INTRODUCTION

1.1 Preamble

Enhanced Oil Recovery (EOR) is a tertiary recovery process which is normally applied after primary and secondary recovery, to mobilize oil trapped in pores by vicious capillary forces. Thermal, chemical, solvent and gases are the most common form of various EOR process (Isco, 2007). Due to the decline of oil reserves caused by the rising oil production, and clamours for environmentally friendly practice in EOR techniques, petroleum engineers are currently driving EOR projects towards more efficient techniques. One of such efficient technique is the Air/Flue gas injection which is motivated by inexpensive source of air as well as environmentally friendly carbon-dioxide sequestration. The motivation for the use of air as an injectant in the EOR project is because of its abundance, availability and low cost. It can simply be supplied by the use of a compressor, with overall project having low initial and operating cost in comparison to other EOR methods (JOGMEC, 2011).

Air for increasing oil recovery from reservoirs dates back to the 1940's and early 1950's (Hvizdos *et al.,* 1983) and by the 1960s and 1970, about forty (40) in-situ full field or pilot projects had been undertaken throughout the world with North America topping such projects (Pwaga *et al*., 2010). This technique, apart from laboratory studies has been implemented in fields such as West Hackberry in Louisiana, Horse Creek North and South Dakota, Zhongyuan and Liaoche oil fields in China, H field in Indonesia, South Bridge in California and other countries such as Romania, United Kingdom, Japan, Canada, India, Argentina, Venezuela have maintained laboratory and field studies too (Sakthikumar *et al*., 1996; Ren *et al*., 1999; Mendoza *et al*., 2011; Niu *et al*., 2011; Iwata *et al*., 2001; Xia *et al*., 2004; Zhu *et al*., 2001). Air

has also been used in heavy oil recovery and enhancement of this technique can lead to significant light oil production (Surguchev *et al*., 1998).

An alternative to air injection is the flue gas (which contains nitrogen and carbon-dioxide) produced from the combustion of oxygen contained in the air to sweep oil. This EOR technique, when applied to light oil is known as light oil air injection while in heavy oil reservoir, it is called in-situ combustion. (Kuhlman, 2004; Teramoto *et al*., 2006; Turta *et al*., 2007; Li *et al.,* 2009).

Some studies carried out to describe criteria as well as performance of air injection projects gave positive results even though experimental condition could not mimic the adiabacity of the reservoir (Sakthikumar *et al.,* 1996). Temperature regimes, heat energy content, pressure and temperature dependence during oil combustion were also studied using simple Arhennius type model which assumes constant kinetic parameters throughout the reaction (Hvizdos *et al.*, 1983; Elgibaly, 1998; Niu *et al*., 2011; Li, *et al.*, 2009). There have been few researches which reports on the complexities of combustion reaction of crude oils where kinetic parameters fluctuate or the alteration of the oxidations zones.

1.2Problem Statements

The following are the problems, research gaps in literature and previous studies on enhanced oil recovery with reference to light oil air injection projects.

1. Despite the several thermal and kinetic studies carried out on Enhanced oil recovery, there has been no research that addresses how the kinetic parameters fluctuate during the combustion process for the benefit of oil recovery.
2. Arrhenius type of equation and simple nth order model have been used to study oxidation of oil and these do not adequately capture the complexity of the reaction (such as the trend of activation energy as reaction progresses), therefore, the need to study other models and techniques.

3. Very few and scanty literatures exist that captures the various oxidation reaction zones of crude oil.
4. Interaction parameters of temperature, pressure, extent of air oxidation and sulphur content on crude oil recovery have received low discussions in literatures, hence the need to focus attention on them for the benefit of enhanced oil recovery especially in countries like Nigeria where EOR is yet to be fully practiced.

1.3 Justifications of Research

This sections highlights the benefits of this research.

1. This study will provide insight into improved oil recovery from low producing/ abandoned wells.
2. The iso-conversional approach will help capture the complexity of crude oil oxidation reaction.
3. The findings will benefit upstream companies operating in Nigeria currently at the secondary production stage and at verge of abandoning the wells.
4. This will also help the federal Government of Nigeria during negotiations of oil well sales.
5. It will open up researches and studies on catalytic potential of Nigeria's mine tailings.

1.4 Aim and Objectives of Research

The aim of this research work was to investigate the kinetics, combustion of air and combustion air products for enhanced oil recovery.

This aim was achieved by the following objectives:

1. Using differential iso-conversional method to describe oxidation of crude oils in-situ reservoir.
2. Studying oxidation behaviours of crude oil in an adiabatic environment to verify non-isothermal differential scanning calorimetry (DSC) results.
3. Using tailing as catalyst to alter oxidation characteristics of crude oils.
4. Studying the combined effect of parameters of reservoir conditions such as temperature, pressure, gas content on oil recovery.

1.5 Scope of Research

The scope of this research are focussed on:

1. Combustion behaviours and kinetics of the oxidation reaction of low pressure reservoir of light crude oils.
2. The use of mine tailings to improve the reactions for the benefit of improved oil recovery.
3. Modelling of air injection process with respect to the progress of oxidation kinetics with temperature.
4. The use of crude oil databank and PVT tests to analyse the enhanced oil recovery process for Nigerian crude oils.

CHAPTER TWO

2.0 LITERATURE REVIEW

2.1. Oil Recovery Processes

Hydrocarbons in nature accumulate in geological traps underneath the earth surface called reservoirs; these reservoirs are porous and permeable and are usually trapped by water or an impermeable rock in its bank. These oil reservoirs are usually classified based on the mechanism of their production which are; water-drive, Gas cap drive and the dissolved gas drive reservoir (Lake *et al*., 2014).

There are three major distinct stages in the life of an oil well; these are the primary, the secondary and the tertiary stage otherwise known as the enhanced oil recovery.

The primary recovery has several mechanisms of oil production, but most importantly, production occurs at natural pressures of the reservoir i.e the reservoir energy is used to produce its hydrocarbon contents. Pump installations are necessary when the reservoir pressure drops and productions decline. This usually account for 12-15% recovery of original-oil-in-place (OOIP), this percentage is less for heavy oils but higher for lighter oils (Hawkins & Singhal, 2004).

The secondary stage is necessary after the primary stage, this is when the natural pressure has depleted and production has subsequently declined, most practices in the secondary stages include gas and water injections which were initially present in the reservoir. This technique allows the injectants to sweep the oil to the producer while still maintaining reservoir pressure (Donaldson *et al*., 1989; Baviere, 1991). This type of recovery is due to energy given to the reservoir by the injection of water or gas. Water flooding is very attractive in a reservoir that has a large water aquifer and this type of recovery accounts for an additional 15-20% OOIP over primary.

Tertiary recovery also known as Enhanced Oil Recovery (EOR) and historically comes after the secondary stage which requires the introduction of technique that improves reservoir oil flow to the producer. This may involve injection of fluids that are miscible/near miscible with oil (typically carbon dioxide), steam, air and other formulations polymers. This method recovers additional 10-15% over the secondary methods (Schumacher, 1980; Donaldson, 1989; Sorbie, 1991; Wassmuth 2012; Sheng 2013).

2.2.1 Water drive reservoir

Water drive reservoir, as the name implies involves a large water aquifer which is the main driving force in this mechanism. The pressure from the large water aquifer drives the oil and gas to the well bore while the reservoir pressure still maintained for a long period of time, see Figure 2.1a (Tarek, 2006).

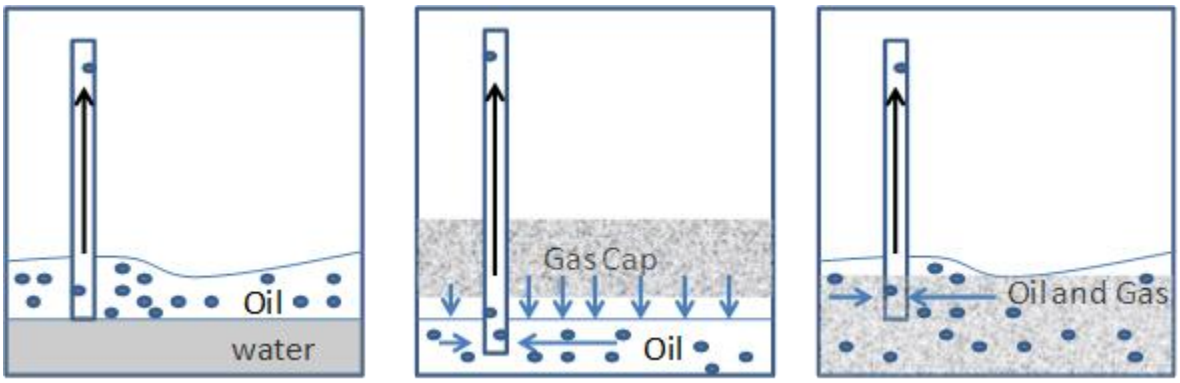
2.2.2 Gas cap drive reservoir

The reservoir which has a gas-cap drive, in which the gas initially in the oil has been liberated to form a cap above the oil so that the oil can be produced under the influence of the gas cap pressure is known as the Gas Cap Reservoir. These productions continue at steady state unless there is production in gas from the gas cap which reduces the driving pressure of the gas, although there are cases of both water and gas cap drive occurring simultaneously (Tarek, 2006; Oliver *et al*., 2008). This is illustrated in Figure 2.1b

2.2.3 Solution gas reservoir

This is also called a volumetric reservoir and solution-gas reservoir. The dissolved gas held in solution (as in Figure 2.1c) in the oil is the drive mechanism. This reservoir gas is actually in the liquid phase at atmospheric condition so when there is pressure drop below the bubble point a two phase (gas and oil)

exists and this eventually poses a weak driving force as compared to a water drive or gas cap (Tarek, 2006).



(a) Water drive (b) Gas-cap drive (c) Solution gas drive

Figure 2.1: Reservoir classification based on drive mechanism (Source: Glover, 2016.)

A summary of conditions of reservoir drive mechanism was also given by Jahn *et al.*, 1998 as shown in Table 2.1.

Table 2.1: Reservoir drive mechanisms for oil production

Drive mechanism	**Initial condition**
Water drive	Saturated or undersaturated oil
Gas cap	Saturated oil with gas cap
Solution gas	Undersaturated (no gas cap)

2.2 Enhanced Oil Recovery (EOR) Concept

The engineering activity applied to various oil reservoirs for the purpose of producing more hydrocarbons is termed enhanced oil recovery. This technique involves injection of material that was not initially present in the reservoir and the measure of the ability of such technique to recover more oil

other than the natural depletion is its EOR efficiency (Mogensen *et al.,* 2009). Shallow reservoirs have more viscous oil compared to deeper reservoirs and this has led to various thermal techniques to recover them. The economics of many EOR processes have so many uncertainties unfortunately, thereby requiring screening studies to be performed on each reservoir before arriving at a decision to proceed on a particular EOR technique (Ray & Wesson, 1982). It should also be noted that no single EOR technique has been discovered to be applicable to all reservoirs as a unified method; therefore, techniques are usually developed to address reservoirs with particular/specific characteristics (Donaldson *et al*., 1989).

Enhanced oil recovery (EOR) is a tertiary recovery process which is normally applied after primary and secondary recovery, applied to mobilize oil trapped in pores by vicious capillary forces. Thermal, chemical and solvent/gases are the most common form of various EOR process (Burger and Sahuquet, 1972; Isco, 2007). Figure 2.2 shows a summary of EOR classifications as described by several authors (Alvarado and Maveric, 2010; Thomas, 2008; Button *et al.*, 2004; Mogensen *et al.*, 2009). EOR is divided into two major parts; the thermal and the non-thermal. The thermal which is the major focus of this research involves oxidation which is instigated by oxygen present in air to produce flue gases which have been studied to be miscible with oil thereby increasing sweep efficiency of oil for incremental oil recovery.

Air injection and In-situ combustion uses the CO_2 and heat respectively for incremental oil recovery (Veld and Phillips, 2010). The main focus of this research is the use of flue gas for incremental oil recovery taking advantage of CO_2 injection. Figure 2.2 can also be seen to show the pathway of EOR techniques with highlights on the CO_2 path. It can be seen that though CO_2 is highlighted under thermal recovery, it is still part of the non-thermal EOR when considering CO_2 production off site and injecting it underground unlike the thermal in which the CO_2 is generated underneath the reservoir. The nature of

crude oil (API) gravity will determine the EOR technique. Heavy oil with API gravity less than 24 (specific gravity greater than 0.91) undergoes an in-situ combustion while light oil air injection for (24< API <44, SG<0.91) and at reservoir temperatures less than 300^{o}C (Greaves *et al*., 1998; Greaves, 2004). There are cases of middle oil combustion which usually occurs at the transition zone between heavy and light oil (Kok *et al*., 2004).

The major concept of this research is to combust a small amount of reservoir crude oil in-situ to produce flue gases which in turn becomes miscible with the crude oil. This miscibility which helps to reduce the viscosity of the oil coupled with swellings, re-pressurisation and thermal effects further improves incremental oil recovery.

In this research, iso-conversional methods and simple Arrhenius equation was used to study the behaviours of crude oil combustion reactions. The effect of sulphide mineral tailings on the onset oxidation temperature of crude oil was studied for the potential of instigating oxidation in-situ reservoir combustion. This therefore makes it possible for more abandoned oil wells to be revisited for production in and economic and environmentally manner.

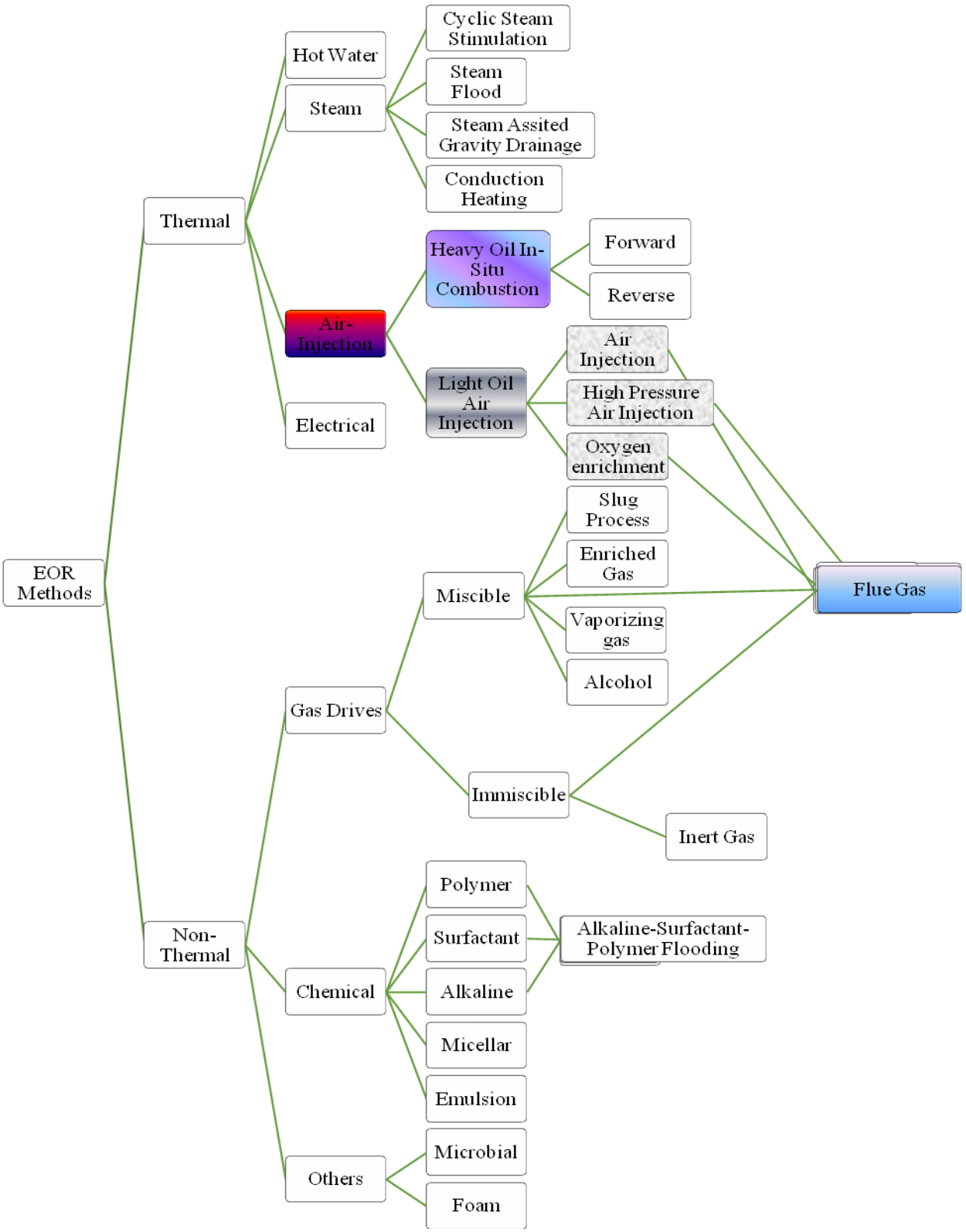


Figure 2.2: Classification of Enhanced Oil Recovery (Button *et al.*, 2004., Thomas, 2008., Mogensen *et al.,* 2009 and Alvarado & Maveric, 2010.)

2.3 Enhanced Oil Recovery (EOR) Methods

Enhanced oil recovery methods can be basically classified into thermal and non thermal methods. Thermal methods involves heat playing a lead role, they were initially intended for heavy oil and tar sands recovery but recently has been introduced to lighter oil for production of gases to improve recovery (Guo et al., 2007; Gutierrez *et al*., 2009).

Non-thermal process on the other hand does not have heat playing prominent role in oil recovery. It involves injection of fluids such as water, and flue gases (Al-Anazi, 2007). The thermal methods are the most advanced form of EOR with respect to field experience and technilogy. Initially suited for heavy oils of 10-20 ^{o}API and tarsands of API gravity less than 10, this process vapourises some of the oil and the heat produced to reduce the viscosity of the oil. These effects mobilises the oil to the producer (Green and Willhite, 1998). Recent application has been in the light oil reservoirs where the initial oil consumed is used for combustion to produce flue gas which drives the oil. Thermal methods have also been practiced in different countries with positive results recorded in canada, United States of America, Venezuela and Indonesia (Taber *et al*., 1997; Shokoya *et al*., 2005; Teramto *et al*., 2006). The different types of thermal recovery are discussed in this section.

2.3.1. Hot water injection

Hot water has historically been injected into the reservoir to reduce oil viscosity and make it flow more readily and there are other many similar variations of this such as the steam injection processes (Figure 2.3) (Sola and Rashidi, 2008). They both have high efficiencies at shallow wells, low sand thickness and high oil saturation (Teodori *et al*., 2006).

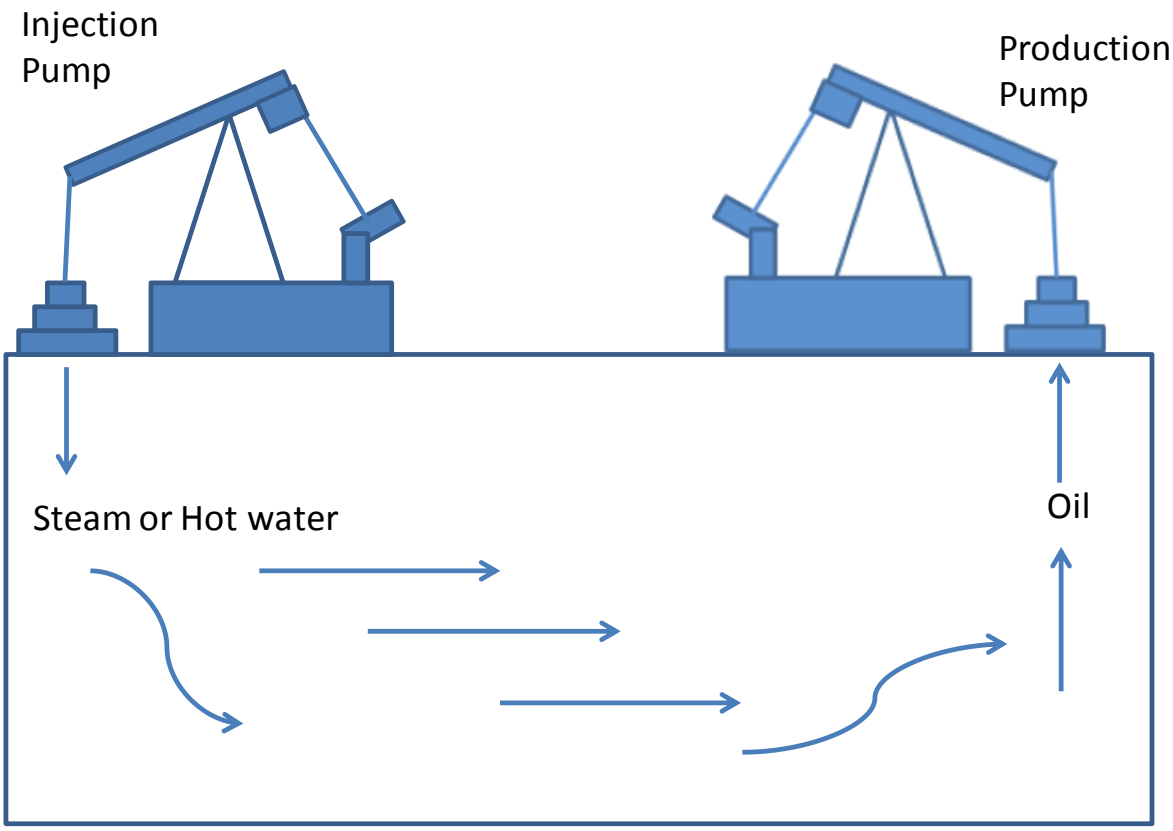


Figure 2.3: Steam or Hot water injection (Source: National Research Council, 2013).

2.3.2. Steam injection (Huff and Puff)

The cyclic steam injection occurs in three stages, they are the steam injection, the soak and the production. The injection of steam is usually done for a month and the well shut for few days to allow for heat distribution through out the well, this period is known as the soak period while the final stage is the production of the less viscous oil. Production continues until productivity drop and another round of cycle is carried out. This method is practiced on shallow reservoirs (<3000 fts) and heavy oil deposits (Amarnath, 1999).

2.4 Air Injection for Enhanced Oil Recovery (EOR)

This is another form of gas injection enhanced oil recovery (EOR) but the gas injected in this case is air. It shows a promising EOR technique for reservoir of various characteristics such as high temperature, low permeability and also light oils (Sarma & Das, 2009). The mechanism of oil recovery can be classified into two types; where the air injected into the reservoir, the oxygen in air combust with a small amount of oil to generate heat which inturn reduce viscosity. It is called in-situ combustion but if injected air generates flue gas for the purpose of miscibility/sweeping gas in a light oil reservoir, it is called light oil air injection. JOGMEC, 2011). The breakdown of thermal EOR method is illustrated in Figure 2.4.

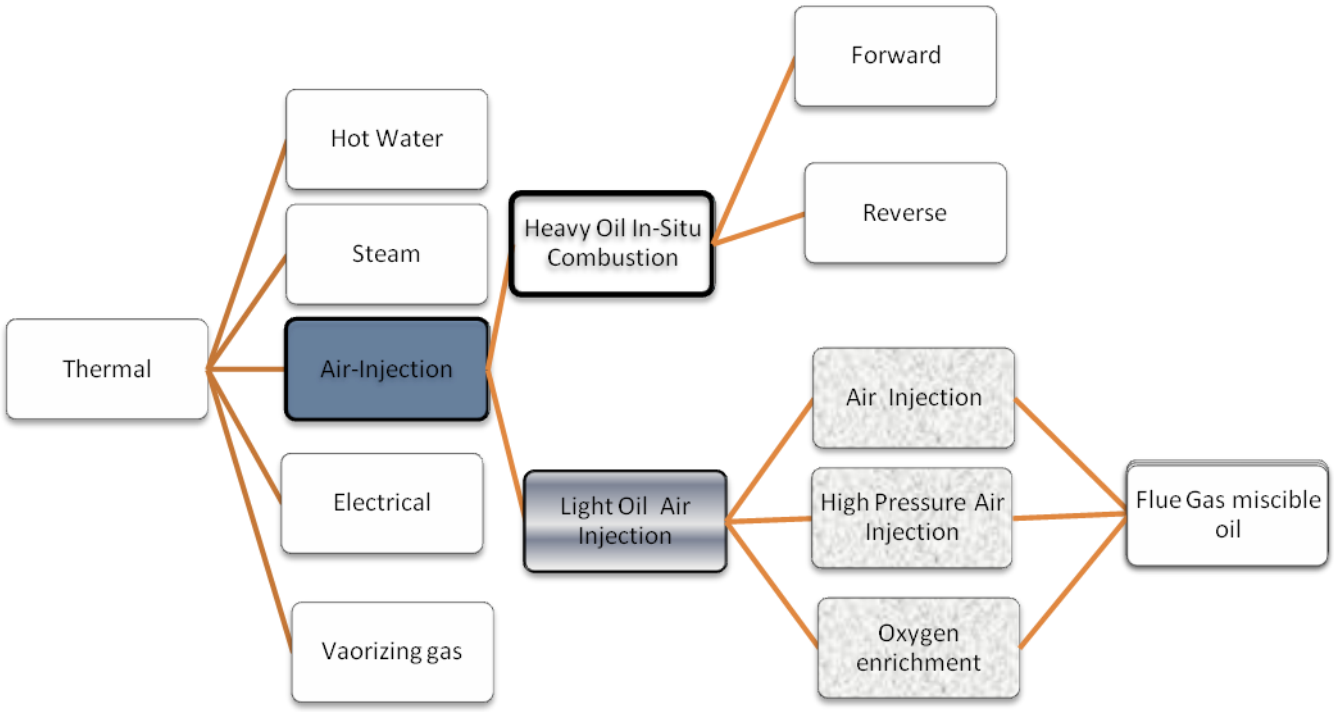


Figure 2.4: Air Injection Route in Thermal EOR Process. (Source: Thomas, 2008).

The various light oil air injection are classified into air, oxygen enrichment and high pressure air injection depending on conditions set for the reservoir. Air injection process illustrated in Figure 2.5 shows where

air is used to improve oil recovery. The air is injected is injected in zone A by the injector. The oxygen in air is consumed as shown in the oxygen profile at zone B where oxidation reaction occurs. In Zone C, oxidation of part of the oil with air generates heat as well as products of combustion and flue gases such as CO_2, CO and unreacted N_2 gases. Zone D shows the displacement of oil by oil viscosity reduction or flue gas sweeping as the cases may be depending on whether it is an in-situ combustion or low oil air injection. Finally, at zone E (producer section) where the displaced oil is collected and incremental production of original oil in place (OOIP) is recorded.

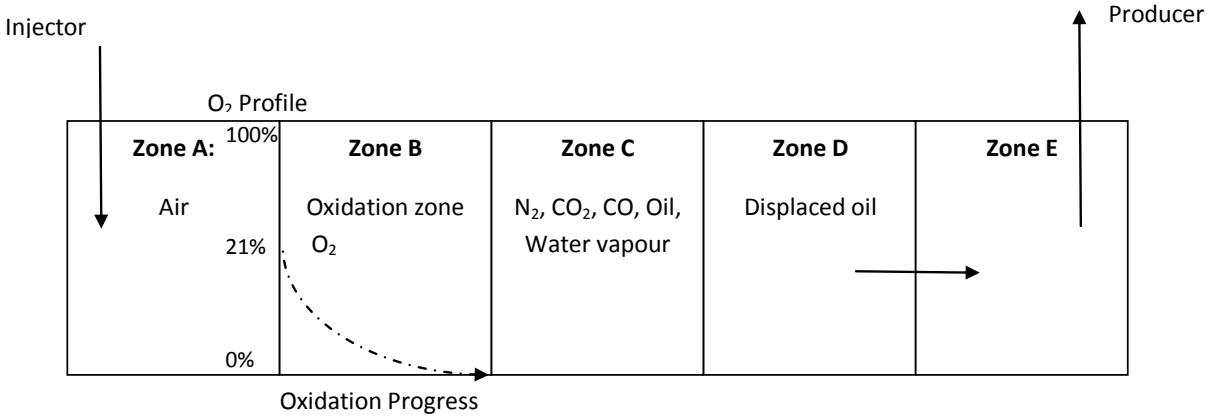


Figure 2.5: An air injection process diagram. (Source: Sarma and Das, 2009).

2.4.1 In-situ combustion

This method is also called fire flooding. Injected air may range from normal air (21% O_2) to enriched air (95% O_2) (Shahani & Hansel, 1987). This process is usually applied to heavy oils and tar sands in which very high tempearures of 350-600^{o}C may be required (Turta & Singhal, 2001). Fuel content is one unique factor that influences the success of these kind of projects. The amount available for combustion and amount of coke that is deposited in the reservoir due to thermal cracking in the reservoir (Donalson *et al.*, 1989).

2.4.2 Light oil air injection

Air injection for enhanced oil recovery is increasingly receiving considerable attention after secondary water flood process (Kuhlman, 2000). This is due to the abundance and low cost of air. A high pressure air injection (HPAI) has also been applied to light oil reservoirs and study based on performance has led to several proposal or estimating recovery factors on such projects (Gutierrez *et al*., 2007).

This method involves the injected air to combust a small fraction of oil to produce flue gases which is responsible for reservoir oil displacement. Xia *et al*., (2004) outlined major benefits of light oil air injection to be because the source of air is inexpensive (air is cheap), its reaction with crude oil is spontaenous as well as completely consumes the oxygen in air. It also favours high recovery due to immiscible gas displacement, oil swelling, reservoir repressurisation, flue gas stripping and sequestration.

2.5 Kinetics of Thermal EOR

Thermal characteristics of crude oils have been investigated over the years by the use of various analytical techniques. This is due to the fact that crude oil are mixtures of complex hydrocarbon fractions which tend to behave differently from reservoirs to reservoirs, so the need to fully understand its kinetics to help optimise recovery potentials.

2.5.1 Combustion reaction of crude oil

In an air injection EOR, oxygen contained in air reacts with the hydrocarbon fuel (CH_x) at the combustion zone to generate heat, and bi-products of its combustion reaction given by the general stoichiometric equation as described by Mamora (1995).

$$CH_x + \left(1 - \frac{m}{2} + \frac{x}{4}\right) O_2 \rightarrow (1-m)CO_2 + mCO + \frac{x}{2} H_2O \quad (2.1)$$

x = atomic hydrogen-carbon (H/C) ratio of fuel

m = fraction of carbon oxidised to carbon monoxide.

Equation 2.1 was later modified to accommodate for complexes in high temperature oxidation (HTO); The modified form is given in equations (2.2) and (2.3).

$$CH_xO_y + \left(1 - \frac{m}{2} + \frac{x}{4} - \frac{y}{2}\right) O_2 \rightarrow (1-m)CO_2 + mCO + \frac{x}{2} H_2O \quad (2.2)$$

where $y = \frac{2(1-m)}{CO_2}\left[CO_2 + CO\left(\frac{1}{2} + \frac{x}{4m}\right) - O_{2c}\right]$ (2.3)

If fuel is not oxygenated, y = 0, therefore the O/C ratio can be determined from equation 2.3 (experimentally for some oil ranged 0.4 – 0.9) for known values of x and m, H/C ratio can also be determined from combustion tube experiments (determined to be between 1.62 and 1.77 by Mamora (1995).

Dubey (2010) presented general reactions of the various crude oil oxidation zones. See Equation (2.4) to (2.6), the light temperature oxidation (LTO), medium temperature oxidation (MTO) and the heavy temperature oxidation (HT)) zones for crude oils;

LTO: hydrocarbon + O_2 + N_2 = oxygenated compounds + energy + N_2 (2.4)

MTO: hydrocarbon + O_2 + N_2 = coke + energy + N_2 (2.5)

HTO: hydrocarbon + O_2 + N_2 = carbon oxides + water + energy + N_2 (2.6)

Although thermal analysis and calorimetric techniques such as differential scanning calorimetry (DSC), thermo-gravimetric analysis (TGA), pyrolysis gas chromatography, and accelerating rate calorimeter (ARC) have been previously used to study combustion / oxidation behaviours of crude oil (Li *et al*., 2002;

Li *et al*., 2004; Mahinpey *et al*., 2010; Kok & Kesin, 2001), however most of these papers have studied combustion regions (onset, peak and end of exothermic activities), and for its kinetics; a simple Arrhenius kinetic model was used to describe the oil combustion behaviour. These have limitations in terms of accuracy and full description of kinetics of these complex reactions that different crude oil fractions may be undergoing simultaneously.

2.5.2 Oxidation of sulfur containing crude oils

Acidic crude oils are known to be sulphur bearing. Crude oils having sulphur contents greater than 0.15 wt% are known as sour crude while those with less than 0.15% are known as sweet crude. Sulfur content has been studied over the years and discovered to increase as boiling temperature of crude oil fraction increases. The sulfur containing hydrocarbons are known to have high molecular weight which is why up to 70 to 90% of all the sulfur hydrocarbons are concentrated in fuel oil and tar (Erikh *et al*., 1985).

Sulphur in hydrocarbons exists in many forms; as dissolved sulfur, colloidal state, dissolved H_2S, mercaptans, sulfides (thioesters), polysulfides (aliphatic), cyclic and thiophene derivatives. The cyclic and thiophene derivatives are usually found in the kerosene fraction and are extremely difficult to isolate. Thiophenes are thermally stable, and do not react with metals but they dissolve well in sulfuric acid. Resinous and asphaltene part also contain very complex compounds including sulfur, nitrogen and oxygen (Karacan *et al*., 1998; Laredo *et al*., 2004).

Sulphur content is known to be responsible for naphthenic acid corrosion in crude oils (Worden and Smalley, 1996) by two (2) processes; the naphthenic attack and hydrogen sulfide attack (Zhang *et al*., 2006) are shown from equations 2.7 and 2.8 respectively.

$Fe + R\text{-}COOH \rightarrow Fe(RCOO)_2 + H_2$ (Naphthenic attack on Iron (carbon steel) (2.7)

$Fe + H_2S \rightarrow FeS + H_2$ (H_2S corrosion attack) (2.8)

Equation 2.9 shows the regeneration of naphthenic acid with the precipitation of iron sulfide which implies that naphthenic crude seems to be more corrosive with low sulfur at high temperature than the crude oil on high naphthenic value and with high sulfur content (Laredo *et al*., 2004; Georgina *et al*., 2004).

$$Fe(RCOO)_2 + H_2S \rightarrow FeS + 2RCOOH \quad (2.9)$$

Nigerian crude oils are known to have very low sulfur between 0.04 to 0.15 wt% (Chevron Corporation, 2016; TOTSA, 2016). In Niger-delta region, aromatic sulphurs are common such as thiophenes. Dibenzothiophene (DBT), 1-methyl Dibenzothiophene, 4 methyl dibenzothiophene, and 2,3 dimethyl dibenzothiophene (Sonibare, *et al*., 2008). Light crude oils are characteristic of Nigerian crude oils and C_2 - C_6 mercaptans have boiling fraction corresponding to 35-140 ^{o}C. Mercaptans have a characteristic unpleasant smell and can be used as an odorant in gas facilities to warn of gas leaks.

Organic Sulfoxides, sulphate salts and complexes such as thiobenzophenones (TBP) $(C_6H_5)_2CS$ were found to be present in alphaltene fraction of some Nigerian crude oils. These crude oils are found in reservoirs from Belema, Imo and Eket oil fields in the Niger Delta area, Nigeria (Katarzyna *et al*., 2005; Adebiyi and Thoss, 2014).

2.5.3 Oxidation of mercaptans

Mercaptans under the action of heat, form sulfides with evolution of H_2S. In the presence of oxygen, they release H_2O as illustrated from equations 2.10-2.12.

$$\text{At } 300^{o}C,\ 2C_5H_{11}SH \rightarrow C_5H_{11}SC_5H_{11} + H_2S \quad (2.10)$$

$$\text{At } 500^{o}C,\ C_5H_{11}SH \rightarrow C_5H_{10} + H_2S \quad (2.11)$$

and in the presence of O_2, water is released

$2C_3H_7SH + ½ O_2 \rightarrow C_3H_7SSC_3H_7 + H_2O$ (2.12)

2.5.4 Oxidation of aliphatic/cyclic sulphides

Aliphatic sulphides produce corresponding alkenes and hydrogen sulphide gas at 400^oC as shown in equation 2.13.

$C_2H_5SC_3H_7 \rightarrow C_2H_4 + C_3H_6 + H_2S$ (2.13)

Polycyclic suphides such as benzthiophene, thiocycloalkane, dibenzthiophen, and napthothiophene do not readily react with metals, and are very thermally stable (Katarzina *et al*., 2005). They also constitute greater than 70% of Sulphur in high molecular part of petroleum (fuel oil, tar).

2.5.5 Air injection for reservoir oxidation

Combustion or oxidation in-situ reservoir requires the oxidizing agent, heat and the fuel (Yannimaras and Tiffin, 1995; Tiffin and Yannimara, 1997). Combustion of crude oil in the reservoir gives a double effect (1) heat effects: which reduces viscosity of the oil (Kuhlman, 2000; Moore *et al*., 1992) and (2) flue gas sweeps: flue gas mixes with the oil, thereby increasing mobility ratio and eventually leading to enhance flow of oil to the producer (Fraim *et al*., 1997).

A typical crude oil combustion reaction is shown in equation 2.

$C_xH_y + O_2 \rightarrow$ Energy + Flue gas (2.14)

Similar to aliphatic sulphides, disulphides combust to produce flue gases and water as shown in equation 2.16 and 2.17.

$C_3H_7SSC_3H_7 + O_2 \rightarrow 2C_3H_6 + H_2S + SO_2$ (2.16)

$C_3H_6 + 2O_2 \rightarrow CO_2 + CO + CH_4 + H_2O$ (2.17)

This equation can be used to determine volume of oxygen required for flue gas production using the simple mole concept. Equal amount of volume of oxygen will be required for production sulphur containing flue gas, while twice molar volume will be needed to produce the other flue gases from light crude oil.

2.5.6 Amount of air required for enhanced oil recovery

The mole concept is based on ratio of reactants. In Equation 2.16 where the stoichiometry of the aliphatic sulphide and oxygen is 1:1, i.e 1 molar volume (22.4 dm^3) of $C_3H_7SSC_3H_7$ requires 1 molar volume of oxygen to produce 2 molar volume of propene (C_3H_6) and one molar volume each of hydrogen sulphide and sulphur dioxide.

This implies that 22.4 dm^3 of $C_3H_7SSC_3H_7$ will require 22.4 dm^3 of Oxygen for the reaction, which is equivalent to (22.4/21 *100) = 1.07 dm^3 amount of air to produce 44.8 dm^3 of propene and 22.4 dm^3 each of hydrogen sulphide and sulphur dioxide.

Using a Basis of 1 dm^3 = 1000 cm^3 for simplicity,

1000 cm^3 of each reactants i.e sulphide hydrocarbon ($C_3H_7SSC_3H_7$) and oxygen (4761.90 cm^3 of Air) will produce 1000m^3 each of products as shown in equation, i.e 2000 cm^3 of C_3H_6, C_3H_6 and 1000 cm^3 each of H_2S, and SO_2 (2000 cm^3 hydrocarbons and 2000 cm^3 flue gas).

Similarly, for equation 2.17 with stoichiometry of 1 : 2, 1000 cm^3 of C_3H_6 will react with 2000 cm^3 of air (9523.81 cm^3 air) to produce 1000 cm^3 each of CO_2, CO, CH_4, and H_2O (4000 cm^3 flue gas).

2000 cm^3 of hydrocarbon will react with 3000 cm^3 of oxygen equivalent to 14,285.71 cm^3 of air to produce 6000cm^3 of flue gas and 8285.71cm^3 (14285.71cm^3 – 6000cm^3) of unreacted air content which mixes and re-pressurizes the oil in the reservoir to produce 3000cm^3 of Hydrocarbon crude oil.

2.6 Arrhenius Studies of EOR Kinetics

Kinetic studies from TGA or DSC uses the relationship between heating rate and temperature given by Equations 2.18-2.20;

$$K = Ae^{-\left(\frac{E}{RT}\right)} \tag{2.18}$$

The differential dα/dt with conversion of α is also given by;

$$\frac{d\alpha}{dt} = k\ (1-\alpha)^{n}\text{; where } \alpha = (\omega_i - \omega_t)/(\omega_i - \omega_f) \tag{2.19}$$

Let β be the linear heating rate given by $\frac{dT}{dt}$, (2.20)

Combining Equations (2.18) to (2.20) and rearranging gives Equation (2.21)

$$\ln\left[\frac{1-(1-\alpha)^{1-n}}{T^2\,(1-n)}\right] = \ln\frac{AR}{\beta E}\left(1-\frac{2RT}{E}\right) - \left(\frac{E}{R}\right)\frac{1}{T} \tag{2.21}$$

Equation 2.21 can be solved for activation energy when $\ln\left[\frac{1-(1-\alpha)^{1-n}}{T^2\,(1-n)}\right]$ is plotted against $\frac{1}{T}$, The slope will be (E/R) for the correct value of n. In most cases, n is assumed to be = 1, so that a straight line of data would give a slope= (E/R) (Li *et al*., 2002), where;

n = order of reaction

E = activation energy (J/Mol)

K = reaction rate constant (min^{-1})

R =universal gas constant (J/Mol/K)

T = absolute temperature (K)

A = pre-exponential factor

α = fractional conversion (min^{-1})

t = time (min)

β = heating rate (^oC/min)

ω = sample weight

subscripts:

i = initial; t = at time t; f = final

2.6.1 Arrhenius studies of EOR kinetics using oxygen consumption bases

A fuel varying geometry is used in this case so that as reaction progresses, oxygen consumption is related to the Arrhenius equation as shown in equations 2.22 and 2.23 given by Mamora, (1995) and Greaves *et al* (1998) respectively. Equation 2.24 gives a simplified equation for a model based kinetic for the reaction.

$$\frac{qO_{2c}}{AL} = -A_{ri}P_{O_2}^{mi}C_{fi}^{ni}\exp(-E_i / RT) \tag{2.22}$$

$$\frac{d(P_{o2})}{dt} = k.e\exp(-E_i / RT).(P_{O_2}^{n}) \tag{2.23}$$

$$\frac{d\alpha}{dt} = A\exp\left(-\frac{E}{RT(t)}\right)f_\alpha \tag{2.24}$$

where;

q = volumetric flow rate

O_{2c} = oxygen consumed

A = cross sectional area of tube

L= length of sand mix in tube

A_{ri} = pre-exponential factor

P_{o2} = oxygen partial pressure

C_f = instantaneous fuel concentration

E = activation energy

R = universal gas constant

T = absolute temperature

N = order of reaction

i = reaction zone (Light or heavy temperature oxidation)

Reaction rate is proportional to fuel consumption as shown in Equation 2.25

$$\frac{qO_{2c}}{AL} = -\alpha \frac{dC_{fi}}{dt} \tag{2.25}$$

where α is a proportionality constant which has a convention of being positive for high temperature oxidation (HTO) and negative for low temperature oxidation (HTO).

2.7 Kinetics by Iso-conversional Methods

The iso-conversional method has found wide applications in reactions analysis where the decomposition reactions proceeds through multiple stages, where mechanisms are generally unknown or where description of simpler models gives poor results (Iliyas *et al*., 2010). This method is the principle in which reaction rate at constant reaction progress α is only a function of temperature (T). These methods allow for the determination of the kinetic parameter, activation energy (E) i.e dependence of E on α without assuming the explicit form of f(α) which implies E is not constant but vary as reaction progresses. E= E(α). There are three modifications of the iso-conversional method;

(a) Differential (Friedman)

(b) Integral (Flynn-Ozawa-Wall)

(c) Advanced integral based on non-linear procedure (Vyazovkin)

2.7.1 Differential (Friedman)

The advanced thermokinetic software (AKTS) applies this type of modification in its analysis employing the logarithm of reaction rate as a function of reciprocal of temperature. If decomposition follows a single mechanism, then a single pair of arrhenius parameters with simple model as in Equation 2.26 and 2.27. Thermal analysis where there is only one value for activation energy and one for pre-exponential factor, Equation 2.28 will be adequate.

There are various reaction models f(α) as in Table 2.2 but they can be grouped to three (3) major classes (acceleration, decelerations and autocatalytic) when the dependence of reaction progress with time is put into consideration. They have unique characteristic reaction profiles as shown in Figure 2.6.

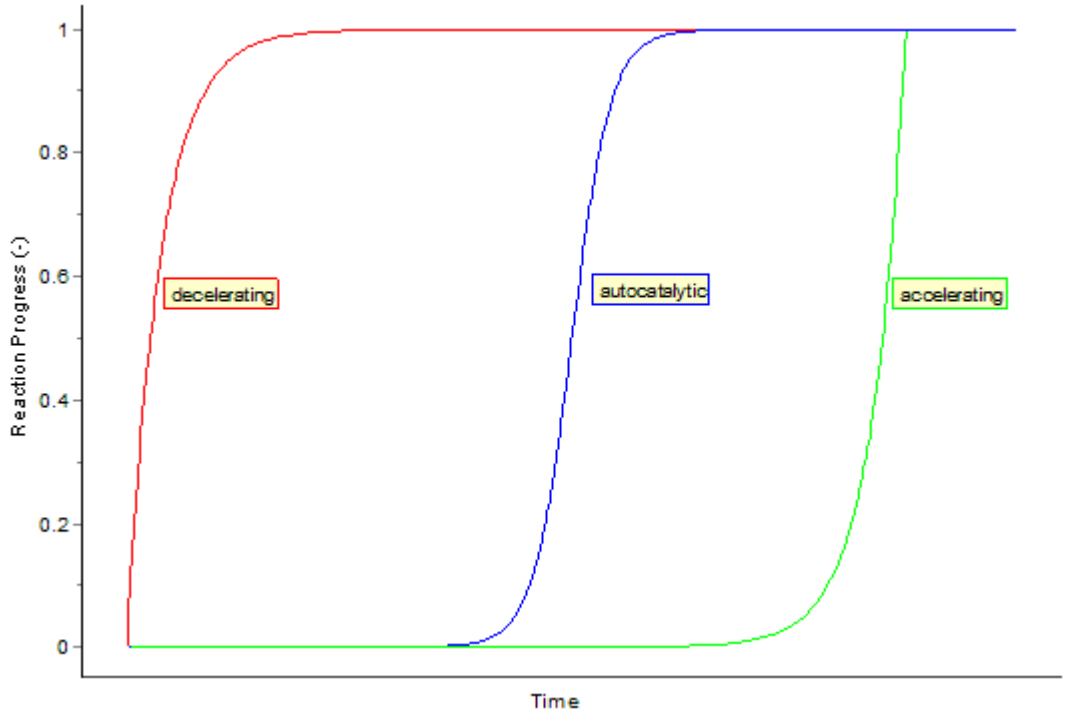


Figure 2.6: Relationship of the reaction progress α vs time for reaction models (Roduit, 2008).

The decelerating model describes a process which records a maximum reaction rate at the beginning of the process and thereafter undergoing a continuos (reaction rate) decrease as the reaction progress from 0 to 1. The common reaction models conforming to these types of reaction profile are the diffusion models (1 dimensional, 2- dimensional and 3 dimensional) and that of the contracting geometry listed in Table 2.2. Homogenous kinetic model that obey this model is given by Equation 2.26;

$$f(\alpha) = (1-\alpha)^n \tag{2.26}$$

where reaction progress (α) ranges from 0 to1, and n is the reaction order.

The autocalytic type has a sigmoidal behaviour where the process accelerates at the begining of the reaction (as soon as the reaction progress exceeds 0) and thereafter decelerates at the end of the reaction (when reaction progress tends to 1). The switch between the accelerating to decelerating gives rise to an intermediate value of extent of reaction (α) where maximum rate of the reaction exists. The Prout-Tompkins model is an example of the autocatalytic model given by the Equation 2.27.

$$f_n = 1-\alpha^{\ n} a^m \tag{2.27}$$

where n is the reaction order and m is a constant.

The accelerating model is the opposite of the decelerating model. The reaction accelerates as the reaction progresses to the end of the reaction. The reaction rate is maximun at the end of the reaction unlike the decelerating where the maximum reaction rate is at the beginning of the reaction. The Power law shown in equation in Table 2.2 is an example of the accelerating reaction model.

Other reaction models such as Avrami-Erofeez, Mampel, nth order have been developed with each having its characteristic model equation.

Friedman analysis is based on the Arrhenius equation as stated in Equation 2.28.

$$\frac{d\alpha}{dt} = Aexp\left[-\frac{E}{RT(t)}\right] f(\alpha) \tag{2.28}$$

where α = reaction progress (-)

$f(\alpha)$ = model function (-)

A = pre-exponential factor (1/s)

E = activation energy (kJ/mol)

T = temperature (K)

t = time (s)

Table 2.2: Wide Variety of Reaction Models f(α)

Reaction Model	f(α)	n	order
nth order	$f_n = (1-\alpha)^n$	1	first order
(Netzsch, 2009 & AG-AKTS, 2008)		2	2nd order
		3	3rd order
Power law	$P_n = n\alpha^{\left(1-\frac{1}{n}\right)}$	1	first order
(AG-AKTS, 2008)		2	2nd order
		2	3rd order
Avrami-Erofeev	$A_n = n(1-\alpha)\left[-\ln(1-\alpha)\right]^{\left(1-\frac{1}{n}\right)}$	1.5	Avrami-Erofeev
(House, 2007)		2	Avrami-Erofeev
Contracting	$R_n = n(1-\alpha)^{\left(1-\frac{1}{n}\right)}$	2	Cylinder
(AG-AKTS, 2008)		3	Sphere
Diffusion	$D_1 = \left(\frac{1}{2\alpha}\right) D_1 = \left(\frac{1}{2\alpha}\right)$	1	1- Dimensional
(AG-AKTS, 2008)			
	$D_2 = \left[-\ln(1-\alpha)\right]^{-1}$	2	2- Dimensional
	$D_3 = 1.5\left[1-(1-\alpha)^{\frac{1}{3}}\right]^{-1}(1-\alpha)^{\frac{2}{3}}$	3	3- Dimensional
Autocatalytic	$f_n = (1-\alpha)^n a^m$	n	n
(CureKinetics, 2008)			

At any time (t), the pre-exponential factor as well as the activation energy is a function of reaction progress. Therefore, Equation 2.28 becomes 2.29.

$$\frac{d\alpha}{dt_\alpha} = A_\alpha f(\alpha) \exp\left(-\frac{E_\alpha}{RT_{t_\alpha}}\right) \quad (2.29)$$

Applying logarithm on Equation 2.29, Equation 2.30 is obtained.

$$\ln\left(\frac{d\alpha}{dt}\right)_\alpha = \ln A_\alpha f(\alpha) - \left(\frac{E_\alpha}{R}.\frac{1}{T_\alpha}\right) \quad (2.30)$$

Eα in this case is apparent activation energy, it is not constant as the reaction progress; pre-exponential factor A, reaction model f(α) and activation energy E are known as the kinetic triplet (Budrugeac, 2005). Simplifying equation 2.30 gives 2.31

$$\ln\left(\frac{d\alpha}{dt}\right)_\alpha = \ln A' - \left(\frac{E_\alpha}{R}.\frac{1}{T_\alpha}\right) \text{ where } A' = A_\alpha f(\alpha) \quad (2.31)$$

So having determined A‘ and E(α) from the equation above, reaction rate and progress can be predicted from (2.32) at any temperature profile.

$$\left(\frac{d\alpha}{dt}\right)_\alpha = A' f(\alpha) \exp\left(-\frac{E_\alpha}{R}.\frac{1}{T_\alpha}\right) \quad (2.32)$$

where α = reaction progress (-)

$f(\alpha)$ = model function (-)

A = pre-exponential factor (1/s)

E = activation energy (kJ/mol)

T = temperature (K)

t = time (s)

2.7.2. *Ozawa-Flynn-Wall analysis*

It is so-called integral isoconversional method. The E(α) are less precise as compared to the diferential Friedman's method. Ozawa, Flynn and Wall developed a method for activation energy determination based of several curves measured at different but constant heating rates into the analysis.

The analysis starts from the Arrhenius equation, $\frac{d\alpha}{dt} = A\exp\left(-\frac{E}{RT(t)}\right) f_\alpha$ with constant heating rate

β=(dT/dt), the integral form of Equation 2.32 is shown in equation 2.33;

$$G(\alpha) = \int_{\alpha=0}^{\alpha} \frac{d\alpha}{f\ \alpha} = \frac{A}{\beta}\int_{To}^{T\ \alpha} \exp\left(-\frac{E}{RT\ t}\right) dt \qquad (2.33)$$

If temperature T_o lies below the onset temperature (temperature of noticeable reaction), T_o is set to zero (0), so that integration of Eqution 2.33 can be carried out and logarithm expression be used in the form of Equation 2.34 and 2.35;

$$\ln G(\alpha) = \ln\left(\frac{AE}{R}\right) - \ln(\beta) + \ln\ p(z) \qquad (2.34)$$

and $p(z) = \frac{\exp(-z)}{z} - \int_{-\infty}^{z} \frac{\exp(-z)}{z} dz$ (2.35)

where $z = \frac{E}{RT}$ and ln p(z) given by an approximation given in Equation 2.36 as;

ln p(z) = 5.3305 - 1.052z (2.36)

and transposing Equation 2.36 yields Equation 2.38.

$$\ln(\beta) = \ln\left(\frac{AE}{R}\right) - lnG(\alpha) - 5.3305 - 1.052\left(\frac{E}{RT}\right) \qquad (2.37)$$

where R = molar gas constant,

β = heating rate

From equation 2.37, A graph of ln β against (1/T) implies a straight line with a slope of (-1.052E/R) at a fixed heating rate β and fixed progress of reaction α. The value of R is known to be constant, therefore, the activation energy as a function of reaction progress can then be calculated.

2.7.3 ASTM E-698

This is based on the assumption that irrespective of the heating rate of the process (β), the maximum of a single step reaction occurs at the same conversion degree. The results obtained from this analysis shows low errors (AG-AKTS, 2008). The method employed the plot of logarithm of heating rate over the reciprocal temperature of the maximum (peak reaction rate), in which the activation energy which is proportional to the slope is calculated (Roduit, 2008).

2.8 Non-Thermal Gas Injection Methods

Non-thermal gas injection methods deals with the different gas injection methods leading to no thermal effect in-situ reservoir. Non-thermal methods are usually applied to light oil of viscosity less than 100 cp, but in recent cases has been applied to oils with viscosity up to 2000 cp. This method includes gas drives (miscible and non-miscible), chemical (polymer, surfactant, alkaline, micellar and emulsion) and others such as microbial and foam (D'Elia-S and Ferrer, 1973; Trushenski *et al*., 1974; Kumar *et al*., 1998; Button, *et al*., 2004; Tiorco, 2009; Oil-Chem, 2010; Armstrong and Windenschild, 2012; Belgravecorp, 2012; NETL, 2012; Statoil, 2012).

These methods as the name implies, do not require heat to generate the flue gas in-situ the reservoir, instead, flue gases are injected from sources outside the reservoir, such as power plants. They are otherwise known as gas drives. These methods do not have the advantage of viscosity lowering due to thermal effect. Gas drives and miscibility are the major driving forces of this technique (Holm, 1986; De La Ossa *et al*., 1998).

Carbon dioxide gas is a known favourable injection fluid for increasing oil recovery. It has the ability to extract or vaporize hydrocarbons from reservoir oil. It is also soluble in oil and its solubility increases with pressure. The dissolved gas in oil readily swells thereby increasing its volume and reducing the overall viscosity of the reservoir oil (Dong and Huang, 2002; Mathiassen, 2003). The effects of swelling and lowering of viscosity makes the oil flow easily to the producer and hence incremental oil recovery. Gas drives can be sub-divided into miscible and non-miscible drives. A miscible drive involves the displacing fluid to be miscible with the reservoir oil, this can take place one time or multiple times. The one-time miscible contact is referred to as first/single contact miscibility (SCM) while the multiple times is called the multiple contact miscibility (MCM). Figure 2.7 shows a miscibility process due to a gas being injected into the reservoir. The mixing zone MZ (around end of zone B and beginning of Zone C) is formed between the displacing fluid and the reservoir causing a piston like displacement (Juttner, 1997). This displacement can occur in two processes called the vaporising and condensing gas drive process (Zick, 1986).

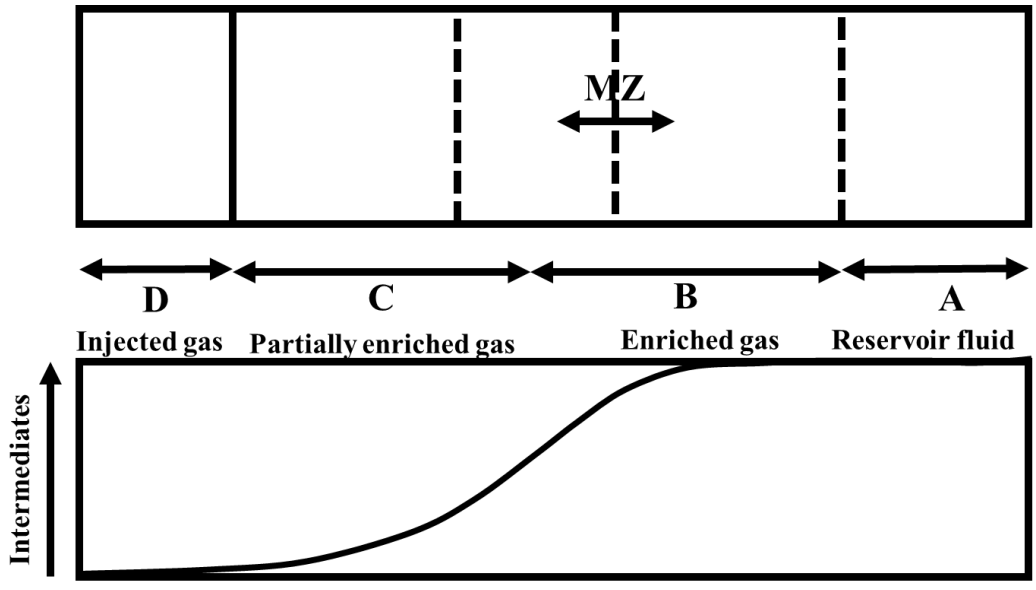


Figure 2.7: Schematic representation of miscible displacement (Juttner, 1997).

Reservoir oil mobility is influenced by two (2) major factors, the capillary number (Nc) and mobility ratio (M). Capillary number is defined by the equation 2.38 given by

$$Nc = v\mu/\sigma \qquad (2.38)$$

where v = Darcy velocity (m/s), μ is the fluid viscosity (Pa.S) and σ is the interfacial tension.

In miscible flooding, interfacial tension reduces to zero and capillary number goes to infinity, and for displacement efficiency to approach unity, mobility ratio (ratio of mobility of displacing fluid to displacing fluid) has to be less than 1.

In a ternary diagram, the major difference between a single and multiple contact miscibility is that in the former, the tie line that joins the injector gas and the oil does not pass through the two (2) phase region while in the later, the tie line passes through the 2 phase region as illustrated in Figure 2.8.

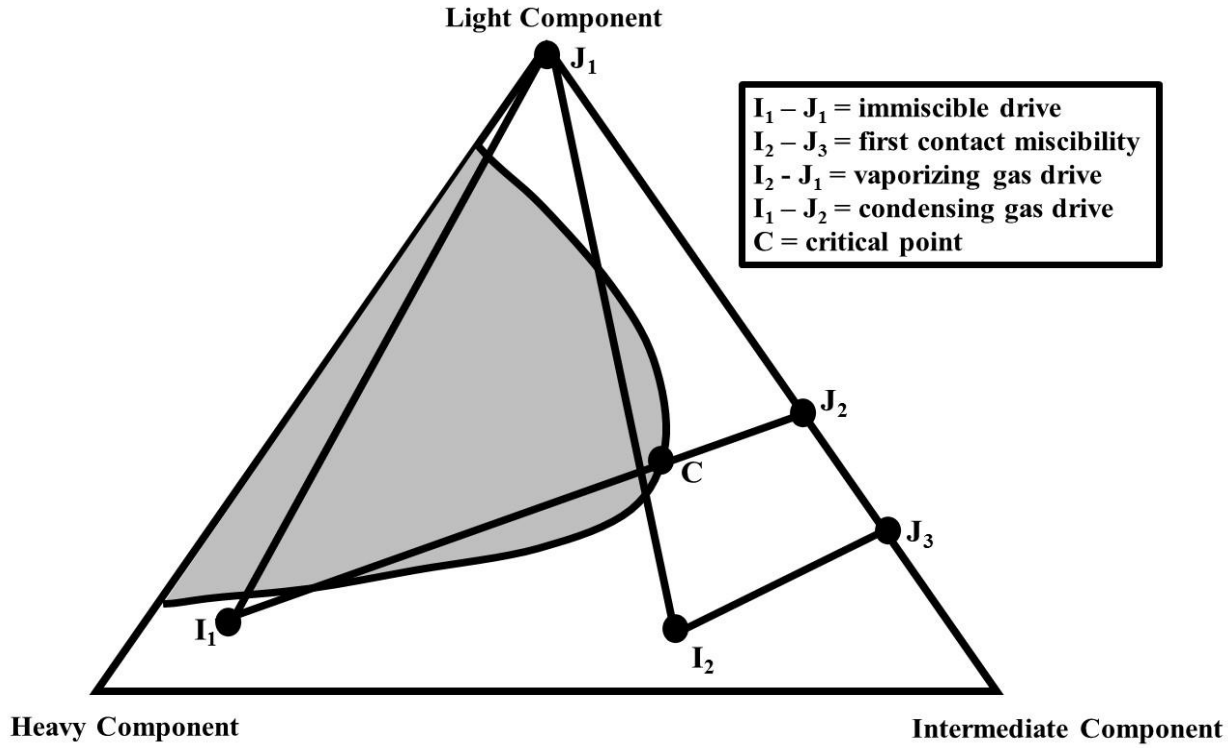


Figure 2.8: Ternary diagram illustrating miscible and non-miscible drives (Lake *et al*., 2014).

2.8.1 Vaporising gas drive

The vaporising gas drive is illustrated in a ternary diagram (Figure 2.9) in which the reservoir oil is on the same side of the critical tangent (the tangent on the critical point C). This process is a Mix-Flash-Move mechanism, in that the line I (injected gas) to O (reservoir Oil) which passes through the two (2) phase region has mixture M_1, and then flashes to I_1 and O_1 of gas and oil respectively. O_1 becomes the new oil concentration and the injected gas mixes with it to flash to I_2 and O_2. This process continues until the tie line coincides with critical tangent. This is where the optimum miscibility is achieved (Danesh, 1998).

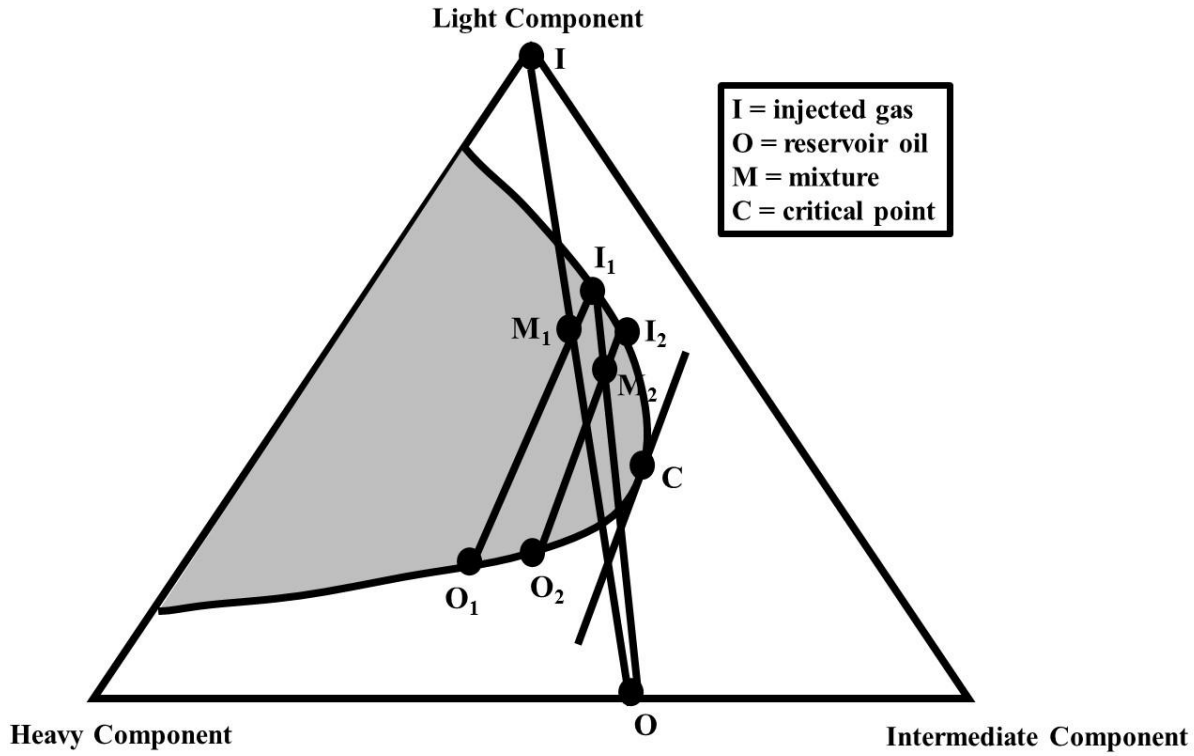


Figure 2.9: Ternary Diagram illustrating Vaporising gas drive (Pederson and Christenson, 2007).

2.8.2. Condensing gas drive

This gas drive mechanism is shown in the ternary diagram, Figure 2.10. It has the injected oil on the same side with the critical tangent while the reservoir oil is on the opposite side. Miscibility also develops from the mixing of the injected gas (I) and oil (O) to form a mixture M_1 which flashes to I_1 and O_1. The injected gas further mixes with the oil O_1 to produce mixture M2 which also flashes to I_2 and O_2 respectively. This Mix-Flash-Move process continues until the tie line from injected gas to the oil coincides with the critical tangent at the optimum miscibility (Orr, 2007).

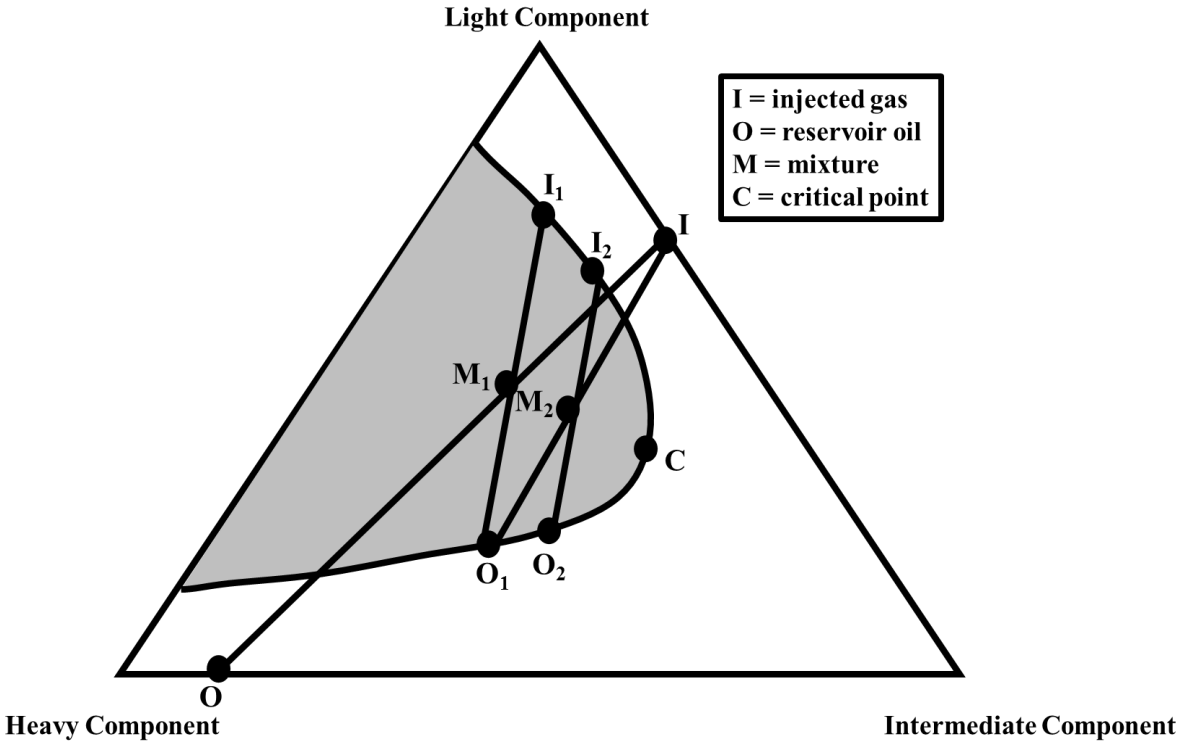


Figure 2.10: Ternary Diagram illustrating Condensing gas drive (Danesh, 1998)

2.8.3 Immiscible gas drives

Immiscible drives are the other methods which do not fall strictly under chemical or miscible categories. These may include inert gas flooding (Farouq & Thomas, 1994). The tie lines shown in Figure 2.11 all pass through the two (2) phase region and unlike the miscible drives, it does not mix, flash or move.

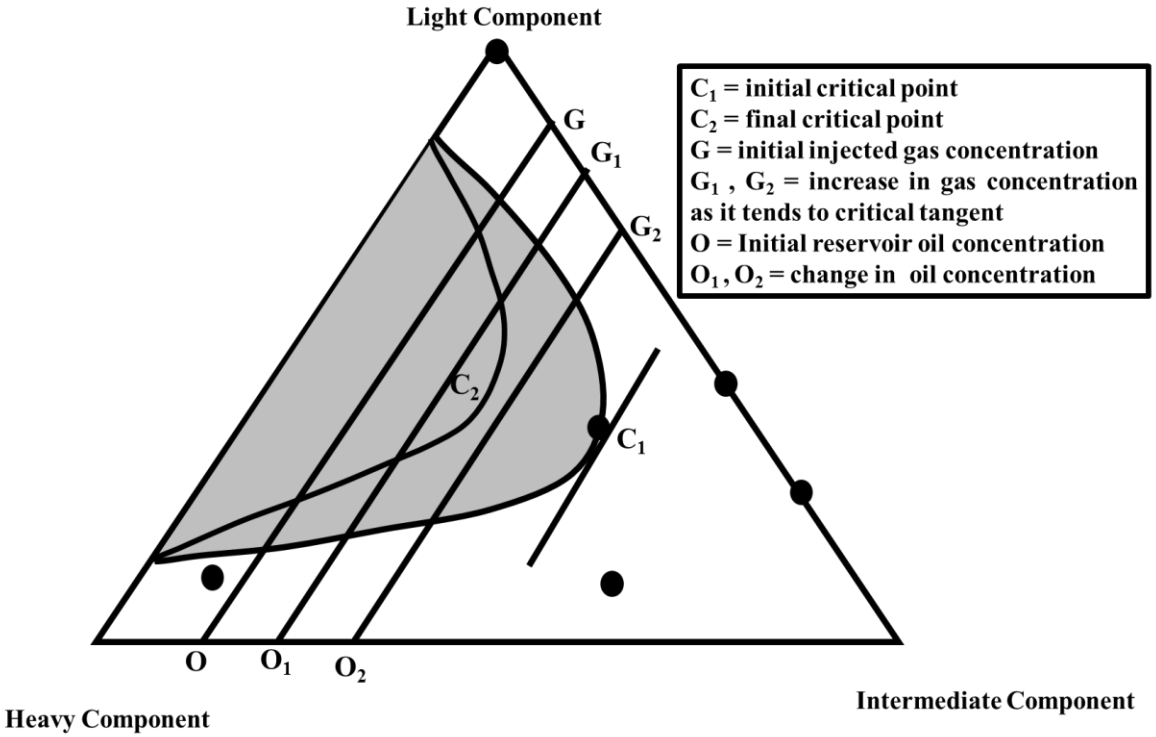


Figure 2.11: Ternary diagram illustrating Immiscible gas drive (Pederson and Christenson, 2007)

The injected gas (G) and reservoir oil do not have any initial partial mixing (M) which is usually observed in miscible gas drive (condensing and vaporising). Miscibility is only achieved by enrichment or pressure increase. The injected oil could be enriched by changing its composition or by enriching it with the intermediate fluid (C_2) so that injected gas G can move its concentration to G_1 and G_2 to make the injected gas closer to the critical tangent. The point where the tie line passes the critical tangent is the point of miscibility. Pressure increase in used to shrink the critical tangent from C_i to C_{ii} so that injected gas say G_2 and oil (O_2) could easily achieve single phase mixing when it coincides with the critical tangent (Orr, 2007).

2.9 Reservoir Fluid Studies and Experiments

Crude oils are complex mixtures consisting basically of hydrocarbons and compounds of nitrogen, sulphur, oxygen, carbon dioxide and metals in lower concentrations (Tarek, 2007). The major and minor constituents affect the behaviour (physical and chemical properties) of the reservoir oils. Reservoir management requires reliable and accurate description of phase behaviour and volumetric data of crude oils (Danesh, 1998). The volumetric data of the oils which mimic reservoir conditions are determined experimentally as a function of Temperature and Pressure. The relationships of pressure, volume and temperature obtained from these experiments helps to optimize reservoir performances from the reservoir fields.

Generally, the laboratory tests used to characterise reservoir oil sample can be classified into three (3). They are Primary tests, Routine tests and the Special laboratory PVT tests.

2.9.1 Primary tests

These are simple routine tests carried out on site. They include specific gravity tests and gas to oil (GOR) ratio of the produced hydrocarbons.

2.9.1.1. Specific gravity (sg) tests

Density of oil is the ratio of mass of oil per unit volume. Crude oil density is pressure dependent due to presence of gas as its constituents and it is specified by the oil specific gravity (s.g) which is the density of the oil relative to that of pure water both measure at standard conditions. However, it is common to use the API gravity which is related to the specific gravity given in Equation 2.39 given by;

$$API = 141.5/s.g - 131.5 \quad (2.39)$$

In the field, the sample of oil is brought to a specific temperature. The test sample is then transferred to a hydrometer that has been brought to the same temperature. The hydrometer is then lowered into the sample and allowed to settle. When equilibrium is reached in temperature, the reading is taken and converted to standard measurement by the use of Petroleum Measurement Tables.

2.9.1.2 Gas to Oil ratio (GOR)

Solution Gas to Oil Ratio (GOR) is the amount of gas dissolved in oil at reservoir condition. It is also the volume of stock tank gas which will dissolve in a unit volume of stock tank oil when both are transferred to a given temperature and pressure. The ratio is defined in terms of gas and oil which reaches the surface during production (McCain, 1989). The GOR is given by equation 2.40 and determine by method shown in Figure 2.12.

$$GOR = \frac{\text{Volume of gas produced at surface condition}}{\text{Volume of oil entering stock tank condition}} \quad (2.40)$$

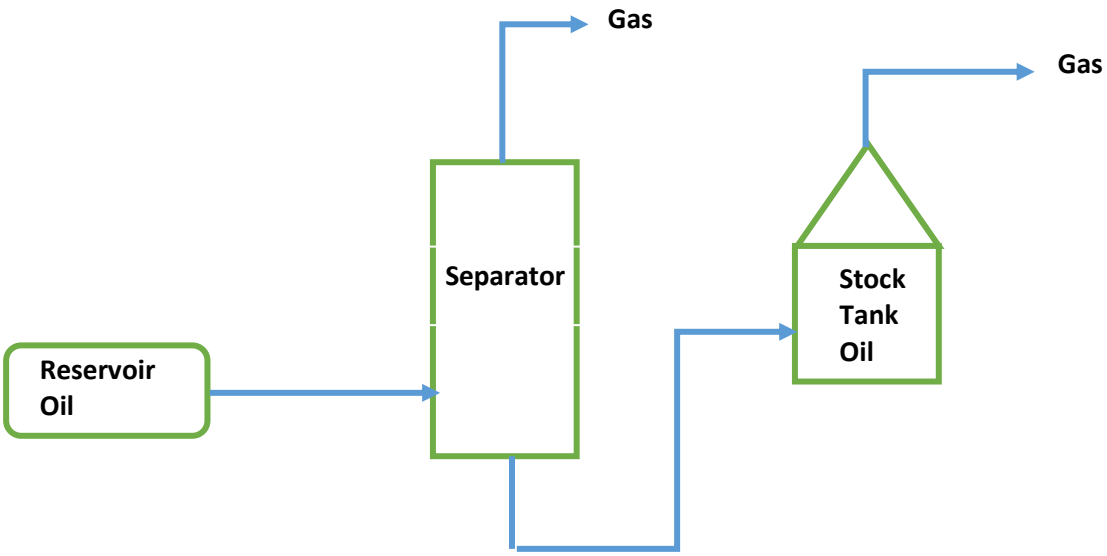


Figure 2.12: Schematic diagram illustrating method for determining gas to oil ratio

2.9.2 Reservoir hydrocarbon oil routine tests

Routine tests are tests carried out regularly to characterise the produced reservoir hydrocarbon oil. These tests include compositional analysis, constant composition expansion, differential liberation, separation tests and constant volume depletion.

2.9.2.1 Compositional analysis of reservoir fluids

Reservoir fluid samples when obtained at the early stages of the hydrocarbon oil reservoir closely resembles that of the original oil in place. That means reservoir oil samples of relatively young oil reservoirs have properties that closely approximates the reservoir property of the oil when the well was first discovered. Analysing these fluid sample reduces the chances of free gases to be present in the reservoir zones (Tarek, 2007).

The compositional description of the hydrocarbon is carried out in 2 phases, the gaseous analysis and the oil analysis. The gas and oil for the analysis are obtained from the Gas to oil ratio method shown in Figure 2.10. The combination of the separator liquid and the separator gas composition gives the reservoir oil composition. The separator gas (in the first and second stage) composition is carried in one step by capillary column chromatography while the stock tank oil is carried out in two steps. The first step is used to analyse the light cut (less than C7 fraction) while the second step is for the C7+ fractions (Jaubert *et al*., 2002).

2.9.2.2 Constant composition expansion (CCE) tests

Constant composition expansion otherwise known as constant mass expansion (CME) experiments are usually performed of gas condensate or crude oil to simulate pressure volume relationships of the hydrocarbon. It is conducted to determine the bubble point pressures at selected temperatures (usually reservoir). It is also conducted to determine the dew point pressure, isothermal compressibility, compressibility factors, and total hydrocarbon volume as a function of pressure (Tarek, 2007).

The experimental procedure involves the hydrocarbon been kept in a cell at reservoir conditions and the pressure reduced in steps at constant temperature as shown in Figure 2.13 where $P_1 < P_2 < P_3 < P_4 < P_5$ (Pederson and Christenson, 2007). If P_{sat} is the saturation pressure, P_1 and $P_2 > P_{sat}$, $P_3 = P_{sat}$ and P_4, $P_5 < P_{sat}$. The change in volume is monitored with respect to total cell volume V_{tot} given by equation 2.30:

$$V_{tot} = V_{ng} + V_{no} \quad (2.30)$$

where n is the stage number.

V_1 is the volume of oil at reservoir pressure P_1. At Pressure 2 lower than P_1, the corresponding Volume is V_2. At saturation point, P_3 is the saturation pressure and the corresponding volume V_3 = Vsat. At Pressure P4, lower than the saturation pressure, gas volume V_{4g} and corresponding oil volume of V_{4o} is noted.

Further decrease in pressure to P_5 leads to gas volume V_{5g} and a corresponding oil volume V_{5o}. The saturated volume (V_{sat}) is used as reference point and the relative volume (V_{rel}) = (V_{tot}/Vsat) reported.

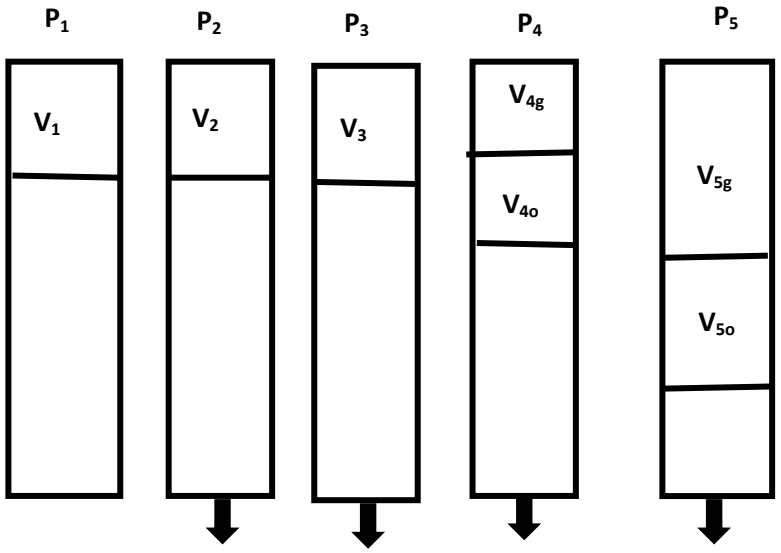


Figure 2.13: Schematic diagram of a constant composition expansion experiment (Tarek, 2007).

2.9.2.3 Differential liberation (vaporization) experiment

The experiment is conducted by first transferring the oil into a cell fixed at reservoir temperature. The experiment is usually started at saturation pressure and pressure reduced in a stepwise manner to liberated the gas and flashed to standard conditions as illustrated in Figure 2.14. The procedure is repeated up to 10 - 15 times to end at standard conditions (Tarek, 2007). The primary data of each stage comprises of oil formation factor which is defined as the oil volume at actual pressure divided by residual oil volume at standard condition; the solution gas to oil ratio which is the standard gas volume liberated from oil in stages that follow divided by the residual oil volume; the gas formation factor defined as the volume of gas at actual condition divided by gas volume at standard condition; and finally the gas gravity which is gas molecular weight divided by the molecular weight of atmospheric air (Pederson & Christenson, 2007).

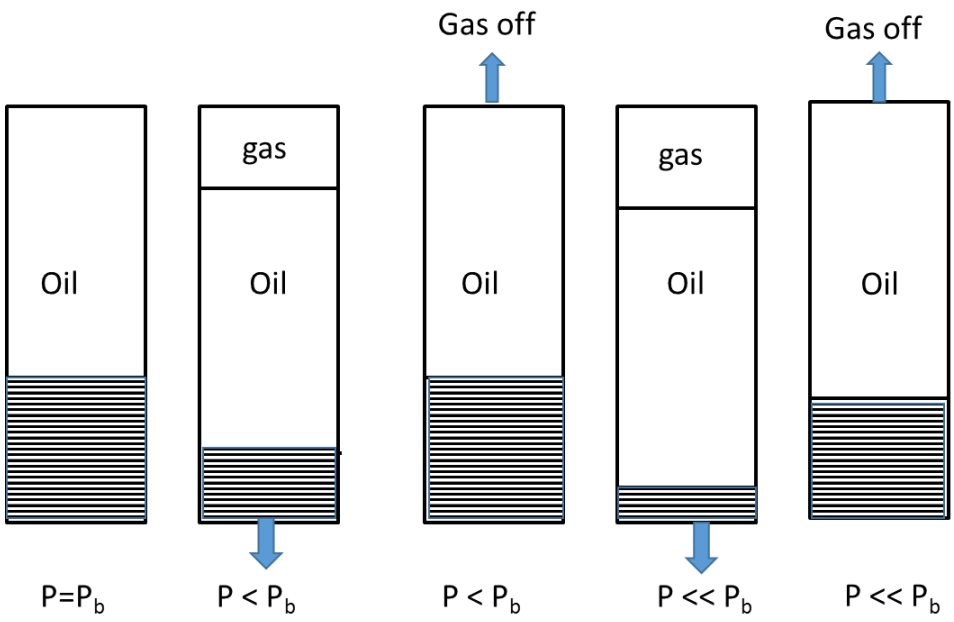


Figure 2.14: Schematic diagram of a differential liberation experiment (Tarek, 2007)

2.9.2.4 Separator tests

Separator tests otherwise known a flash separation tests are carried out to determine the changes in volumetric behaviours of reservoir fluids as it passes through the separator or series of separators. It is carried out on the original oil at bubble point conditions. These separators precedes the stock tank where the reservoir fluid is eventually collected at standard conditions (Tarek, 2007). The behaviour of reservoir fluid behaviour is affected by the conditions (temperature and pressure) of the surface separators. Separator tests provide essential information about the optimum surface operation of the separators to maximise the oil production in the stock tank.

The laboratory procedure for separator tests involves the following: the reservoir fluid is first charged into a PVT cell at reservoir conditions of temperature and it bubble point pressure. A small amount of oil is then removed at constant pressure and flashed through series of multistage separators at fixed temperature and pressure as shown in Figure 2.15. The gas liberated at each separator stage is then collected and its volume (Vo) and specific gravity measured. The remaining oil in the stock tank is also measured (Vst). The total solution gas to oil ratio and gas formation volume factors are calculated. The procedure is then repeated at different separator pressures and fixed temperatures (Pederson and Christenson, 2007).

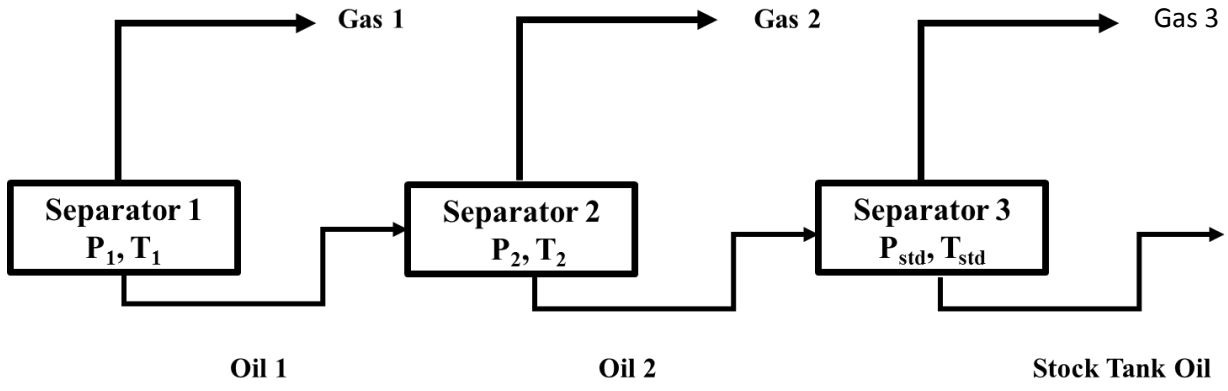


Figure 2.15: A schematic representation of a three-stage separator experiment (Tarek, 2007)

Separator tests when combined with differential liberation tests provides a means of obtaining some PVT parameters such as the differential oil volume formation factors, solution gas solubility, and relative total volume required for petroleum engineering calculations.

2.9.2.5 Constant volume depletion test (CVD)

Constant volume depletion tests involve the simulation of reservoir depletion performance and compositional variation on gas condensates and volatile oils. Its secondary purpose is to generate information on volumetric changes taking place with the well stream when operated at standard conditions. The experiment is carried out by transferring the reservoir fluid into a PVT cell at a fixed temperature T, (often at reservoir temperature (Pederson and Christenson, 2007). The test is started at saturation pressure (P_{sat}) where a known composition Z_i and volume (V_{sat}) are recorded and the compressibility factor Z_{sat} is calculated using the real gas equation $Z_{sat} = PV_{sat}/n_iRT$. (n_i is initial no of moles of the gas).

The volume is then reduced in a stepwise manner by opening a valve on the top of the cell which allows the gas deplete as shown in Figure 2.16. At each volume depletion stage, the pressure and volume readings are taken and corresponding compressibility factor (Z) calculated (Tarek, 2006).

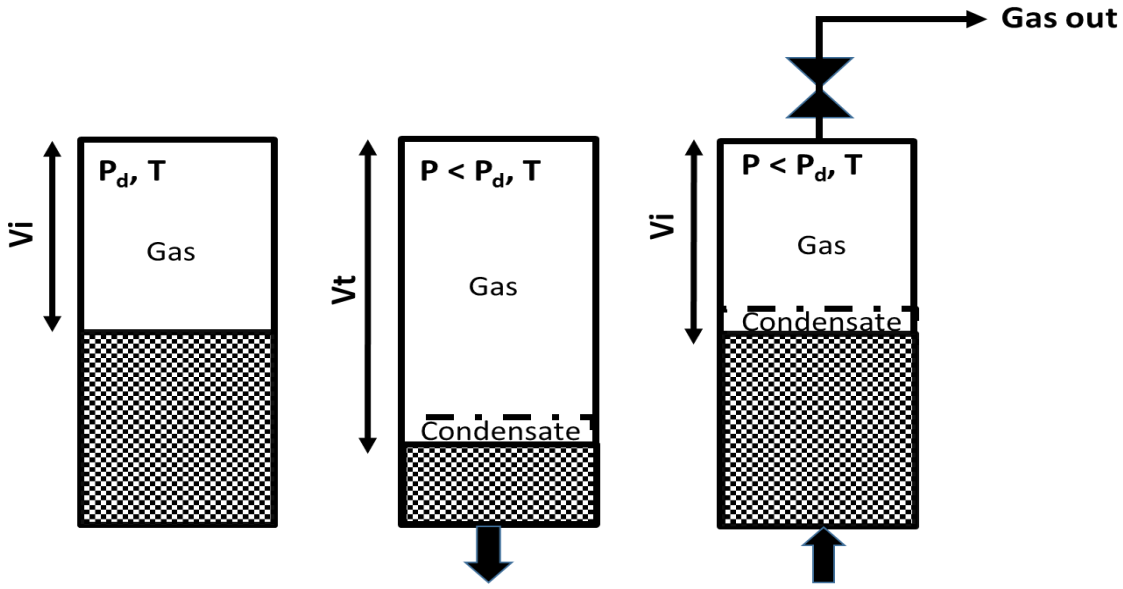


Figure 2.16: Schematic representation of a constant-volume depletion test (Tarek, 2007)

During the stages of pressure depletion, a second phase retrograde liquid is formed (condensate). The fluid is then brought to equilibrium and the retrograde (V_L) and gas volume (V_g) measured. The retrograde volume is recorded as a percentage of initial volume (V_i) which basically represents retrograde liquid saturation (S_L) where $S_L = 100* (V_L/ V_i)$. Mercury is then injected into the PVT cell at constant pressure and an equivalent volume of gas removed simultaneously. When the initial volume (Vi) is reached, the mercury injection is stopped as shown in Figure 2.16. This step mimics a reservoir producing only gas with an immobile retrograde liquid remaining in the reservoir.

The composition of the remove gas is then analysed and its volume at standard condition recorded. The moles of gas produced, gas compressibility and the 2-phase compressibility factor are also calculated.

This steps are repeated several times until a minimum test pressure is achieved, after which the quantity of gas and retrograde liquid remaining in the PVT cell are recorded.

2.9.3 Special laboratory PVT tests

These tests are carried out for very specific applications. Slim tube experiment and swelling test may be carried out for gas injection enhanced oil recovery such as miscible gas injection or gas cycling scheme.

2.9.3.1 Slim tube experiment

This involves the injection of miscible gas in reservoir oil. Gases such as nitrogen, carbon dioxide or natural gas are often injected into the reservoir during enhanced oil recovery (EOR) of depleted oil wells (Tarek, 2006). The miscibility of these gases in the oil favours EOR which implies that the gas and oil form one phase independent of mixing ratio. Miscibility in reservoir usually occurs at the gas-oil front or in between and allows for complete displacement of reservoir oil.

In situations where gas is not completely soluble in the oil, gas break out occurs. This is when some of the insoluble gas forms the gas phase of a higher mobility compared to the oil. This then leads to the subsequent production of the injected gas also knows as gas cycling through the reservoir (Pederson and Christenson, 2007).

Slim tube is a one-dimensional model reservoir, with a narrow tube packed with sand or glass beads with a length between 5 to 40 m as shown in Figure 2.17.

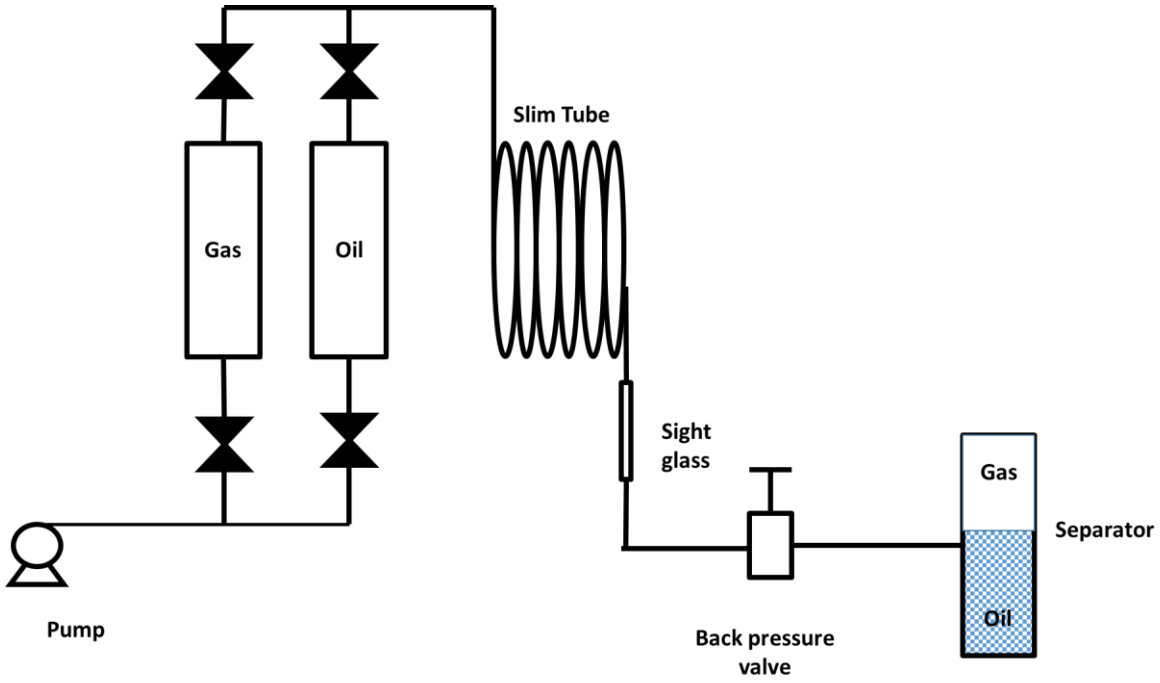


Figure 2.17: Schematic Diagram of a Slim Tube apparatus (Tarek, 2007)

The Slim tube experimental procedure involves the tube initially saturated with oil at reservoir temperature above the bubble point pressure. The oil is then displaced by an injectant gas forced through the inlet and the pressure controlled by the back pressure valve (Pederson and Christenson,

2007). The pressure drop is significantly low, therefore the entire displacement process considered a constant pressure process. The effluent of the tube is flashed at standard conditions and the rate of recovery, density and composition of the products measured (Danesh, 1998). The gas breakout is monitored by measuring the gas to oil ratio and/or the effluent gas composition (Tarek, 2006).

2.9.3.2 Swelling tests

Swelling tests are usually conducted on reservoirs that are to be depleted by gas injection or dry gas cycling scheme. This is started on a reservoir oil, at saturation pressure in a PVT cell operated at reservoir temperature. A known amount of gas is injected into the cell containing the oil (Tarek, 2006). The pressure is then increase at constant temperature until all the injected gas is dissolved in the reservoir oil. The pressure and the swollen volume of the dissolved gas in oil are then recorded. More gas is injected and pressure increased until all the gas goes into solution with the oil as shown in Figure 2.18. The procedure is repeated for a number of stages and pressure and volume recorded correspondingly (Pederson and Christenson, 2007).

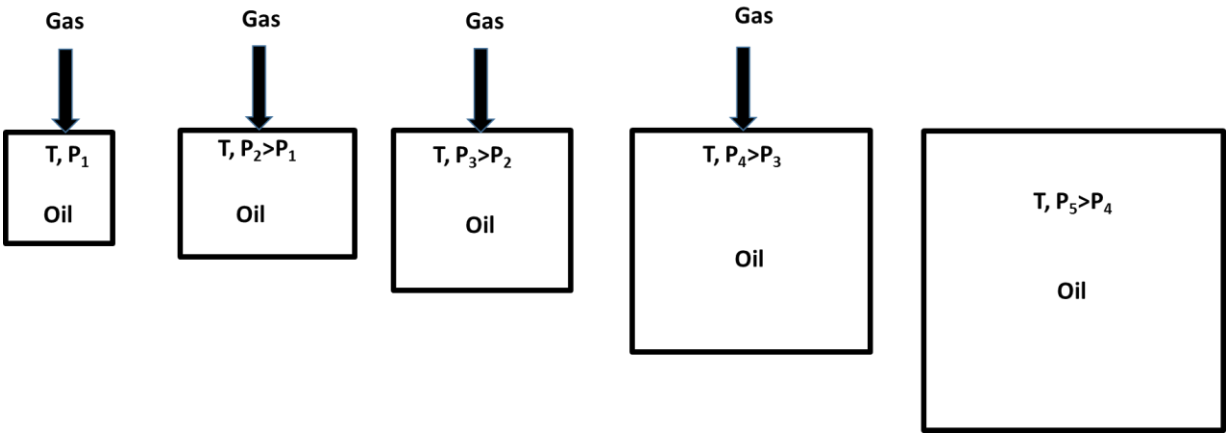


Figure 2.18: Schematic Representation of Swelling Test (Tarek, 2007)

Swelling tests are generally carried out to investigate gas injection operations in a reservoir. The dissolution of the gas in the oil causes swelling of the oil and the saturation point of the oil also

increases. This increase in volume and saturation pressure are very important factors in the process of gas injection for Enhanced oil recovery (Andrei *et al*., 2010). Data generated from swelling tests include the relationship between saturation pressure and amount in volume of gas injected, the volume of saturated fluid mixture compared to the volume of the original saturate fluid (Pederson and Christenson, 2007).

CHAPTER THREE

3.0 MATERIALS AND METHODS

3.1 Materials and Equipment

This section provided the list, details and manufacturers of material and equipment used in the course of the study. These are tabulated in Tables 3.1 and 3.2 respectively.

3.1.1 Materials and utilities

Table 3.1 List of materials and utilities used in the enhanced oil recovery study

S/no	Materials/Utilities	Details	Manufacturer/Source
1	Crude Oils	Offshore Newfoundland, Canada	Offshore Newfoundland, Canada
2	Mine tailings	Sulfide mineral tailings	Voisey Bay tailings site, Newfoundland and Labrador
3	High Pressure gold pans and lid	Pressure resistance Crucible, M20. 081reu02.	Swiss Institute for the Promotion of Safety and Security.
4	Spherical Bomb test cells	ARCTC-SS316L-L-C-E; thickness of 0.5 mm, stem 3.17 mm; burst pressure of 425 bar and mass of 8.6g.	Thermal Hazard Technology, UK
5	Epoxy Resin	Epoxy tooling resin	ARYA Chem, Canada
6	Nut and Ferrule sets	Nut and Ferrule (1/4, 1/8, 1/16) with adaptors.	Swagelok, Atlantic Valve & Fitting Co. New Brunswick, Canada.
7	Compressed medical air	CO2-103L-295-500; 6.32 m^3	Air Liquid, Canada Inc.
8	Distilled water	Distilled water	Chemistry Department. Memorial University of Newfoundland.
9	Nitrogen gas	SPG-NIT1AL44, Size 6.32 m^3	Air Liquide Canada Inc.

3.1.2 Equipment

The following Equipment listed in Table 3.2 were used in the course of this study.

Table 3.2 List of Equipment used in the enhanced oil recovery study.

S/no	Equipment	Details	Manufacturer/Model
1	Viscometer	Digital viscometer	Brokfield Ultra viscometer, Model DV-E
2	Differential Scanning calorimeter	With Gas controller GC 2000	Mettler Toledo, Model no 822e
3	Accelerating rate calorimeter	Designed to Dow patents 1980 and 1984.	Thermal Hazard Technology, UK
4	Mineral liberation analyzer	MLA software developed by Julius Kruttschnitt mineral research group	FEM MLA 650 F
5	Rotary micro riffler	Aluminum bowl, 120 cm^3 capacity Spinning riffler	Quantachrome Cooporation, Europe
6	PVTsim 19.0 software	Reservoir simulation software	Calsep PVTsim

3.2 Experimental Procedure

This section details the series of methods employed to achieve desired results in the study of air injection for the enhancement of improved oil recovery.

Physical properties of the oils were first determined using a density bottle and a rheometer. Thermal properties were then studied using thermal instruments such as the differential scanning calorimetry (DSC) and the accelerating rate calorimeter (ARC), correlations were also used to determine the API gravity and the specific heat capacity of the oils. Minerals analysed using a Mineral Liberation Analyser (MLA) were used to study their effect on crude oil oxidation.

3.2.1 Viscosity determination

The Brookfield Ultra Viscometers / Rheometers was used to determine the viscosity of the crude oils. It was turned on, leveled and auto-zeroed. The level was adjusted using the three feet on the bottom of the base and confirmed using the bubble on the top of the head. The crude oil sample to be measured was poured into the cylindrical holding container. The standard spindles supplied with the viscometer was then used with a 600 ml low form Griffin beaker. The water bath was then connected and maintained at 25^{o}C and viscosity reading taken for all the samples. Viscosity was calculated from the plot of shear stress (dynes/cm^{2}) vs shear rate (1/s), where the slope of the proportional line is the viscosity.

3.2.2 Specific heat capacity determination

Heat capacity of the crude oils were determined using the correlation from Manning and Thompson (Manning, 1995). Equation 3.1 expresses the Manning and Thompson correlation.

$$C_p = \left(2 * 10^{-3} * T - 1.429\right) * SG + \left(2.678 * 10^{-3}\right) * T + 3.049 \quad (3.1)$$

where;

Cp = specific heat capacity (kJ/ kg. ^{o}C)

T = Temperature (^{o}C)

SG = Specific gravity of oil at 15^{o}C.

3.2.3 Differential scanning calorimetry (DSC) tests

Mettler Toledo with gas controller GC2000 as shown in plate 3.1 was used to carry out Dynamic DSC on eight (8) crude oil samples. Nitrogen gas flow rate of 200 ml/min was used for the tests. An amount of 5 ± 0.5 mg of oil sample was enclosed in a high pressure gold pan and ramped at

10, 8, 4 and 2 K/min after pre-calibration of the instrument. Each test was conducted at least twice to ascertain good experimental reproducibility. It was ensured that the atmosphere was dry and flow of nitrogen gas was maintained to eliminate air.

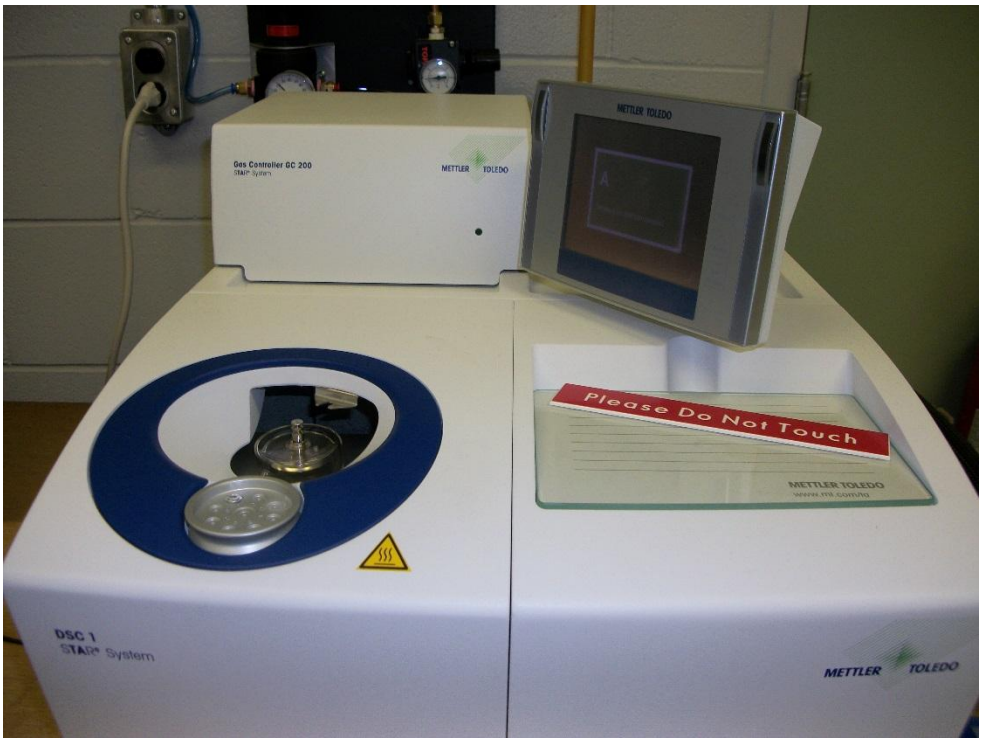


Plate 3.1: DSC system by Mettler Toledo with gas controller GC 2000

3.2.4 Accelerating rate calorimeter (ARC) tests

Samples of crude oil (5 $\pm$ 0.5 g) with mine tailings were examined using an ARC. The sample was loaded in an ARC stainless steel test cell. The cell containing the sample was fixed to the top heater before being connected to the temperature thermocouple and the pneumatic pressure line. The setup was now lowered into the cylindrical heater and balanced to a stable position before the ARC door was locked. The ARC was then powered on, with sample and test cell information imputed and the calibration file uploaded to a "Heat-wait-seek" algorithm which is the main operational mode of the ARC system as shown in Figure 3.1. The sample's temperature was

raised (heat) to a set temperature (T) before proceeding to the (wait) period (time t = 15 minutes) where thermal equilibrium was attained (i.e. the difference between temperature of the test cell (bomb) and its surrounding tends to zero). The ARC then proceeded to the seek mode where if the self-heat value exceeds a set threshold (dT/dt = 0.02 ^{o}C/min) an exotherm mode is activated until the self-heat falls below the threshold. If the self- heat falls below the threshold (Tonset), the sequence of "heat-wait-seek" is re-started for the next heat step, If not, the test goes to cool mode when the end temperature reaches the final experiment temperature (T_f). After the cool mode, the test goes idle and stops. The test data was then exported for analysis when the end temperature was reached.

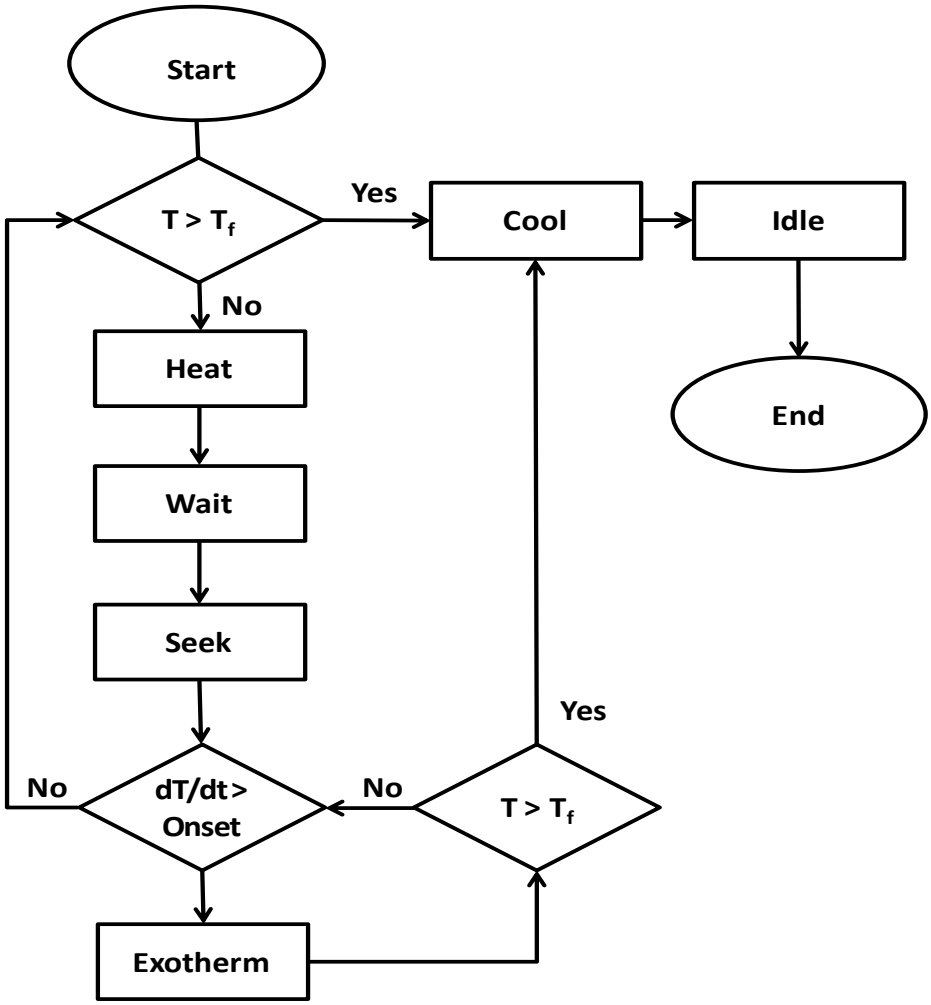


Figure 3.1: The Algorithm Logic of Heat-Wait-Seek Operation in ARC

3.2.5 Mine tailing preparation

Tailings sourced from Newfoundland, Labrador, which were stored under water, were first sampled by drilling a cylindrical core from the sample. The collected sample was then dried in air at a temperature of 25 ^{o}C in a fume hood. The dried sample was grounded using a mortar and ceramic pestle before being taken to a riffling machine (Plate 3.2).



Plate 3.2: The Rotary Micro Riffler

The Rotary Micro Riffler which has eight (8) collection points, and each collection points was used for sampling. The collections at these various points represented aliquots of the parent sample. Aliquots of 10 - 20 g of the sample was then mixed with pure graphite powder to prevent particle cohesion and embedded in round mould epoxy blocks to harden as shown in Plate 3.3. The diameter of the round blocks were 30 mm each.



Plate 3.3: Tailing Samples in round mould prepared for Mineral Liberation Analysis

A cross section of the epoxy block was then cut from the mould, and the surface of the analytical surface was then grounded and polished in several steps until the demands of electron-beam imaging and analysis were matched. The polished samples were then cleaned and coated with carbon and made ready for the Mineral analyzer.

3.2.6 Mineral liberation analyser (MLA) for mine tailings studies.

The polished sample as obtained from section 3.2.4 was then taken into the Mineral Liberation Analyzer (MLA) equipment shown in Plate 3.4 for mineral and constituent analysis. The FEI MLA 650F has a state-of the-art automated quantitative mineralogy software which combines a large specimen chamber automated Scanning Electron Microscope (SEM) and multiple Energy Dispersive X-ray detectors. It uses a technique which relies on backscattered electron imaging (BEI), to measure the average atomic number which helps in grain boundary discrimination. MLA software developed at Julius Kruttschnitt Mineral Research Centre (JKTech) was used to determine its constituents.

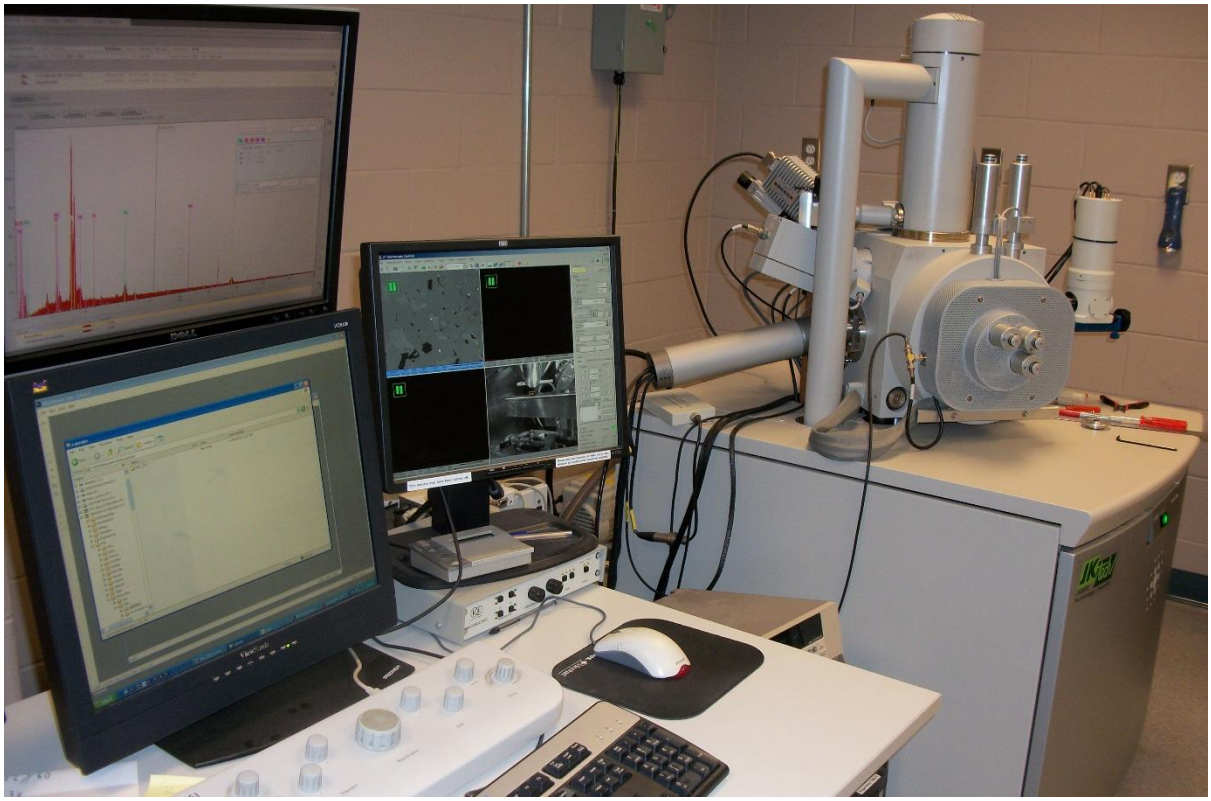


Plate 3.4: The FEI Mineral Liberation Analyzer (MLA)

3.2.7: PVTSim 19 and design expert software simulation for oil recovery analysis

Crude oil pressure-volume-temperature (PVT) properties were obtained from a crude oil databank (Jaubert *et al*., 2002). This was matched with several Nigerian oils (Bonga, Escravos and Brass River) with respect to specific gravity and sulphur content. Corresponding experiments such as isothermal constant mass expansion and isothermal differential vaporization obtained from Jaubert *et al*., (2002) were regressed and tuned in the PVTsim 19 software. The regression with high fit and low deviation was saved. Design expert software was used to generate experimental runs for 4 factor and 1 response analysis. The factors included reservoir temperature, pressure, sulphur content and amount of injected O_2 (Oldenburg *et al*, 2001 and Evamy *et al*., 1978). Oxygen concentration used varied from 0% to 100% while oil recovery generated from the simulated slim tube experiment was recorded as the response. This experimental runs obtained from the design expert were fed into the PVTsim for the slim tube experiment. The recovery obtained from the experiment was re-inputted into the design expert for statistical analysis.

CHAPTER FOUR

4.0 RESULTS AND DISCUSSION

4.1 Properties of the Crude oils

Table 4.1 shows the viscosity, API and specific heat capacity properties of the analysed crude oil samples.

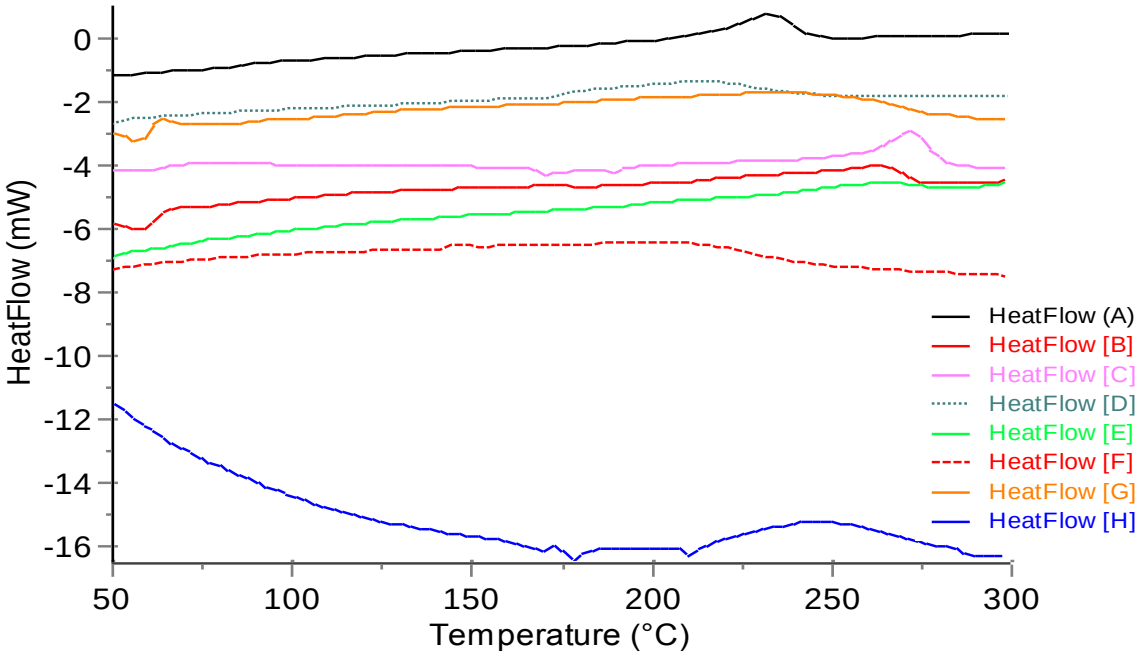
Table 4.1 Property of the crude oil samples

Crude Oil Sample	Viscosity (cP)	API gravity	Specific Heat Capacity (kJ/kg.K)
A	5.44	46.96	1.888
B	7.90	44.06	1.926
C	4.99	30.21	1.910
D	25.70	40.02	1.833
E	11.90	41.91	1.898
F	8.18	38.98	1.882
G	24.90	32.46	1.846
H	10.11	46.91	1.889

The samples have their API gravity greater than 10 and less than 48 which corresponds to a class of oil identified as light crude oil (Danesh, 1998). The oils viscosity also ranged in the zone of light, non-viscous oil while the oil specific heat capacity ranged from 1.83 kJ/kg.K to 1.93 kJ/kg.K.

4.2 Thermal Behaviours of Crude Oils using DSC

Thermal behaviour of all the reservoir crude oils was first carried out in the DSC ramped at 10 K/min and the obtained DSC thermograms are depicted in Figure 4.1. Three (3) of the samples (A, B, and C) showed clear peaks of oxidation between 130°C and 300°C, which is an indication that they have measurable exothermic signals. The temperature range between the onset and the endset falls in the low temperature oxidation zone and makes them a probable candidate for high pressure air Injection (HPAI) EOR (Kok *et al*., 2004; Li *et al* 2005; Kok, 2008).



A

Figure 4.1: DSC thermograms of crude oil samples at 10K/min (Refer to Table 4.1 for properties of samples A-H).

Therefore, the DSC thermograms of the samples that had measurable exothermic signals were then further ramped at 8, 4 and 2 K/min and at least three (3) best thermograms were saved and exported to

the AKTS and NETZSCH software. These were then used for iso-conversional and model based kinetics simulations as presented in the next Sections.

4.3 Thermal Kinetics of DSC thermograms of crude Oils

Several models are available to determine kinetic parameters such as activation energies for reactions. This includes Arrhenius, Ozawa–Flynn–Wall, Kissinger–Akahira–Sunose, Friedman e.t.c. (Drici and Vossoughi, 1985; Kok, 1997; Kok *et al*., 2004; Iliyas *et al.*, 2011; Gundogar and Kok, 2014; Li *et al*., 2014). In this study, iso-conversional method by Friedman due to its applicability to autocatalytic reaction and higher reliability when compared to the Ozawa-Flynn-Wall analysis or the nth order model (Budrugeac, 2005).

Figures 4.2 – 4.5 presents the reaction progress as a function of temperature for Samples A, B, C and A* (Sample A* is sample at 10% water saturation). The figures were obtained using the advanced thermo-kinetic software (AKTS). The oxidation reaction follows an autocatalytic behaviour similar to those illustrated in Figure 2.6. The reaction curves were then further analysed in the AKTS software for iso-conversional and model based simulations.

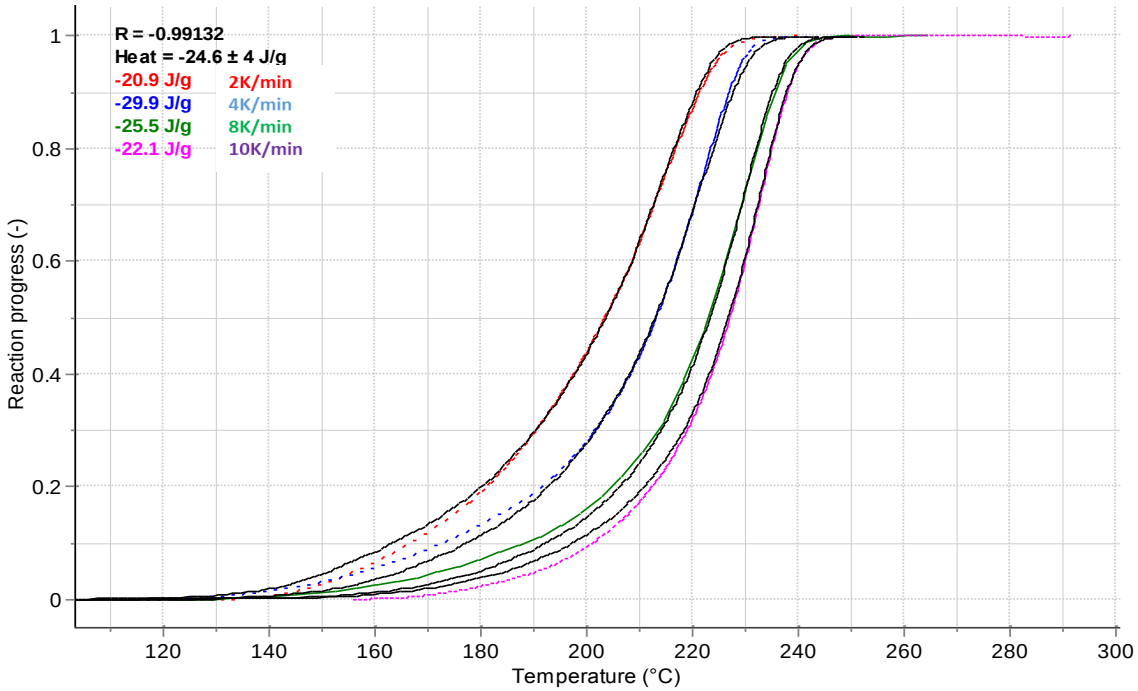


Figure 4.2: Reaction Progress as a function of Temperature for Sample A

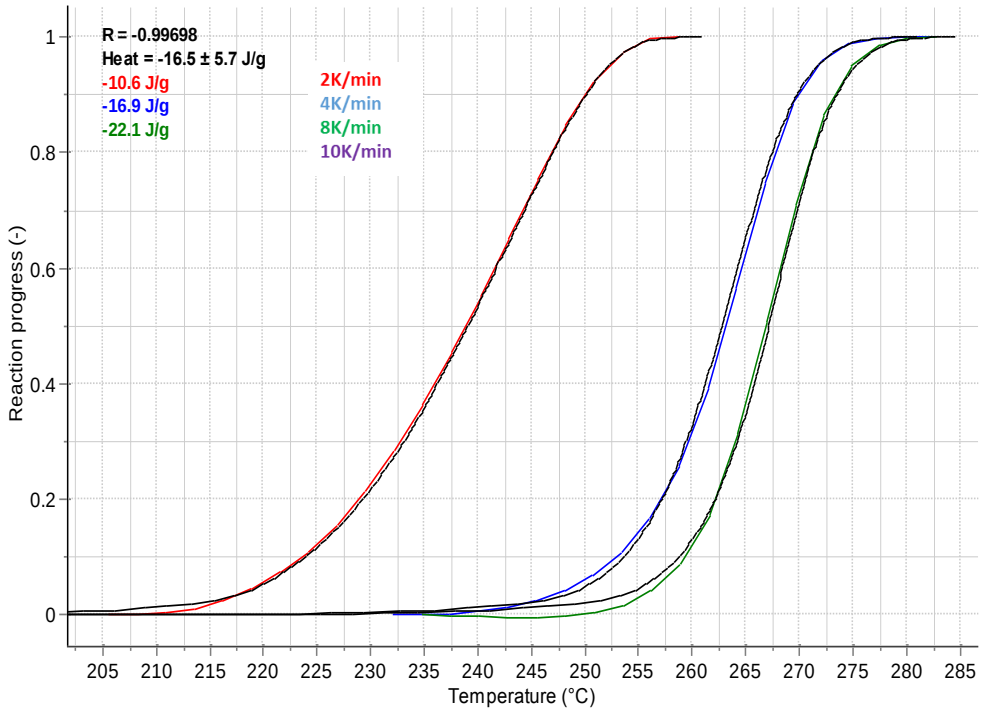


Figure 4.3: Reaction Progress as a Function of Temperature for Sample B

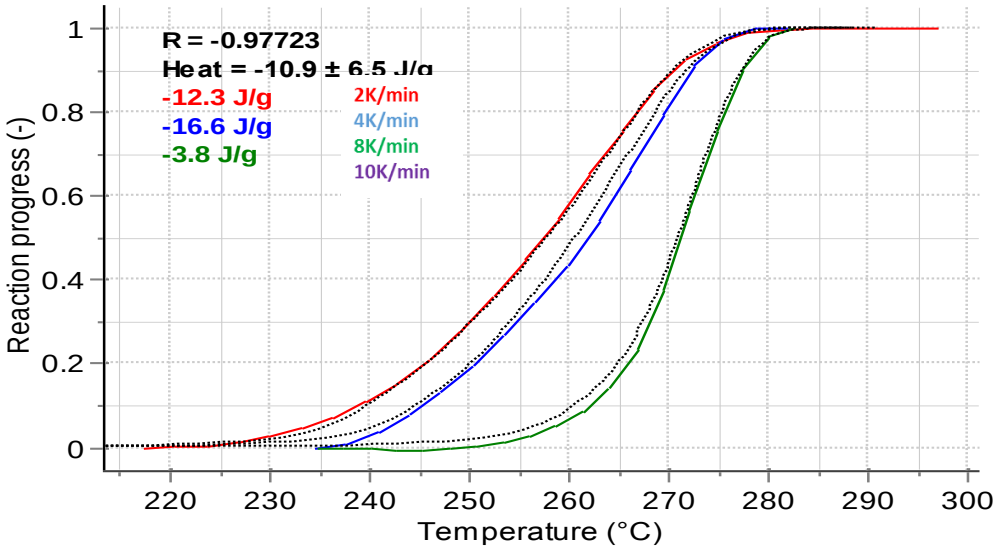


Figure 4.4: Reaction Progress as a Function of Temperature for Sample C

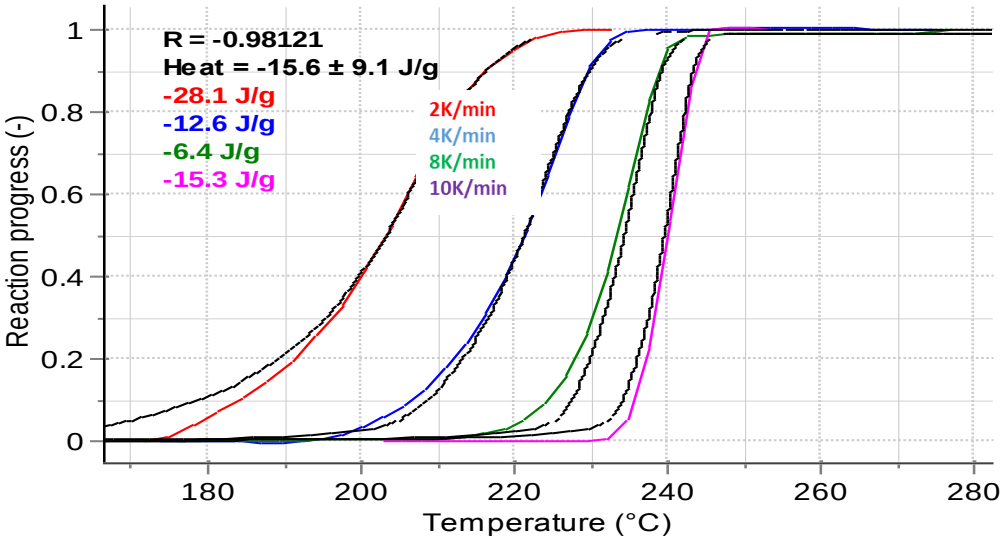


Figure 4.5: Reaction progress as a Function of Temperature for Sample A*

Thermograms (of the different ramp rates) of each of the samples were then modelled to generate enthalpy of the oxidation reaction. These simulations involved processes such as slope correction, curve

cutting, and a tangential sigmoid bases line carried out to generate high value for regression (r) correlation. This was to ensure high reliabiltity of the results obtained. Sample A had the highest average enthalpy change of -24.6 ± 4 J/g while samples B and C had -16.5 ± 5.7 J/g and -10.9 ± 6.5 respecively. Sample A saturated with 10% water (A*) had a drop in enthalpy change (-15.6 ± 9.1 J/g) and also a shift in onset temperature. Chen *et al.* (2012), reported a very high oxidation zones of 424 °C to 755 °C for vacuum residue. A very high enthalpies of 470 J/g to 1222 J/g was also reported for the reaction. This observation was due to high temperature oxidation of oils where cracking and coke deposition occurs (Kok *et al*., 1997; Kok and Gundogar, 2013). However, the low temperature oxidation reaction for these crude oil is enough to cause significant drop in oil viscosity thereby favouring flow of oil (Sarathi, 1998).

Figure 4.6 – 4.9 presents the oxidation reaction rate of the crude oils as a function of temperature at various ramp rates. It is vividly shown that the onset, peak and endset temperatures of the oxidation reaction at various ramp rates as expected, shifted to the right as ramp temperature increased.

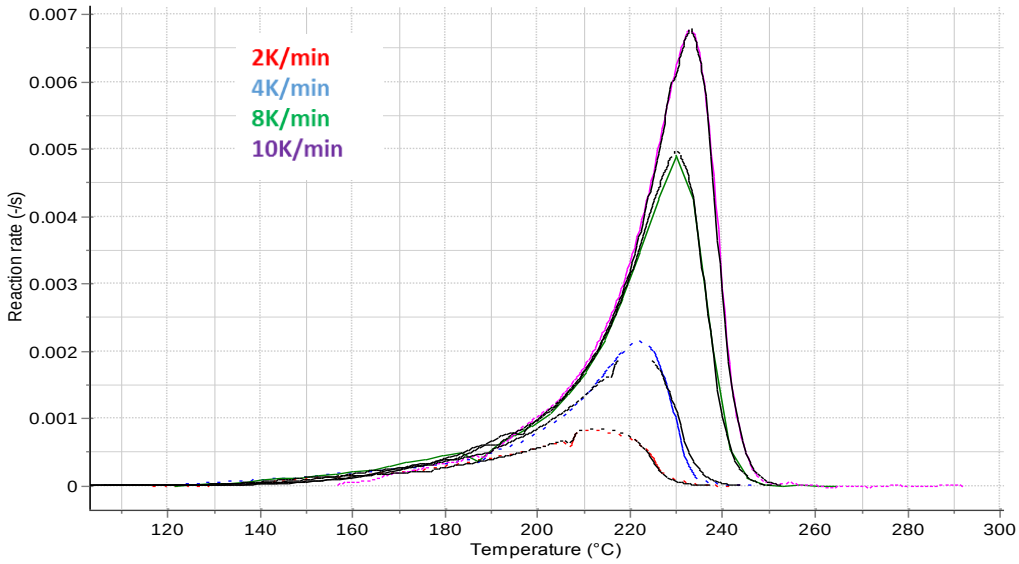


Figure 4.6: Reaction rate for Sample A at different ramp rates.

Sample A at 2 K/min ramp rate can be seen to have an onset at 120 ^{o}C through peak of 210 ^{o}C and an end set temperature of 240 ^{o}C. At a higher ramp rate of 4 K/min, it had onset, peak and endset at 120 ^{o}C, 220 ^{o}C and 240 ^{o}C respectively. At 8K/min it was 120 ^{o}C, 230 ^{o}C and 244 ^{o}C respectively and 120 ^{o}C, 235 ^{o}C and 250 ^{o}C respectively at 10K/min. The average onset, peak and endset temperatures within this reaction zone (taking the average at 2 K/min, 4 K/min, 8 K/min and 10 K/min) is 120 ^{o}C for onset temperature, 223.75 ^{o}C for peak temperature and 243.5 ^{o}C for endset temperature.

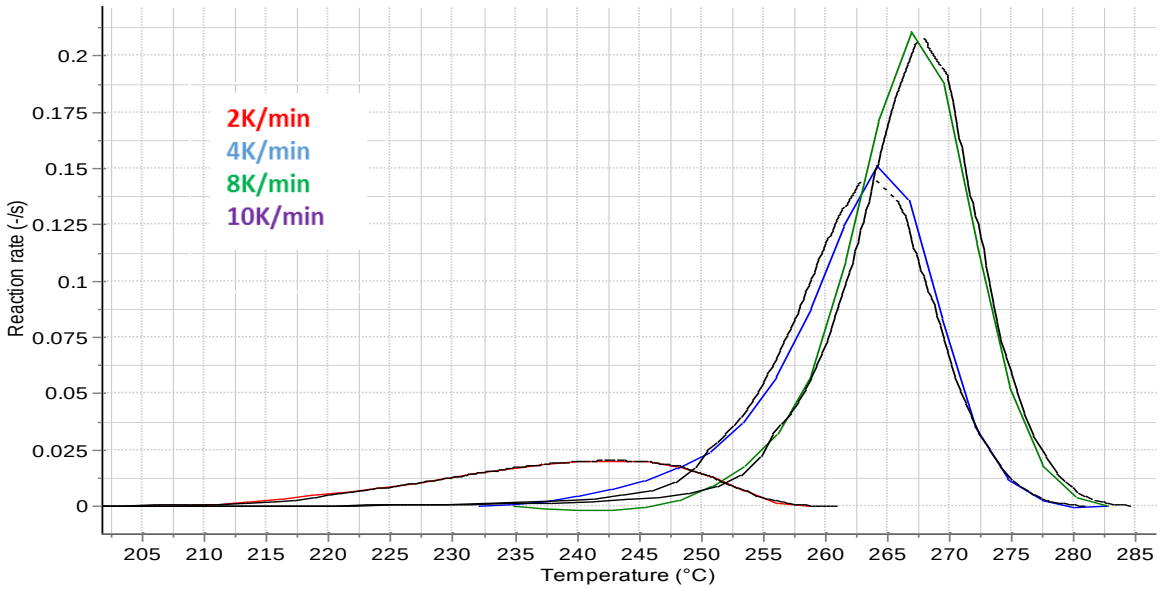


Figure 4.7: Reaction rate for Sample B at different ramp rates.

Figure 4.7 shows the reaction rate for sample B similar to sample A with respect to shift in reaction zones as the ramp rate is raised. The average onset, peak and endset are 215 ^{o}C, 245 ^{o}C and 260 ^{o}C respectively.

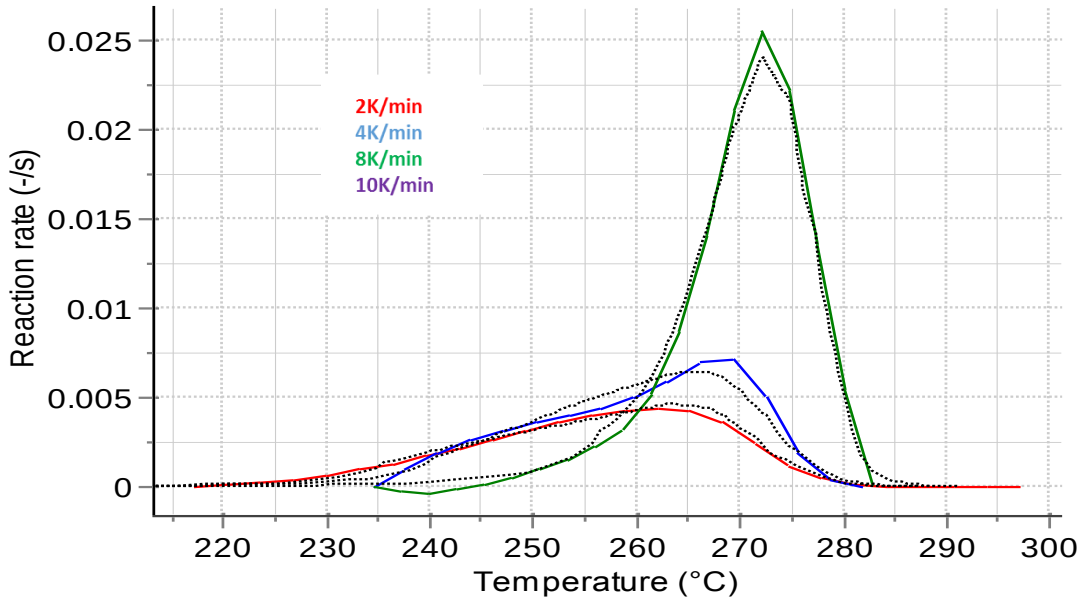


Figure 4.8: Reaction rate for Sample C at different ramp rates.

Figure 4.8 shows the avaerage temperature zone for sample C. The average onset peak and, endset is calculated to be 231.67 ^{o}C, 268 ^{o}C and 281 ^{o}C. This sample had a higher temperture oxidation zone compared to samples A and B, as a result of its low API and probably more asphaltene content (Kok and Gundogar, 2013).

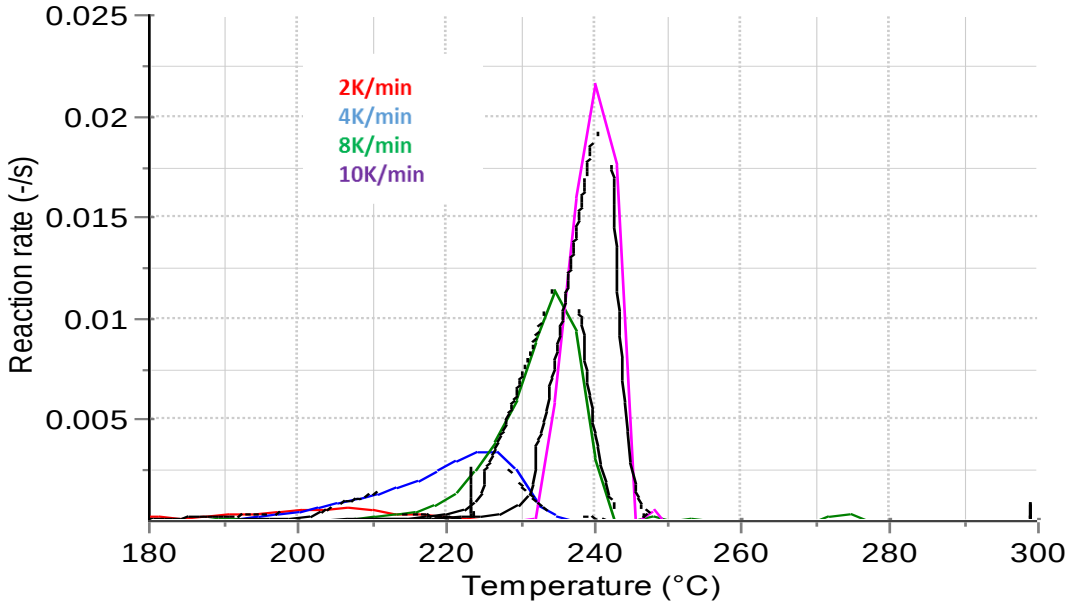


Figure 4.9: Reaction rate for Sample A* at different ramp rates.

Figure 4.9 shows the reaction rate of Sample A* at different ramp rates. It was observed that the temperature zone had a shift to 206 ^{o}C, 21.67 ^{o}C and 240.67 ^{o}C at onset, peak and endset respectively whereas Sample A had 120 ^{o}C for onset temperature, 223.75 ^{o}C for peak temperature and 241 ^{o}C respectively. This is evident in comparing Sample A and Sample A*. The onset oxidation temperature of Sample A* was delayed by about 86^{o}C and its enthalpy reduced by 9 J/g. This implies that water content in Sample A* crude oil affected the oxidation and thermal properties of the crude oil. Therefore, a mature reservoir with high water-cut would be less favourable for HPAI compared to reservoirs with lower water cut even though it has its oxidation temperature zones within the limits.

All of the the three (3) oil samples have their onset, peak and endset temperature within the range of 130 – 290 ^{o}C which are within the low temperature oxidation regimes confirming the suitability for samples for HPAI (Li *et al*., 2005; Kok, 2008).

Figures 4.10 to 4.13 shows the activation energy of the samples based on the ASTM E-698. This was obtained using the iso-conversional method**.**

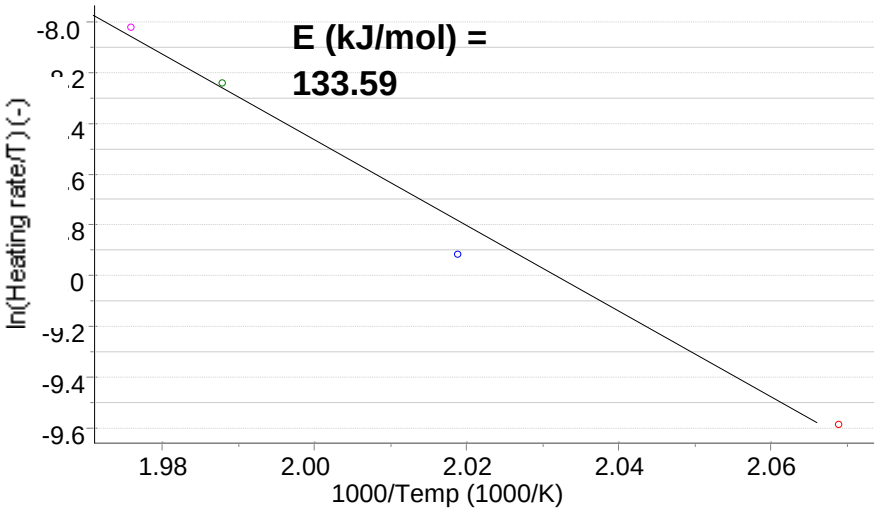


Figure 4.10: Apparent Activation Energy of Sample A based on ASTM E-698

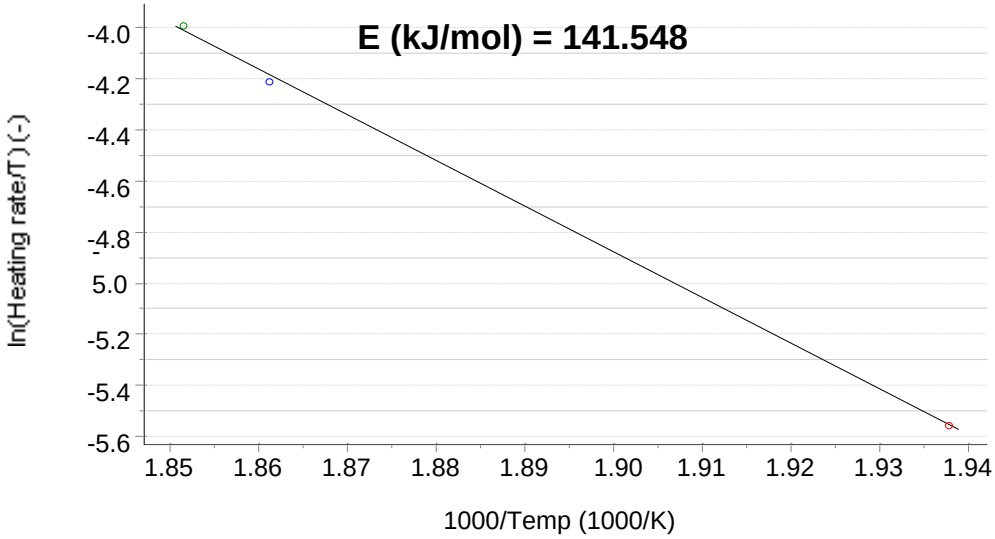


Figure 4.11: Apparent Activation Energy of Sample B based on ASTM E-698

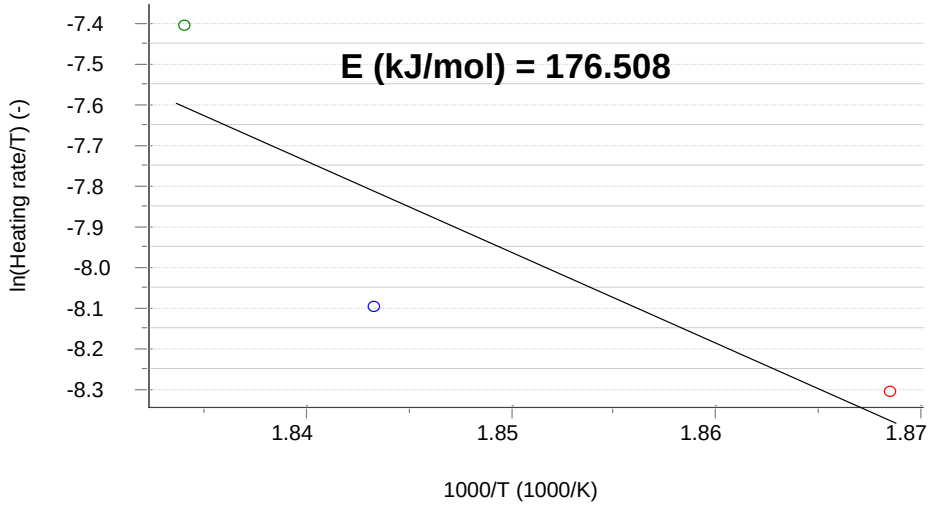


Figure 4.12: Apparent Activation Energy of Sample C based on ASTM E-698

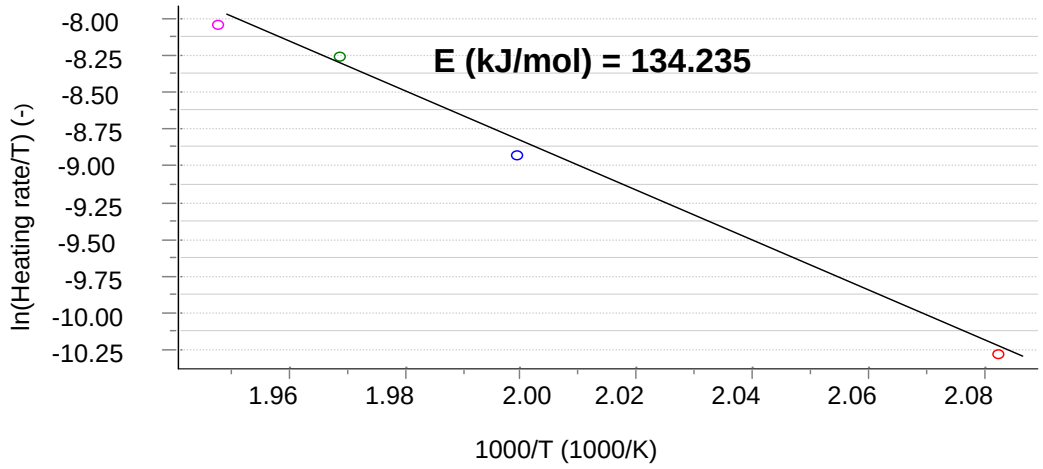


Figure 4.13: Apparent Activation Energy of sample A* based on ASTM E-698

Sample A with the lowest onset temperature had the lowest activation energy while Samples B and C which are of lower API gravity and a delayed onset. This behaviour can be attributed to higher molecular weight paraffin and / or more polycyclic aromatic contents in the heavier crude samples (Abu-Khamsin, 2003; Li *et al*., 2004). These values of activation energies were observed to be close to that obtained for Raman, Bulgurdy and Huntington beach reservoirs located in Turkey (Kok, 1997). Generally, light oil

undergo low temperature oxidation and the activation energies of the low temperature oxidation zones have been obsevred to be lower than the activation energies of high temperature oxidation zones (Kok *et al*., 1997; Kok, 2012; Li *et al*., 2014).

Figures 4.14 to 4.17 show the behaviour of activation energy and pre-exponential factor as the oxidation reaction progresses using the Friedman's differential iso-Conversional method.

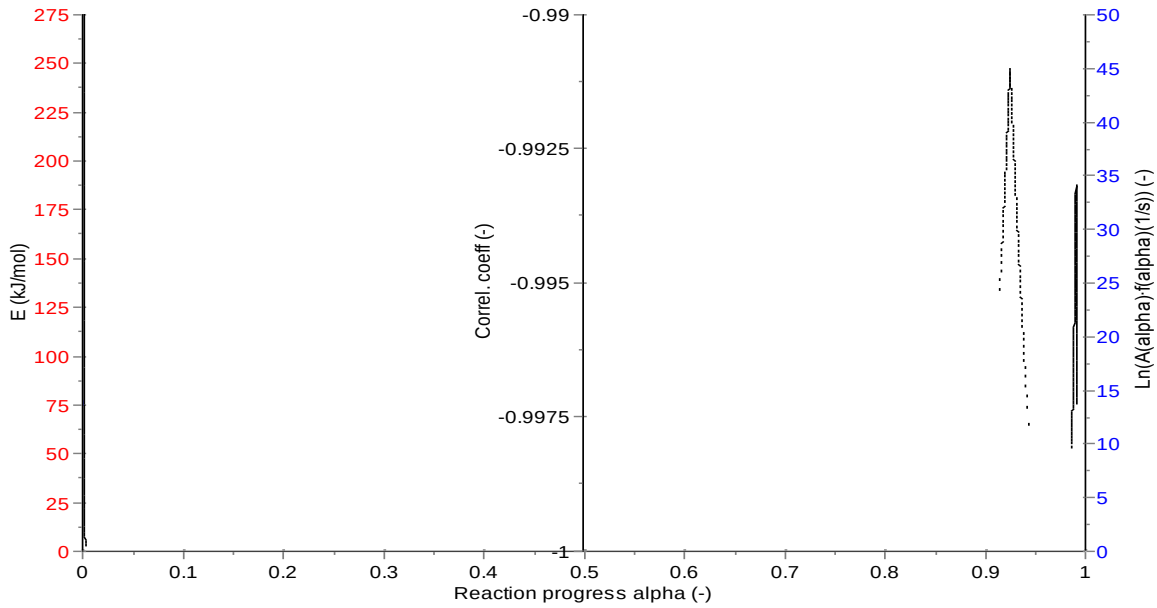


Figure 4.14: Activation energy and pre-exponential factor as a function of reaction progress for Sample A

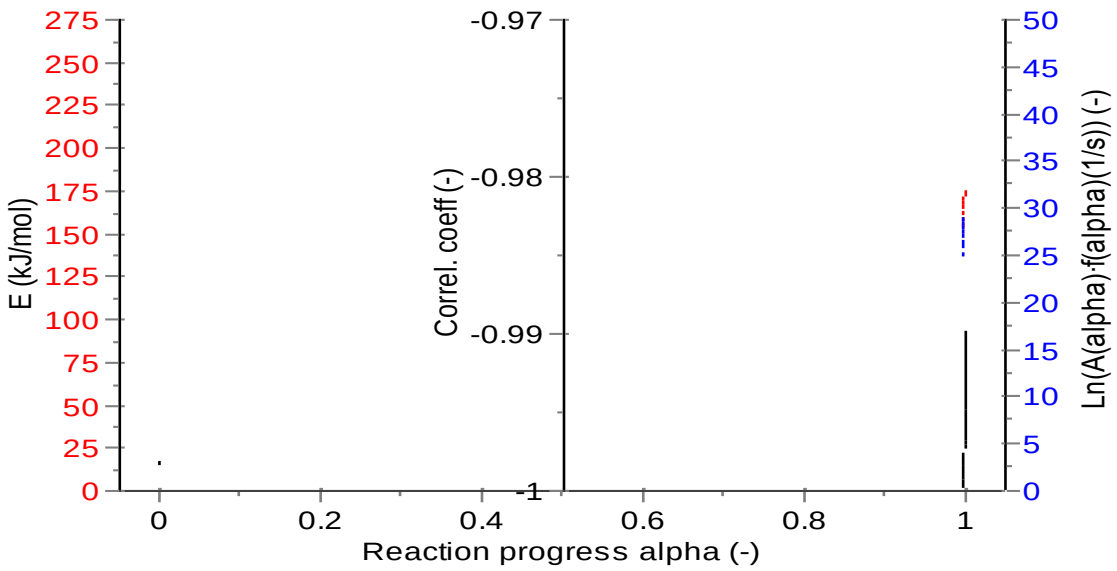


Figure 4.15: Activation energy and pre-exponential factor as a function of reaction progress for Sample B

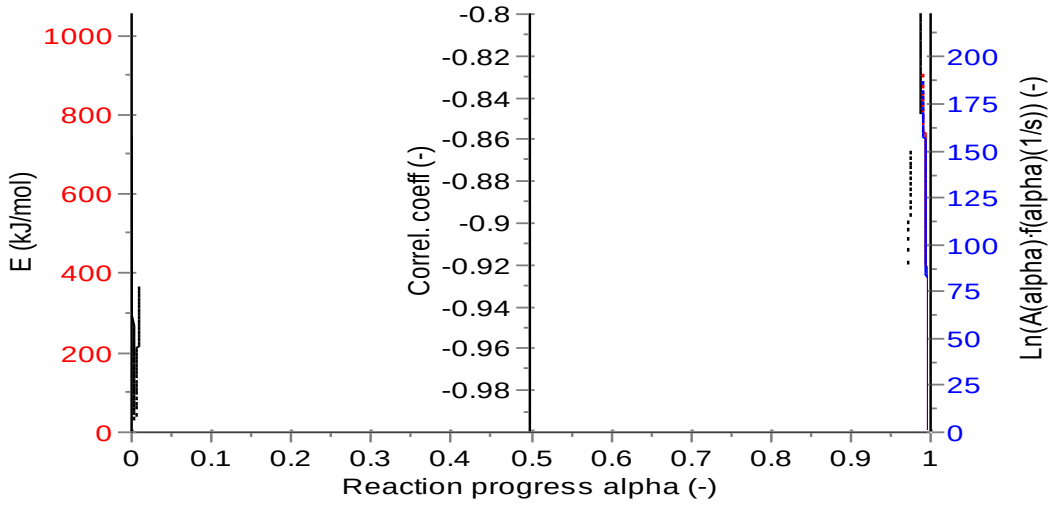


Figure 4.16: Activation energy and pre-exponential factor as a function of reaction progress for Sample C

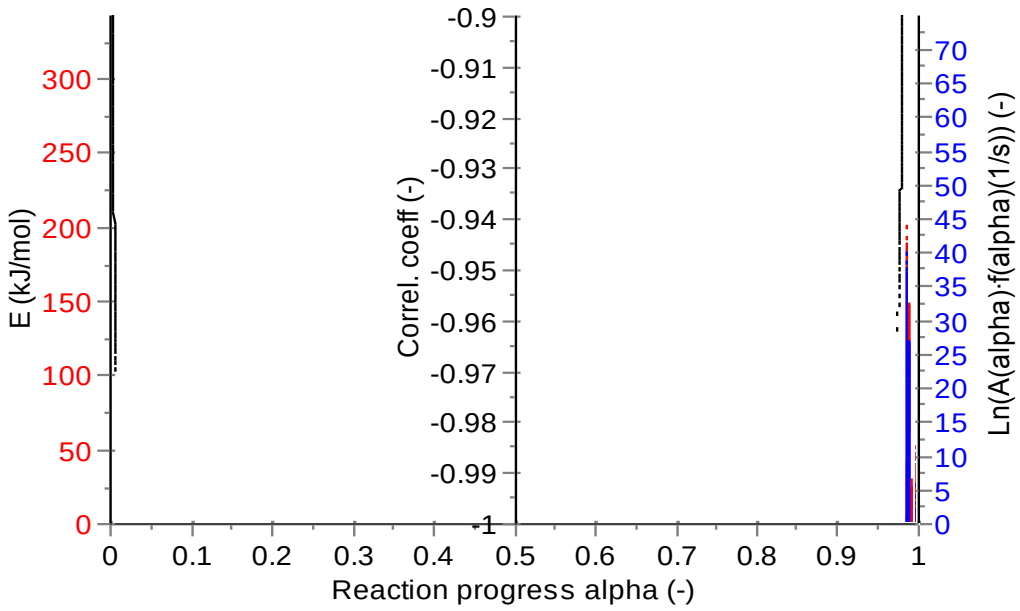


Figure 4.17: Activation energy and pre-exponential factor as a function of reaction progress for Sample A*

A common observable trend in the study was the increase in the activation energy as the reaction progressed and also the peaks at some points which confirms the complexities in crude oil oxidation reaction. This is an indication that the ASTM method is a simplified form of assumed constant activation energy throughout the reaction (AG-AKTS, 2008). Sample A had peaks at reaction progress of 0.7, 0.90 and 0.95 while only a peak was observed at 0.7 for Sample B and Sample C had a peak at 0.9. Sample A* had at 0.85.

Figure 4.18 shows the nth order kinetic model to compare the experimental and simulated DSC thermograms. Despite the statistical good fit (r^2 = 0.98), the nth order failed to precisely predict the obtained thermogram at 10K/min. The estimated activation energy of sample A obtained from the model based method given by 178.34KJ/mol is over 33.48% larger than the estimated activation energy obtained by the ASTM E-698 as tabulated in Table 4.2. Such a large deviation in the kinetic parameter

estimation could adversely affect the accuracy of field evaluation of high pressure air injection processes (Montes *et al*., 2010; Sheng, 2013).

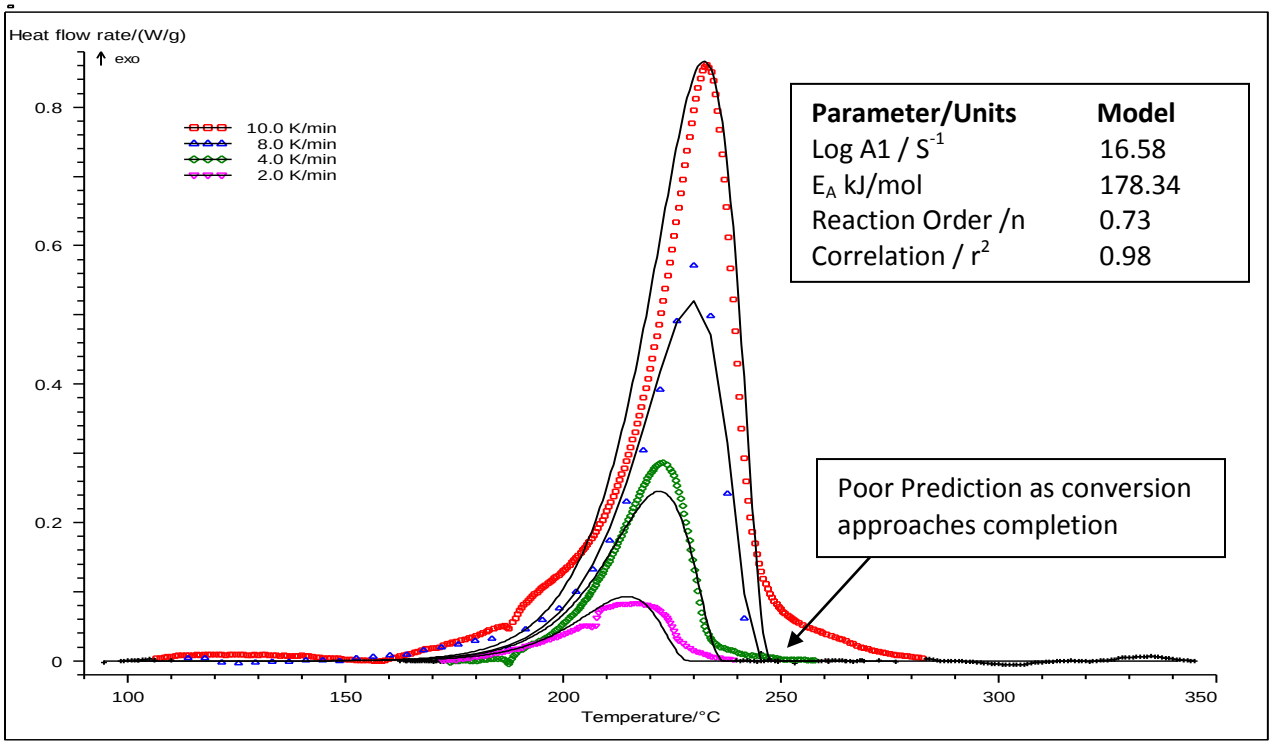


Figure 4.18: Comparison of experimental DSC thermograms with n^{th} order model prediction for sample A

The summary of findings are presented in Table 4.2. The ASTM E-698 and the model based parameter (which assumes a constant activation energy) falls within the range of the Friedman's apparent activation calculations. It was also observed that the lighter crude (low specific gravity or high API gravity) had a lower onset oxidation temperature and higher enthalpy of reaction as shown in Table 4.2. Crude oil sample with water content of 10% saturation had a reduced enthalpy and onset temperature, although its activation energy based on ASTM E-698 calculations was not affected as much as it varied in the Friedman's.

Table 4.2 Summary of physical and thermodynamic properties of the four (4) crude oil samples that showed clear/consistent peaks.

Sample	API	μ	-ΔH	T_{onset}	T_{Peak}	T_{offset}	Friedman's	ASTM	Model based

		(cP)	(J/g)	(°C)	(°C)	(°C)	E_a (kJ/mol)	E_a (kJ/mol)	(kJ/mol
A	46.963	5.44	24.6	140	210	240	50-235	133.6	178.34
B	44.058	7.90	16.5	215	245	260	25-175	141.6	Low R^2
C	30.214	4.99	10.9	220	265	285	100-900	176.5	Low R^2
A*	46.963	5.44	15.6	180	225	240	50-200	134.3	Low R^2

Low R^2: Not recorded due to low correlation coefficient.

4.4 The use of Mine Tailings as catalysts in crude oil oxidation reactions

This section presents the study of how the oxidation behaviours of crude oils was enhanced by the use of mine tailings as catalysts. These findings will encourage further study on how to optimise the catalyst obtained in the tailings for enhanced oil recovery as well as screening studies for candidate reservoirs. The backscattered image of tailings obtained from Newfoundland Labrador, Canada as well as the color code corresponding to its constituents are shown in Appendix A. Pyrrhotite mineral was observed to be the most abundant mineral in the tailings analysed with an amount of 83.51 wt%. The summary of the constituents obtained in the mineral liberation analysis are presented in Table 4.3.

Table 4.3: Mineral and Chemical Constituents of the Tailings

Mineral Constituents	Amount (wt%)	Chemical Elements	Amount (wt%)
Pyrrhotite	83.51	Iron	61.08
Magnetite	10.29	Sulphur	30.06
Plagioclase	2.06	Silicon	1.16
Amphibole	0.68	Aluminum	0.46
Orthopyroxene	0.37	Calcium	0.31
Olivine	0.31	Magnesium	0.31
Pentlandite	0.32	Oxygen	5.35
Others	2.46	Others	1.27
Total	100	Total	100

The pyrrhotite rich mine tailings was found to have high iron and sulphur content of 61.08 wt% and 30.06 wt% respectively. These constituents are known to have self heating properties which can be used to influence oxidation (Qiu and Sego, 2001; Iliyas *et al.*, 2011).

Several studies on mine sites in Nigeria have been conducted over the years. Some mine sites around the north to the east of Nigeria have been noted to contain tailings rich in sulphide associated minerals. The Arufu mining district below the river Pii tributaries in Benue State Nigeria have been found to be rich in lead, zinc and cadmium. It has also been recorded to contain minerals such as biotite, diotite, sandstone, limestone and shale. Most importantly, studies reveal it contained sulphide associated with the Pb-Zn minerals (Adamu and Nganje, 2010). In Abakaliki district of Enyingba, Ebonyi state, there exist sites which contains minerals such as pyrite (trace amount of Pyrite mineral is found in the Newfouldland, Labrador tailings) and chalcopyrite which undergoes oxidation to produce heat (Onyeobi and Imeokparia, 2014). In South-East Nigeria, along river Nyaba, Enugu, the quality of water around the mine drainage was studied and found to be contaminated with flouride, potasium and sulphates of concentrations up to 512 mg/L which exceeds the world health organisation (WHO) standard (Nganje *et al*., 2010). These mineral containing sulphides could be a potential self heating agents which can aid oxidation of crude oil for the purpose of enhanced oil recovery. They can be found at Kaduna, Kogi, Benue, Enugu and Ebonyi states as shown in Figure 4.19.

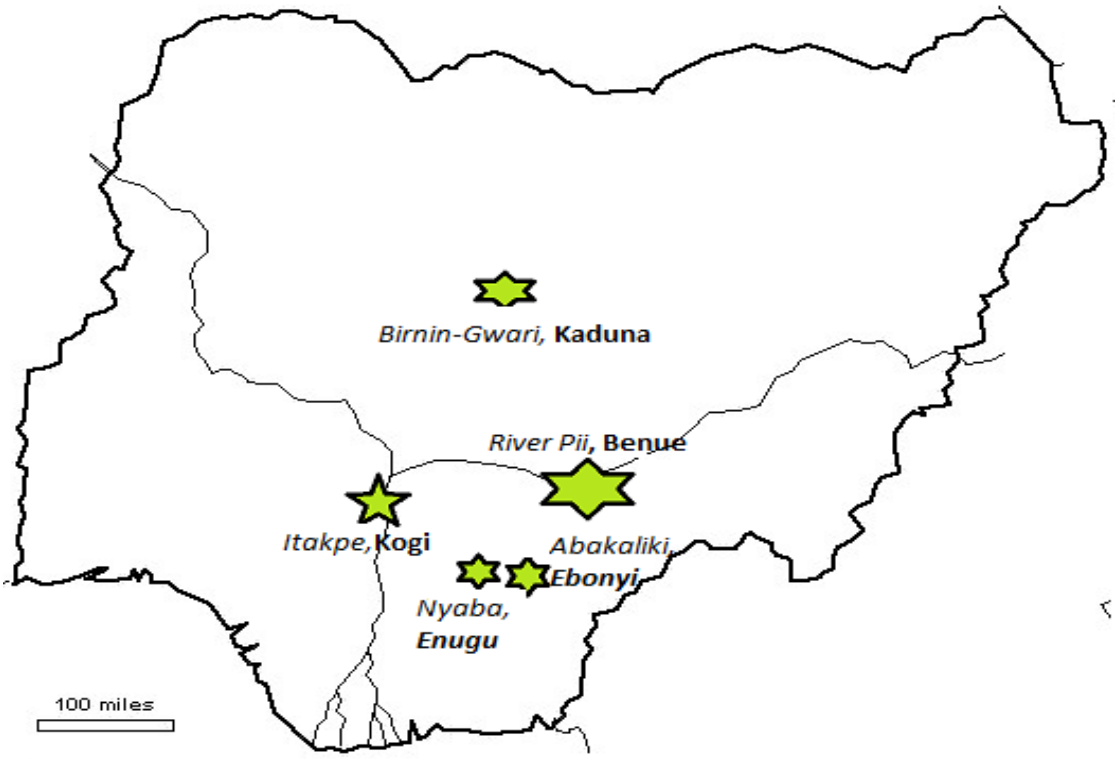


Figure 4.19: Sulphide Associated Mineral sites in Nigeria

In Itakpe, Kogi State, an iron ore processing site has access to rich minerals of haematite, quartz and other several metallic minerals such as iron (III) oxide (Fe_2O_3), iron (II, III) oxide (Fe_3O_4), silicon oxide (SiO_2), alumina (Al_2O_3), calcium oxide (CaO), magnesium oxide (MgO), pottasium and sulphur (Ajaka, 2006). Quartz-gold-sulphide minerals also exist at the Birnin Gwari artisanal gold mining area of the north-western part of Nigeria which is known to have high lead content (Waziri, 2014). Several mines are yet to be explored while around Kaduna, there is a new discovery of mineral rich in high grade Nickel (Ali, 2016; Ezeamalu, 2016; Nwakalor 2016).

These associated sulphide minerals are in most cases responsible for the oxidation or self-heating behaviour of the minerals. This is a potential for oxidation instigation for crude oil for the purpose of enhanced oil recovery which could be beneficial for Nigerian crude oil production in the future. The

future when Nigeria will turn to its depleted oil wells for economic and environmentally friendly methods of production.

Figure 4.20 shows several differential scanning calorimeter (DSC) thermograms overlay of varrying amount of tailing (sourced from Newfoundland and Labrador, Canada) used in the study of improved oxidation of crude oils. Tailings amount of 0%, 5%, 10% and 20% was preliminarily carried on a crude oil to observe the oxidation behaviour before further replicating it in an accelerating rate calorimeter. The ARC is known to be much more sensitive and time consuming test and can easily mimic an adiabatic condition when compared to the DSC. It can be noted that the onset oxidation temperature of the reaction was lowered as the tailing concentration increased. At 0% tailings, the onset oxidation temperature was 160 ^{o}C which dropped to 152 ^{o}C with 5% tailings. It further dropped to 148 ^{o}C and 107 ^{o}C at 10% and 20% tailings concentrations respectively. This is an evidence of oxidation enhancement of crude oil which is beneficial for enhanced oil recovery.

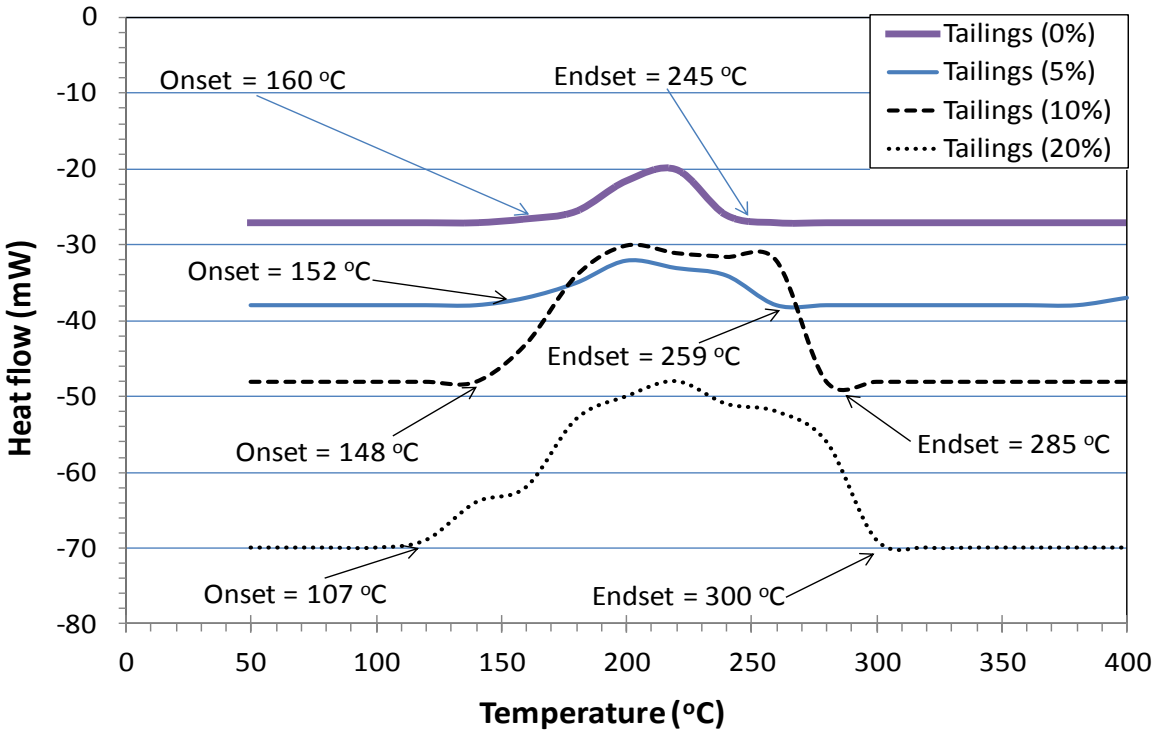


Figure 4.20: DSC thermograms of varying amount of tailings in crude oil

Solid minerals such as sandstone, limestone, silica, nanoclay had been reported to enhance oil combustion and thus improved oil recovery (De los Rios *et al*., 1988; Celebioglu and Bagci, 2002; Kök *et al*., 2005; Kok, 2011; Kok, 2012; Rezaei *et al*., 2013). This is an indication therefore that the observation of onset temperature lowering will enhance oil recovery from the reservoir. Hence, similar experiment was conducted in an accelerating rate calorimeter to take advantage of its adiabatic condition. The results are presented in Figures 4.21 to 4.26 which shows the temperature and pressure profile of crude oil combustion reaction with varying concentration of tailings (0% to 40%).

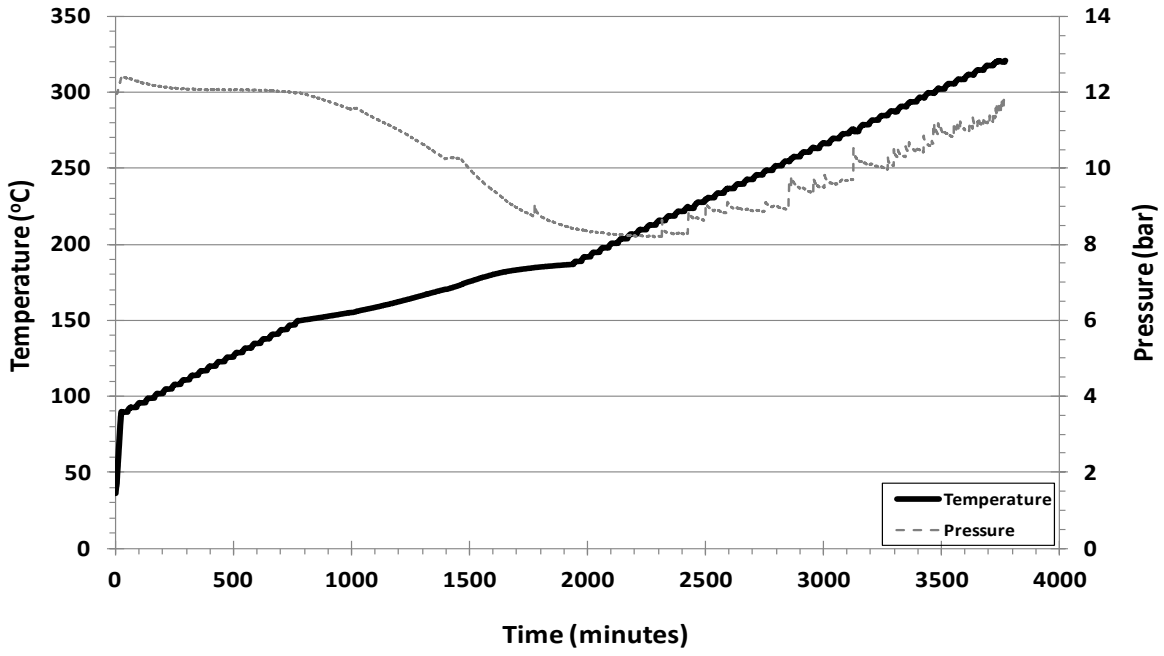


Figure 4.21: Temperature / Pressure profile of crude oil without tailings

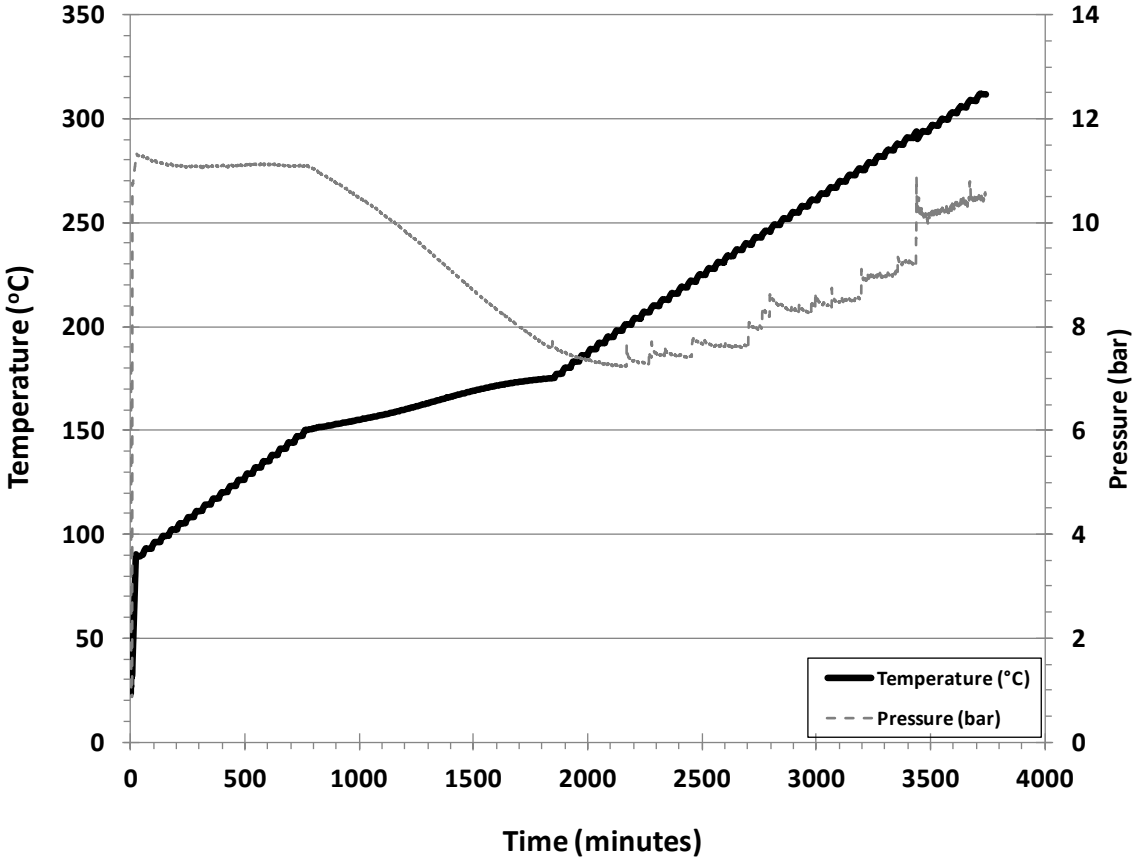


Figure 4.22: Temperature / Pressure profile of crude oil with 5% tailings

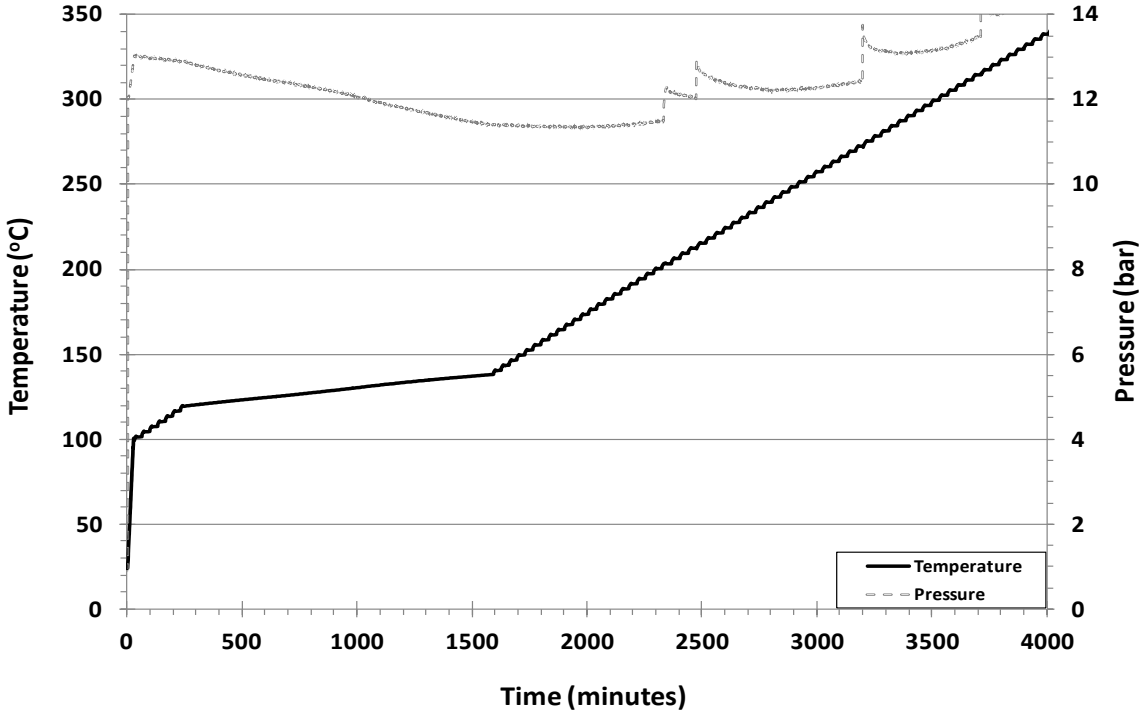


Figure 4.23: Temperature / Pressure profile of crude oil with 10% tailings

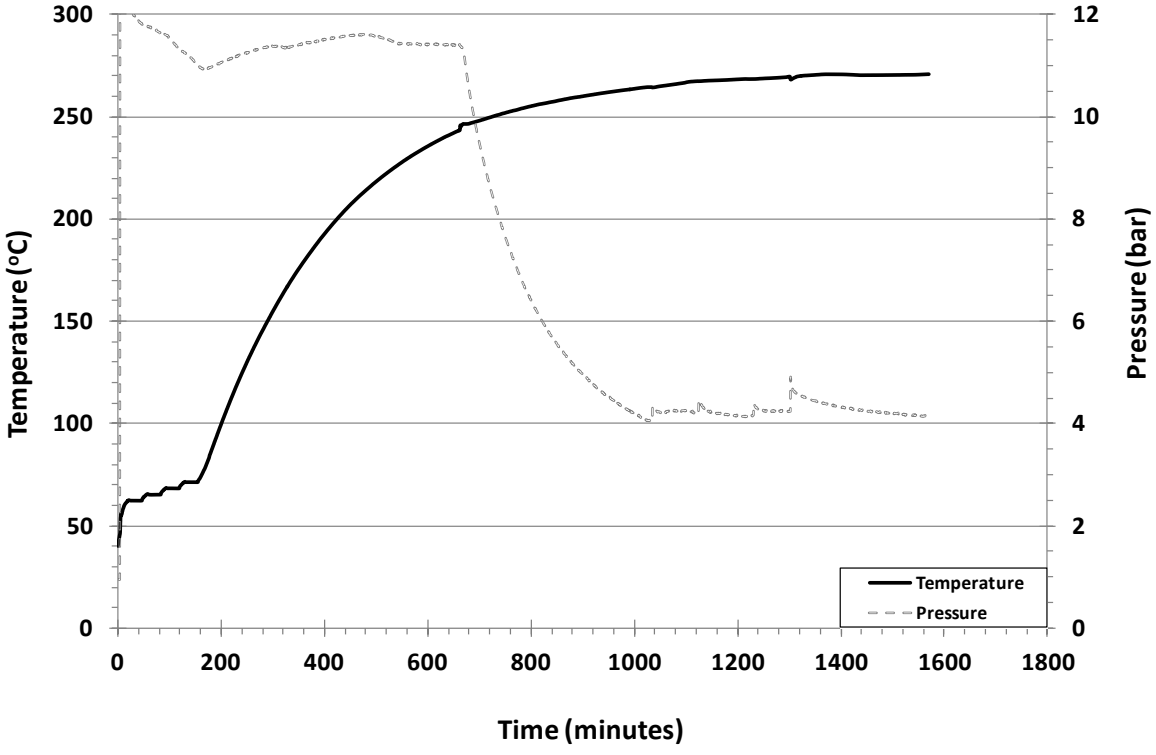


Figure 4.24: Temperature / Pressure profile of crude oil with 20% tailings

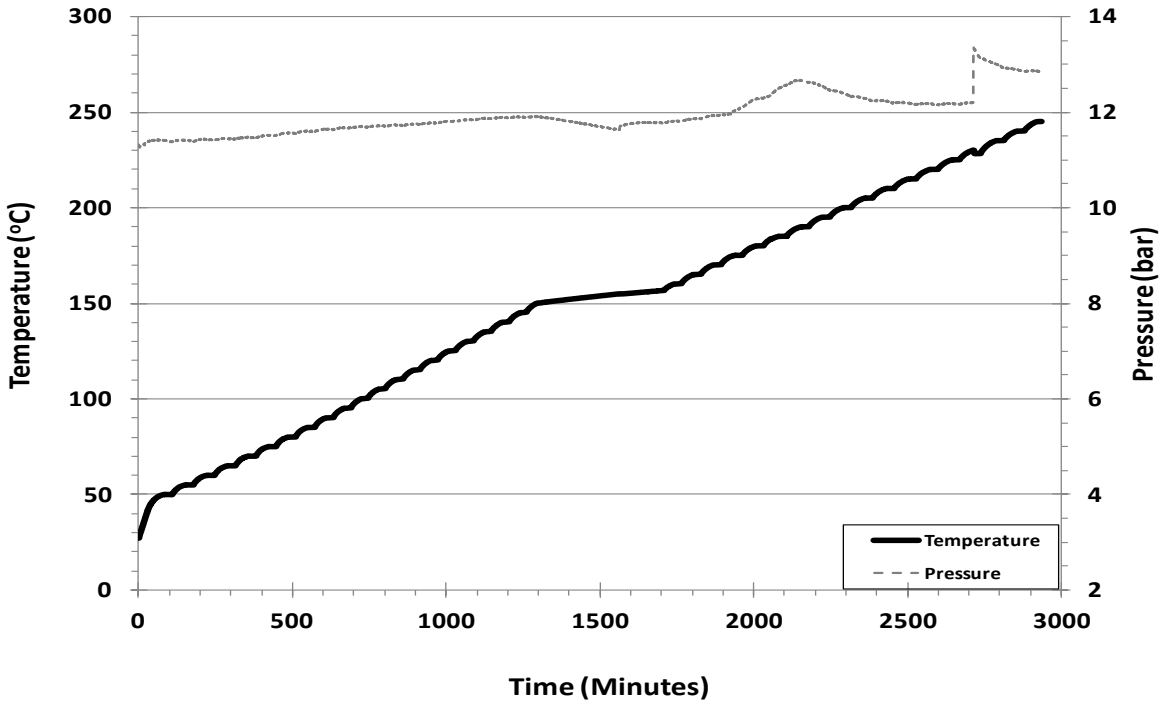


Figure 4.25: Temperature / Pressure profile of crude oil with 30% tailings

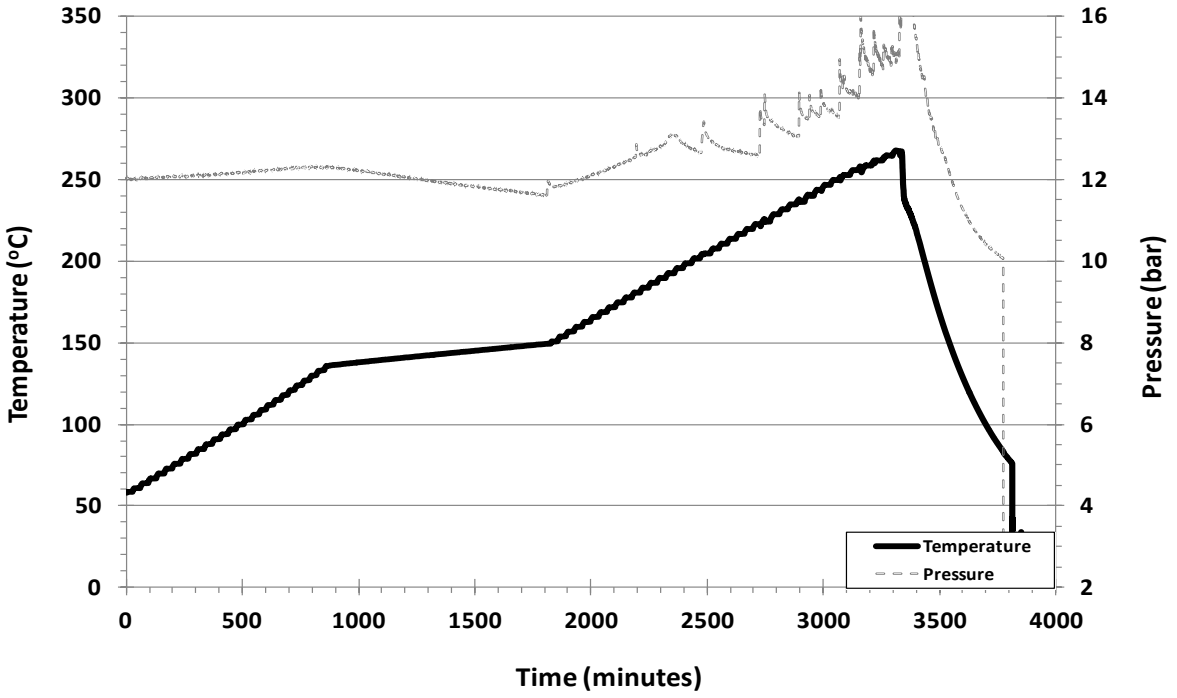


Figure 4.26: Temperature / Pressure profile of crude oil with 40% tailings

It was observed that as the amount of tailing increased, the onset oxidation temperature dropped until 20% then it increased with further increase in tailing to 30%. The increase observed in the onset temperature as the tailings was increased from 20% to 30% could be as a result of oxygen deficiency for the combustion reaction behaviour. An increase after that caused a drop in onset oxidation temperature at 40%.

Figure 4.27 illustrates the effect of tailings amount on temperature onset, peak and endset of the oxidation reaction of the crude oil at varying tailings amount. It can be observed that temperature range was highest of 63.9 ^{o}C for crude oil with 20% tailings. This implies oxidation reaction can occur over the wide temperature rage making it an advantage for air injection EOR.

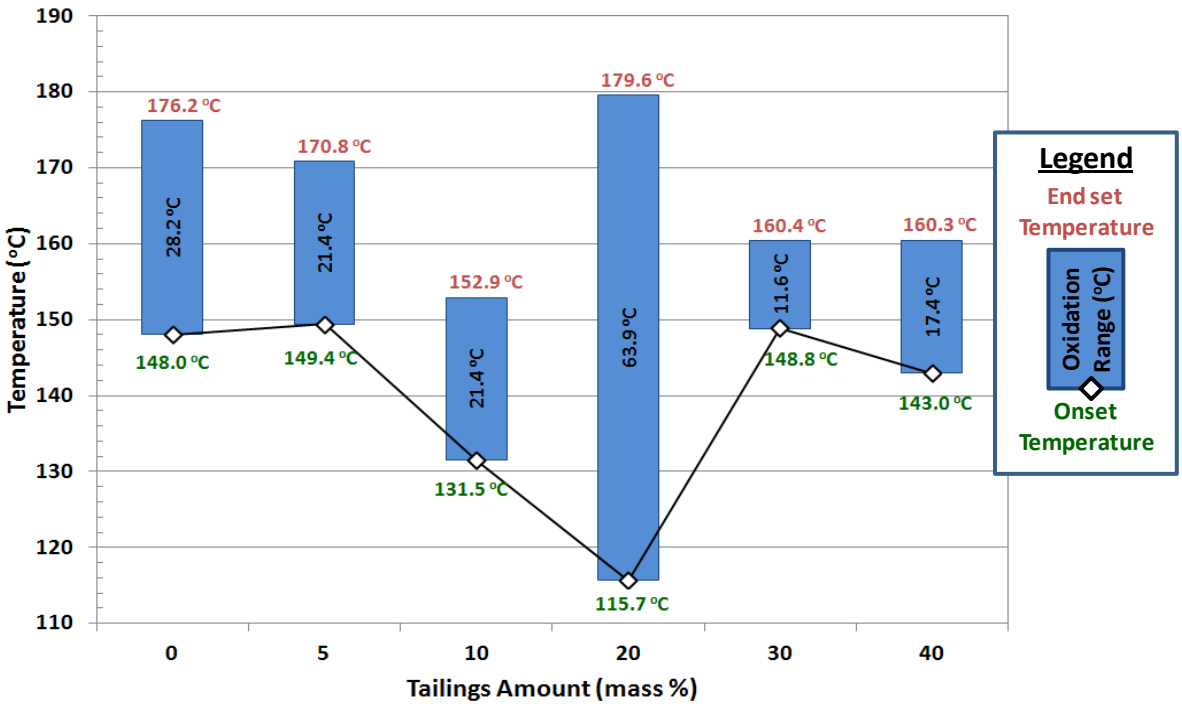


Figure 4.27: Effect of amount of tailings on Onset temperature, Oxidation range and End set temperature during oxidation reaction of crude oils

Tailings at optimum amount would favour oxidation, and hence production of flue gases which will enhance miscibility and eventually an improved oil recovery of an aged well (Sarathi, 1998; Kok, 2012; Shokrlu *et al*., 2013).

A summary of ARC test results is shown in Table 4.4. It shows the mean temperatures and pressure of the oxidation zone including their respective standard deviation. Full details including reproducibility data is shown in Appendix B. The 20% tailings which recorded the highest standard deviation in its onset temperature was further subjected to box plot (Appendix B, Figure B1) which shows reasonable data reliability.

Table 4.4: Summary of the Temperature-Pressure Data Obtained from an Accelerating Rate Calorimeter test including standard deviation.

Tailings wt%	**T_{onset} ^{o}C**	**T_{endet} ^{o}C**	**T_{range} ^{o}C**	**P_{onset} bar**	**P_{endset} bar**	**P_{range} bar**
0.0	148.0 ± 1.9	176.2 ± 10.8	28.2 ± 8.9	11.9 ± 0.2	9.8 ± 1.5	2.1 ± 1.6
5.0	149.4 ± 0.3	170.8 ± 2.8	21.4 ± 2.6	11.7 ± 0.3	9.9 ± 1.2	1.8 ± 1.9
10.0	131.5 ± 11.5	152.9 ± 14.5	21.4 ± 3.0	12.7 ± 0.2	11.5 ± 0.2	1.2 ± 0.3
20.0	115.7 ± 9.9	179.6 ± 20.8	63.9 ± 27.5	11.2 ± 0.3	8.8 ± 1.2	2.4 ± 1.1
30.0	148.8 ± 1.0	160.4 ± 4.7	11.6 ± 5.7	12.0 ± 0.1	11.6 ± 0.2	0.4 ± 0.3
40.0	143.0 ± 7.1	160.3 ± 9.9	17.4 ± 2.9	12.3 ± 0.1	11.6 ± 0.0	0.7 ± 0.0

The onset oxidation temperature lowering of crude oil makes it a candidate for air injection EOR prospect. This is further illustrated in Figure 4.28 where reservoir oil exhibits an onset oxidation temperature higher than its reservoir temperature. The tailing added to the oil helped to lower its onset

temperature to reservoir temperature thereby making the reservoir a candidate for air injection EOR project.

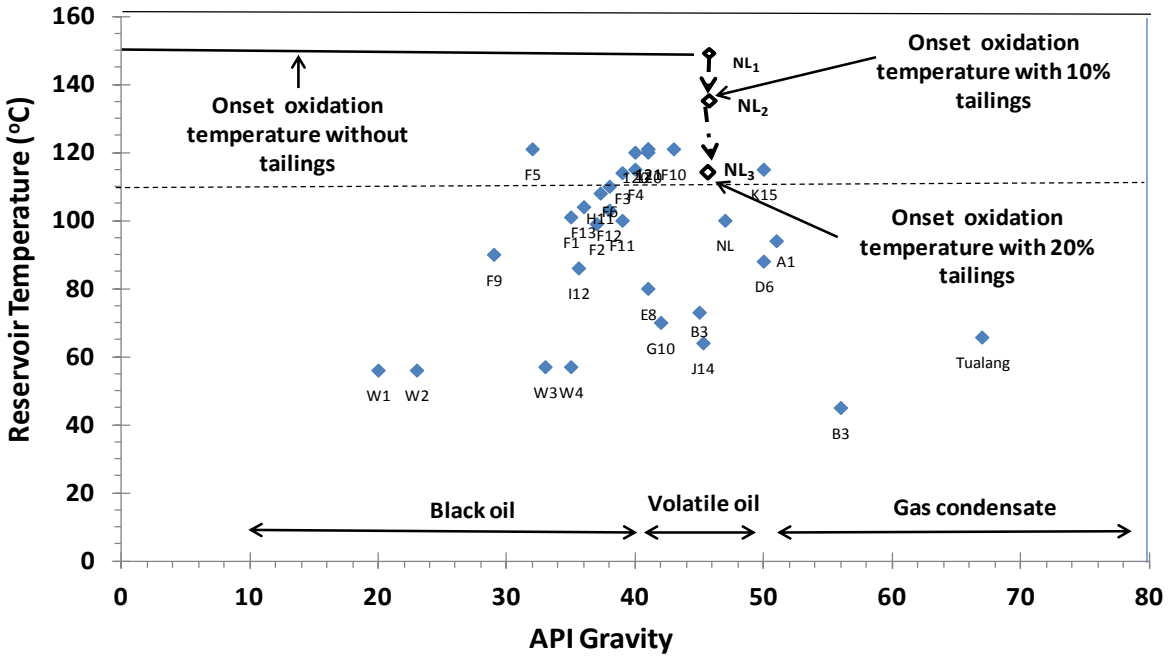


Figure 4.28: Theoretical effect of tailings on onset temperature and oxidation reaction based on Reservoir conditions

Figure 4.28 shows the potential of onset temperature lowering during an EOR process. Petro-physical (reservoir temperature and API) properties of various crude oil reservoirs around the world (Standing, 1947; Masters *et al*., 1987; Jaubert *et al*, 2002) was used to demonstrate this concept. Reservoir temperatures are usually lower than the oil's spontaneous combustion temperature in air. For an air injection EOR to be applicable, combustion must be able to take place at the reservoir conditions which mean lowering the onset temperature to the reservoir temperature. Crude oil (NL_1) which had an onset temperature of 150 ^{o}C could combust at 130 ^{o}C with 10% tailings. The onset temperature could be further lowered to make it combust at 115 ^{o}C giving it a higher potential than the previous stages. The figure showed the potential of a large number of reservoirs that will be applicable to this type of EOR if

the combustion temperature of their crude oils can be lowered. The extent of lowering of the onset temperature of reservoir oil increases the chances of its suitability for air injection. Therefore, the higher the possibility of lowering the onset oxidation of the crude oil, the higher the potential for its reservoir to be considered for air injection EOR (Li *et al*., 2004; Kok *et al*., 2004; Li *et al* 2009).

4.5 Effect of Reservoir conditions on Oil Recovery on Nigerian Crude Oil

This section discusses the effect of reservoir temperature, reservoir pressure and reservoir sulphur content on improved oil recovery prospect in Nigeria. The crude oil data obtained from Jaubert *et al* (2002) (Table C.1 – Table C.4) was regressed with the given isothermal expansion data and Isothermal differential vaporization data using the Soave-Redlich-Kwong (SRK) equation of state as shown in Table D.1 – D.5. The lumping method of similar molecular weight was adopted in PVTsim 19. The saturation pressure calculated deviated by 21.26% when calculated using the SRK equation of state. Lumping method to 3 pseudo component (Table E.1 to E.5) was used for tuning which yielded a lower deviation of -9.43 %. The tuned oil properties are presented in Appendix F (Table F.1 to F.5).

An Anova analysis on experimental runs generated from the design of experiment (Appendix Table G.1) is presented in Appendix H (Table H.1). An optimum desirability of one (1) was chosen from the design of experiment analysis and a final equation based on coded factors generated as presented in Appendix H (Tables H.2 to H.4). The 3D plots describing the reservoir property relationship as designed in the experiment is therefore presented in Figures 4.29 to 4.31.

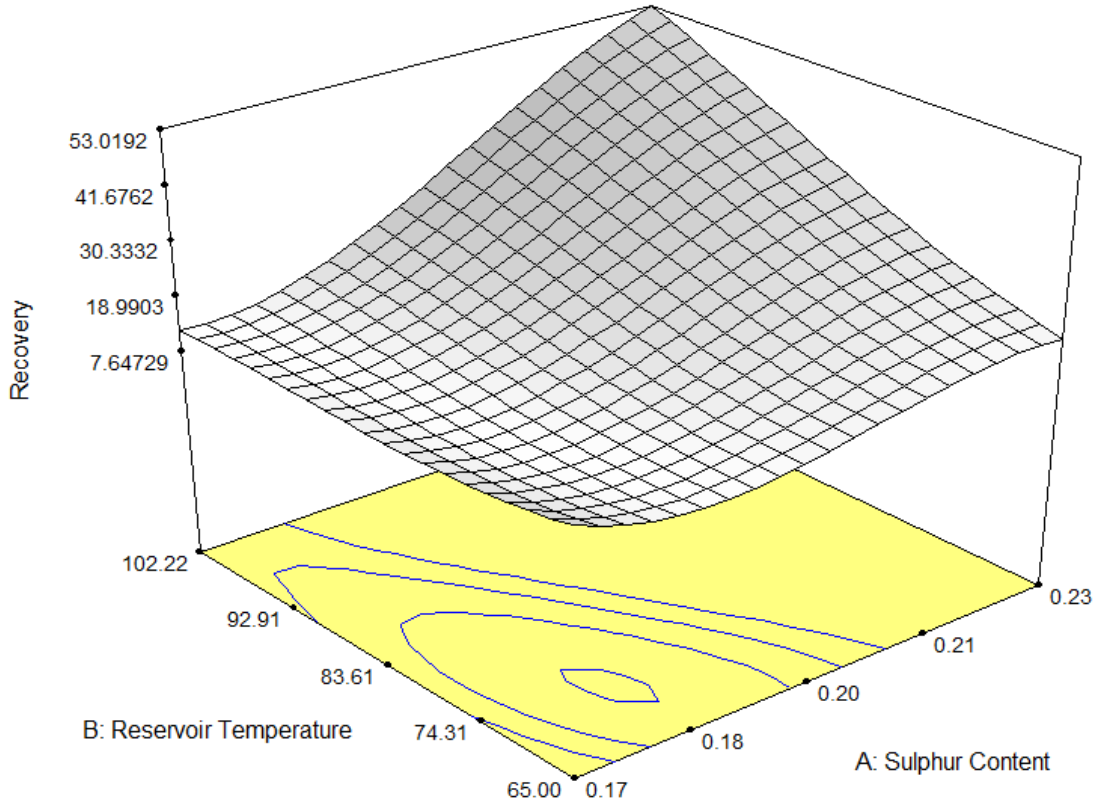


Figure 4.29: Effect of reservoir temperature and sulphur content on oil recovery

Figure 4.29 shows the effect of sulphur content and reservoir temperature on recovery. Although sulphur is not desirable in high amount in the reservoir, an improved recovery of oil as reservoir temperature and sulphur content increased in the reservoir. This can be attributed to the effect of SO_2 as a constituent of flue gas known to influence combustion (Dong and Huang, 2002; Abu-Khamsin, 2003; Niu *et al*., 2011).

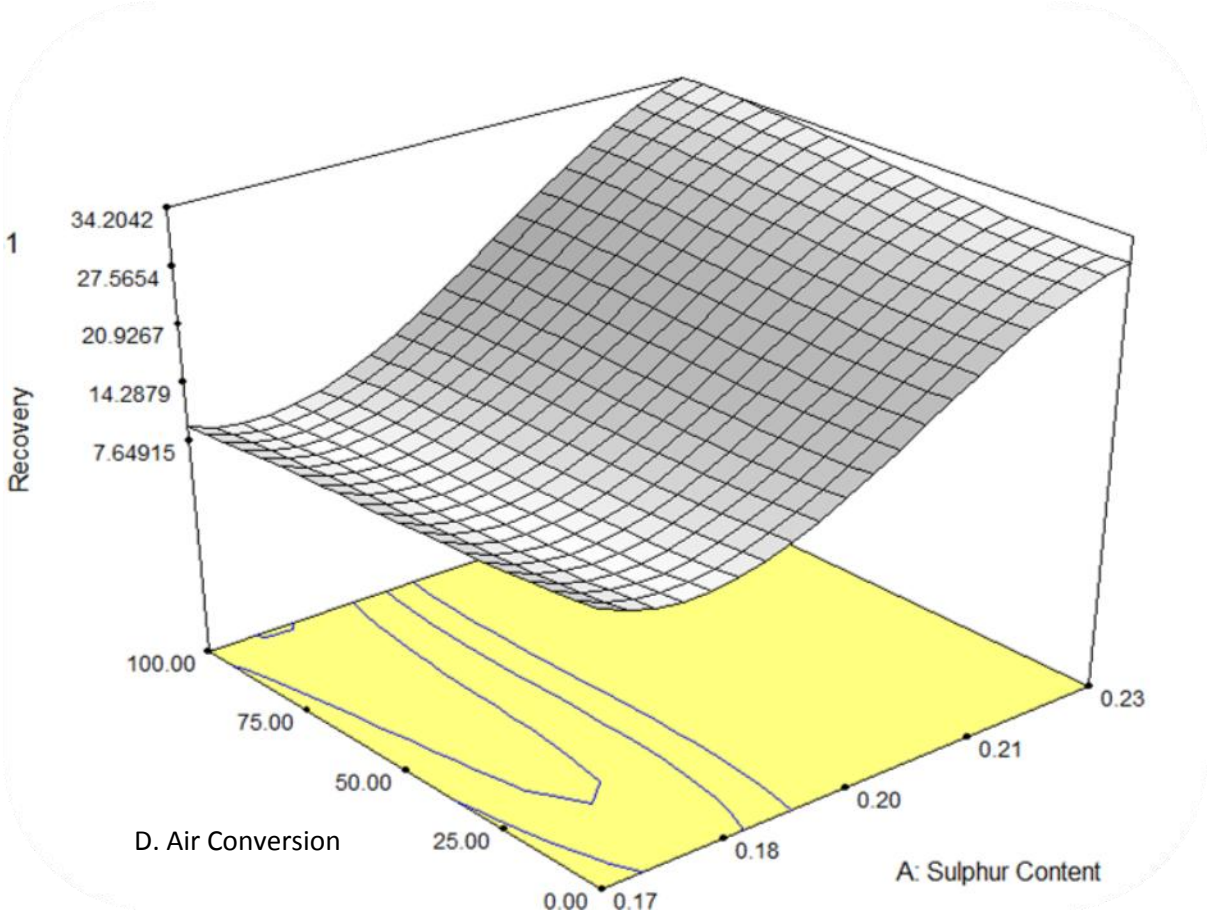


Figure 4.30: Effect of extent of air oxidation and sulphur content on oil recovery

Figure 4.30 shows the effect of the extent of air oxidation and sulphur content on oil recovery. Higher sulphur content in the reservoir as well as increased air conversion by oxidation to flue gas were observed to improve oil recovery in the reservoir. This is in agreement with Figure 4.29 on the positive influence flue gas constituents on oil recovery (Zhu *et al*., 2001; Shokoya *et al*., 2004).

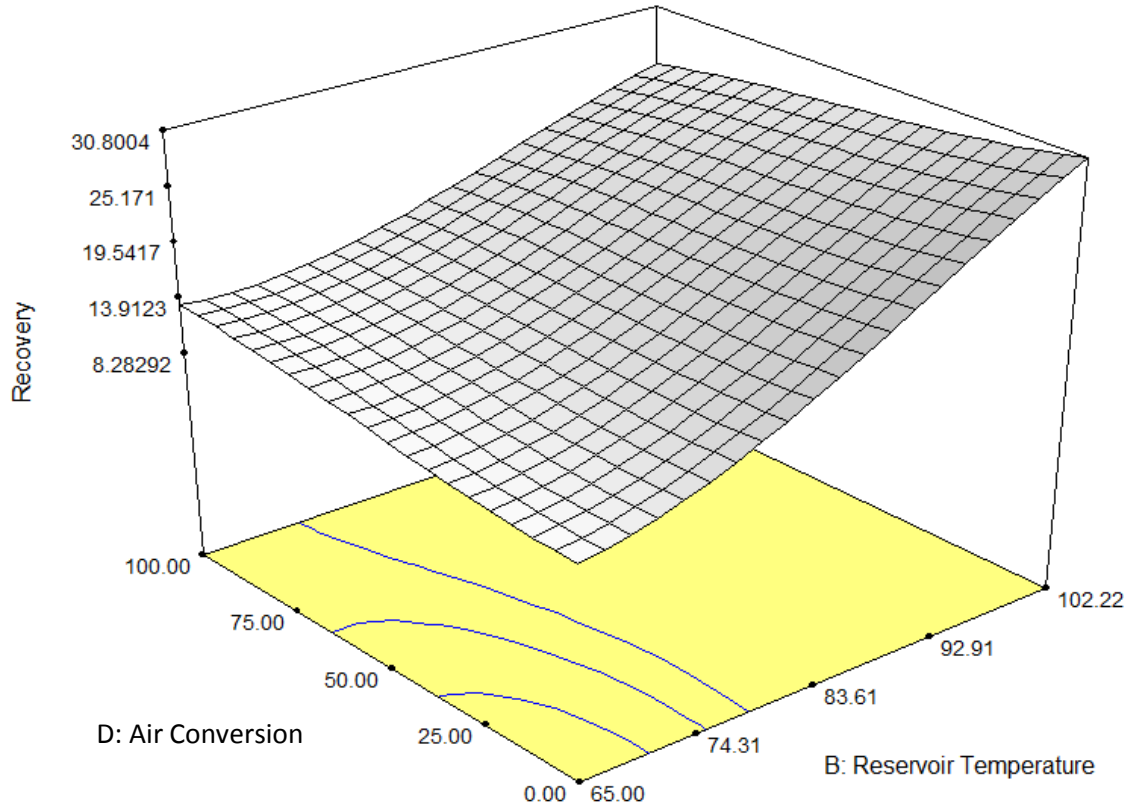


Figure 4.31: Effect of extent of air oxidation and reservoir temperature on oil recovery

Figure 4.31 shows the effect of the extent of air oxidation and reservoir temperature on improved recovery. It was observed that for high yield of improved recovery, Air conversion to flue gas (such as CO_2 which is miscible in oil) and reservoir temperature were high which implied that recovery by air injection is favoured by conversion/oxidation of air to flue gas as well as high reservoir temperature (Moore *et al*., 1992; Mahinpey *et al*., 2010; Niu *et al*., 2011).

CHAPTER FIVE

5.0 CONCLUSIONS AND RECOMMENDATIONS

Based on the thermal and mineral analyses carried out using the light oils, mine tailings, and air combustion product in-situ the reservoir at high temperature and pressures, the following conclusions and recommendations can be made.

5.1 Conclusions

1. The superiority of the iso conversional studies can easily be observed based on the activation energy determination. Sample A when analysed using the iso-conversional method, had a non-constant activation energy between 50 - 235 kJ/mol as the reaction progressed to completion while with the simple Arrhenius model analysis, a constant activation energy of 133.6 kJ/mol was determined for the reaction. This is evident in the other samples analysed.
2. The detected onset oxidation temperatures of the reactions for sample A was in the low temperature oxidation zones (140 ^{o}C) while samples B (215 ^{o}C) and C (220 ^{o}C) recorded their onset oxidation temperature in the medium temperature oxidation zones respectively.
3. The estimated activation energies using the ASTM E-698 method were observed to be higher for the lower API gravity crude samples. Sample A which high API gravity of 46.963 had a low activation of 133.6 kj/mol while sample C with low API gravity of 30.214 recorded the highest activation energy of 176.5 kj/mol.
4. The apparent activation energy using the iso-conversional method increased as the reaction progressed with sample A recording a peak at $\alpha = 0.58$ due to production of flue gases which hampers oxidation reaction hence the larger activation barrier.

5. The oxidation reaction using 20 wt% tailings caused the oxidation reaction to span from the low temperature oxidation zone to medium temperature oxidation zone (where the onset of 106 ^{o}C to enset up to 200^{o}C), thereby increasing its suitability in an EOR project involving a low and medium temperature oxidation reactions.
6. In the study of the use of tailings to lower oxidation temperature of light crude oil in-situ the reservoir, 20% tailings on the crude oil recorded the lowest onset oxidation and highest endset temperature making it a best tailing amount required for an Air injection EOR project of the crude oil.
7. Air injection EOR is favoured by high reservoir temperature, pressure as well as the oxidation of injected air.

5.2 Recommendations

1. Future work should investigate the risk analysis of Air injection projects operating on catalytic enhancements.
2. A comparison of historical data vs simulated data should be carried out for future reliability analysis.
3. A study of Coking problem during air injection projects should be carried out to see effect on overall oil recovery.
4. Although 20% tailings showed the highest temperature lowering of the onset temperature, screening different crude oils for their response to specific tailings is highly recommended before field project.

REFERENCES

Abu-Khamsin, S. A. (2003). The effect of Unsaturates on Low Temperature Oxidation of Crude Oil. *Journal of Pettroleum Science and technology*, 1065-1075.

Adamu, C. I and Nganje, T. N. (2010). Heavy metal contamination of Soil and Surface water in Arufu Lead-Zinc Mining District, Middle Benue Trough, Nigeria. *Ghana mining Journal*. Vol 12: 17-23.

Adebiyi, F. M., and Thoss, V. (2014). Organic and elemental elucidation of asphaltene fraction of Nigerian crude oils . *Fuels*, 426–431.

AG-AKTS. (2008). *AKTS-Thermokinetics software and AKTS-Thermal Safety software)*. Retrieved January 03, 2012, from AKTS-Thermokinetics software: http://www.akts.com

Ajaka, E. O. (2006). Recovering fine Iron minerals form Itakpe Iron Ore Process Tailings. *ARPN Journal of Engineering and Applied Sciences*. Vol. 4, 19-28.

Al-Anazi, B. D. (2007). Enhanced oil Recovery techniques and Nitrogen Injection. *Canadian Society of Exploration and Geophysicists*, 28-33.

Ali, Ahmed (2016, September 2). Dangoma: Inside Nigeria's nickel-rich community. Daily Trust. *Retrieved from www.dailytrust.com.ng*.

Alvarado, V., & Maveric, E. (2010). Enhanced Oil Recovery: An Updated Review. *Energies*, 1529-1575.

Amarnath, A. (1999). *Enhanced Oil recovery Scooping Study*. California : Electric Power research Institute, Inc.

Andrei, M., De Simoni, M., Delbianco, A., Cazzani, P., & Zanibelli, L. (2010). *Enhanced Oil Recovery with CO2 Capture and Sequestration.* Armetella: ENI Exploration & Production.

Armstrong, R. T., & Windenschild, D. (2012). Investigating the Pore-Scale Mechanism of Microbila Enhanced Oil Recovery. *Journal of Petroleum Science and Engineering*, 155-163.

Baviere, M (1991). Basic Concepts in Enhanced Oil Recovery Processes. Springer Netherlands. ISBN 978-1-85166-617-1.

Belgravecorp. (2012, February 12). *Surfactant Flooding*. Retrieved February 12, 2012, from belgravecorp: http://www.belgravecorp.com/Iframe/technology/chemical-injection/chemical-injection_4.php

Budrugeac, P (2002). Differential non-linear isoconversional procedure for evaluating the activation activation energy of non-isothermal reactions. *Journal of Thermal Analysis and Calorimetry.* 68 (1): 131-139.

Budrugeac, P. (2005). Some Methodological Problems concerning the Kinetic Analysis of Non-Isothermal Data for Thermal and Thermo-oxidative Degradation of Polymers and Polymeric Materials. *Polymer Degradation and Stability*, 265-273.

Burger, J. G., & Sahuquet, B. (1972). Chemical Aspects of In-Situ Combustion - Heat of Combustion and Kinetics. *Society of Petroleum Engineers, SPE 3599*, 410-422.

Button, P., Peterson, C., & Morgan, K. (2004). Enhanced Gravity Drainage Through Immiscible CO2 Injection in the Yates Field (Tx). *10th Annual CO2 Flooding Conference* (pp. 1-10). Midland, Tx: SPE-PB.

Celebioglu, D., & Bagci, S. (2002). The effects of metallic catalysts on light crude oil oxidation in limestone medium. *Fuel Processing Technology*, 29-49.

Chen, K., Wang, Z., Liu, H., & Guo, A. (2012). Study on thermal performance of heavy oils by using differential scanning calorimetry. *Fuel Processing Technology*, 82–89.

Chevron Corporation (2016). African Crudes. *Chevron Global Supply and Trading*. CBRES/10C Houston 064095.

CureKinetics. (2008, April 7). *CureKinetics*. Retrieved 12 12, 2011, from Cure Kinetics: www.erfcomposites.com

D'Elia-S, F., & Ferrer-G, J. (1973). Emulsion Flooding of Viscous Oil Reservoirs. *Society of Petroleum Engineers AIME, SPE 4674*, 1-8.

Danesh, A. (1998). *PVT and Phase behaviou of Petroleum Reservoir Fluids.* Amsterdam: Elsevier science BV.

De La Ossa, R. J., Wallens, A. B., Anaya, A. F., & Santos, N. S. (2010). Experimental Evaluation of the Flue-Gas Injection of Barrancabermeja Refinery as EOR Method. *SPE International Conference on CO2 Capture, Storage, and Utilization, SPE 139715*, 1-20.

De los Rios, C. F., Brigham, W. E., & Castanier, L. M. (1998). *Effect of Metallic Additives on the Kinetics of Oil Oxidation Reactions in In-situ Combustion.* Oklahoma: US Deartment of Energy.

Donaldson, E. C., Chilingarian, G. V., Yen, T. F., & Sharma, M. K. (1989). Oil Recovery Processes. In E. C. Donaldson, G. V. Chilingarian, & T. F. Yen, *Enhanced Oil Recovery, II. Process and Operation* (pp. 1-10). Amsterdam: Elsevier.

Dong, M., & Huang, S. (2002). Flue Gas Injection for Heavy Oil Recovery. *Journal of Canadian Petroleum Technology, PETSOC-02-09-04*, 44-50.

Drici, O., & Vossoughi, S. (1985). Study of the Surface Area Effect on Crude Oil Combustion by Thermal Analysis. *Society of Petroleum Engineers SPE 13389*, 731-735.

Dubey, N. K. (2010). Laboratory Investigation on Light Oil Air Injection. *Society of Petroleum Engineers, SPE 138372*, 1-11.

Elgibaly, A. A. (1998). Oil Recovery from Bottom Beds of Kuwait Oil Lakes by Retorting. *Society of Petroleum Engineers International*, 809-823.

Erikh, V. N., Rasina, N. G., & Rudin, N. G. (1985). *The Chemistry and Technology of Petroleum and Gas.* Moscow: Mir publishers.

Evamy, D. D., Haremboure, J., Kemerling, P., Knaap, W. A., Molly, F. A., & Rowlands, P. H. (1978). Hydrocarbon Habitat of Tertiary Niger Delta. *American Association of Petroleum Geologist Bulletin*, pp. 1-39.

Ezeamalu, Ben (2016, August 29) 'World class' nickel discovered in Nigeria, govt. to sign exploration deal with Australian firm. Premium Times. Retrieved from http://www.premiumtimesng.com.

Farouq Ali, S. F., & Thomas, S. (1994). A Realistic look at Enhanced Oil Recovery. *Scientia Iranica*, 219-230.

Fraim, M. L., Moffitt, P. D., & Yannimaras, D. V. (1997). Laboratory Testing and Simulation Results for High-Pressure Air Injection in a Waterflooded North Sea Oil Reservoir. *SPE Annual Technical Conference and Exhibittion* (pp. 655-663). San Antonio: Society of Petroleum Engineers.

George, A. K.-M., Singh, R. N., & Arafin, S. (2008). Thermo-elastic and Thermodynamic Properties of Light and Heavy Crude oil. *Physics and Chemistry of Liquids*, 328-341.

Georgina, L. C., Carla, L. R., Regina, Á. E., & José, C. L. (2004). Naphthenic acids, total acid number and sulfur content profile characterization in Isthmus and Maya crude oils. *Fuel*, 1689–1695.

Glover, P (2016). Reservoir Drives in: Formation Evaluation MSc Course Notes. University of Leeds, UK. http://homepages.see.leeds.ac.uk/~earpwjg/PG_EN/CD%20Contents/Formation%20Evaluation%20English/Chapter%203.PDF

Greaves, M. (2004). *Air Injection – Improved Oil Recover y Strategy for the UK Continental Shelf.* Bath: Business Briefing: Exploration & Production: The Oil and Gas Review.

Greaves, M., Ren, S. R., & Rathbone, R. R. (1998). Air Injection Technique (LTO Process) for IOR from Light Oil Reservoirs: Oxidation rate and displacement studies. *Society of petroleum Engineers, SPE 40062*, 479-492.

Green, D. W., & Willhite, G. P. (1998). *Enhanced Oil Recovery*. Texas: Society of Petroleum Engineers.

Gundogar, A. S., & Kok, M. V. (2014). Thermal characterization, combustion and kinetics of different origin crude oils. *Fuel*, 59-65.

Guo, B., Lyons, W. C., & Ghalambor, A. (2007). *Petroleum Production Engineering: A Computer-Assisted Approach.* Oxford: Gulf Professional Publishing. .

Gutierrez, D., Skoreyko, F., Moore, R. G., Mehta, S. A., & Ursenbach, M. G. (2009). The Challenge of Predicting Field Performance of Air Injection Projects Based on Laboratory and Numerical Modelling. *Journal of Canadian Petroleum Technology*, 23-34.

Gutierrez, D., Taylor, A. R., Kumar, V. K., Ursenbach, M. G., Moore, R. G., & Mehta, S. A. (2007). Recovery Factors in High-Pressure Air Injection Projects Revisited. *Society of Petroleum Engineers International SPE 108429*, 1-12.

Hawkins, B., & Singhal, A. (2004). *Enhanced Oil Recovery Water Usage.* Alberta: Alberta Research Council.

Holm, L. W. (1986). Miscibility and Miscible Displacement. *Journal of Petroleum Technology*, 817-818.

House, J. E. (2007). *Principles of chemical kinetics.* London: Aademic Press.

Hvizdos, L. J., Howard, J. V., & Roberts, G. W. (1983). Enhanced Oil Recovery Through Oxygen Enriched In-Situ Combustion: Test Results form the Forest Hill Field in Texas. *Society of petroleum Engineers of AIME*, 1061-1069.

Iliyas, A., Hawboldt, K., & F, K. (2010). Advanced Kinetics for Calorimetric Techniques and Thermal Stability Screening of Sulfide Minerals. *Thermochimica Acta 501*, 35-45.

Iliyas, A., Hawboldt, K., & Khan, F. (2011). Kinetics and safety analysis of sulfide mineral self-heating. *Journal of Thermal Analysis and Calorimetry*, 53-61.

Isco, T. (2007, October 27). Enhanced Oil Recovery (EOR). *Teledene Isco*.

Iwata, Y., Koseki, H., Janssens, M. L., & Takahashi, T. (2001). Combuston Characteristics of Crude Oils. *Fire and Materials*, 1-7.

Jahn, F., Cook, M and Graham, M. (1998). Hydrocarbon Exploration and Production. Elsevier Science, Amsterdam pp 153-171.

Jaubert, J., Avaullee, L., & Souvay, J. (2002). A Crude oil data bank containing more than 5000 PVT and gas injection data. *Journal of Petroleum Science and Engineering*, 65-107.

JOGMEC. (2011). *Air Injection Technilogy*. Tokyo: Japan Oil, Gas and Metals national Corporation.

Juttner, I. (1997). Oil displacement in Miscible Condition. *Rudarsco-Geolosko-Naftni-Zbornik*, 63-66.

Karacan, O., Kok, M. V., & Karaaslan, U. (1999). Changes in Thermal Properties of Crude Oil Asphaltene induced by NaOH Treatment. *Fuel Processing Technology*, 13-21.

Katarzyna, K., Zofia, K., Katarzyna, M., & Piotr, K. (2005). Oxidation of sulfides to sulfoxides. Part 2: Oxidation by hydrogen peroxide . *Tetrahedron*, 8315–8327.

Kok, M. V. (1997). High-Pressure DSC Application on Crude Oil Combustion. *Energy and Fuels*, 1137-1142.

Kok, M. V. (2008). Non Isothermal Kinetic Analysis and Feasibility Study on Medium Grade Crude Oil Field. *Journal of Thermal Analysis and Calorimetry*, 745-74.

Kok, M. V. (2010). Thermo-oxidative reactions of crude oils. *Journal of Thermal and Analytical Calorimetry*, 411-414.

Kok, M. V. (2011). Characterization of medium and heavy crude oils using thermal analysis techniques. *Fuel Processing Technology*, 1026–1031.

Kok, M. V. (2012). Clay concentration and heating rate effect on crude oil combustion by thermogravimetry. *Fuel Processing Technology* , 134-139.

Kok, M. V., & Gundogar, A. S. (2013). DSC study on combustion and pyrolysis behaviors of Turkish crude oils. *Fuel Processing Technology*, 110-115.

Kok, M. V., & Keksin, C. (2001). Comparative Combustion Kinetics for In-Situ Combustion Process. . *Thermochimica Acta*, 143-147.

Kök, M. V., Hughes, R., & Price, D. (2005). Combustion characteristics of crude oil-limestone mixtures. *Journal of Thermal Analysis and Calorimetry*, 609-615.

Kök, M. V., Pokol, G., Keskin, C., Madarász, J., & Bagci, S. (2004). Light crude oil combustion in the presence of limestone matrix. *Journal of Thermal Analysis and Calorimetry*, 781-789.

Kok, M. V., Sztatisz, J., & Pokol, G. (1997). High-Pressure DSC Application on Crude Oil Combustion. *Energy & Fuels*, 1137-1142.

Kuhlman, M. I. (2000). Simulation o Light Oil air Injection Into Viscous-Dominated and Gravity-Stable Reservoirs. *Society of Petroleum Engineers International, SPE 59331*, 1-10.

Kuhlman, M. I. (2004). Expanded Uses of Nitrogen, Oxygen and Rich Air for Increased Production of Both Light and Heavy Oil. *Society of Petroleum Engineers SPE 86954*, 1-16.

Kumar, S., Yen, T. F., Chilingarian, G. V., & Donaldson, E. C. (1989). Alkaline Flooding. In E. C. Donaldson, G. V. Chilingarian, & T. F. Yen, *Enhanced Oil Recovery: Processes and operations* (pp. 219-230). Netherlands: Elsevier Science Publishers.

Lake, Larry W., Johns, Russell., Rossen, Bill and Pope, Gary. (2014). Fundamentals of Enhanced Oil Recovery. Society of Petroleum Engineers. ISBN: 978-1-61399-407-8.

Laredo, G. C., Carla R. Lo´pez, Regina E. A ´ lvarez, Jose´ L. (2004). Cano Naphthenic acids, total acid number and sulfur content profile characterization in Isthmus and Maya crude oils Fuel 83: 1689–1695.

Li, J., Mehta, S. A., Moore, R. G., & Ursenbach, M. G. (2002). The research of Oxidation and Ignition behaviour of Saturated Hydrocarbon Sample with Crude Oils using TG/DTG and DTA Thermal Analysis Techniques. *Petroleum Society's Canadian International Petroleum Conference* (pp. 1-16). Calgary: Petroleum Society.

Li, J., Mehta, S. A., Moore, R. G., & Ursenbach, M. G. (2009). New Insights into Oxidation behaviour of Crude Oils. *Journal of Canadian Petroleum Technology*, 1-6.

Li, J., Mehta, S. A., Moore, R. G., G, U. M., E, Z., H, F., & Okazawa, N. E. (2004). Oxidation and Ignition behaviour of Saturated Hydrocarbon samples with Crude Oils using TG/DTG and DTA Thermal Analysis Technique. *Journal of Canadian Petroleum Technology*, 45-51.

Li, J., Mehta, S. A., Moore, R. G., Ursenbach, M. G., Ferguson, H., Zalewski, E., & Okazawa, N. E. (2002). The Research of Oxidation and Ignition Behaviour of Saturated Hydrocarbon Sample With Crude Oils Using TG/DTG and DTA Thermal Analysis Techniques. *Canadian International Petroleum Conference*, (pp. 1-16). Calgary: Society of Petroleum Engineers.

Li, J., Mehta, S. A., Moore, R. G., Ursenbach, M. G., Zalewski, E., Ferguson, H., & Okazawa, N. E. (2004). Oxidation and Ignition Behaviour of Saturated Hydrocarbon Samples with Crude Oils using TG/DGT and DTA Thermal Analysis Technique . *Journal of Canadian Petroleum Technology*, 45-51.

Li, J., Mehta, S. A., Moore, R. G., Ursenbach, M. G., Zalewski, E., & Van Fraassen, K. (2005). Chemically Assisted Ignition Technologies for a Light Oil Air Injection Process. *Canadian International Petroleum Conference* (pp. 1-9). Calagary: Canadian Institute of Mining, Metallurgy & Petroleum.

Li, Y.-B., Zhao, J.-Z., Pu, W.-F., Peng, H., Zhong, D., & Hub, Z.-W. (2014). A method based on the Harcourt and Esson equation to estimate the catalytic effect of metallic additives on light crude oil. *Journal of Alloys and Compounds*, 7-13.

Mahinpey, N., Mani, T., & Murungan, P. (2010). Comparative Kinetics and Thermal Behaviour: The Study of Crude Oils Derived from Fosterton and neilburg Fields of Saskatchewan. *Energy and Fuels*, 1640-1645.

Mamora, D. D. (1995). New Findings in Low-Temperature Oxidation of Crude Oil. *Society of Petroleum Engineers, SPE 29324*, 577-592.

Manning, F. S. (1995). *Oilfield Processing; Volume Two: Crude Oil*. Tulsa: PennWell Publishing Company.

Masters, C. D., Attanasi, E. D., Dietzman, W. D., Meyer, R. F., Mitchell, R. W., & Root, H. R. (1987). World resources of Crude oil, Natural gas, Natural bitumen and Shale oil. *12th World Petroleum Congress* (pp. 3-27). Houston, USA: World Petroleum Congress.

Mathiassen, O. M. (2003). *CO2 as Injection Gas for Enhanced Oil Recovery and Estimation of the Potential on the Norwegian Continental Shelf*. Trondheim / Stavanger: Norwegian Petroleum Directorate.

McCain, W. D.Jr (1989). The properties of petroleum fluids. PennWell Books. Tulsa. ISBN-0-87814-335-1.

Mendoza, A. J., Oliveros, D., Arellano, D., Perozo, H., Reinoza, J., & Rivas, A. (2011). New Approach to Upgrade the Combustion In-Situ process by Using an emulsified Additive on Heavy oil from Orinoco Belt. *society of Petroleum Engineeers SPE 145056*, 1-9.

Mogensen, K., Hood, P., Lindeloff, N., Frank, S., & Noman, R. (2009). Minimum Miscibility Pressure Investigations for a Gas Injection EOR Project in Al Shaheen Field, Offshore Qatar. *Society of Petroleum Engineers International, SPE 124109*, 1-20.

Montes, A. R., Gutierrez, D., G, M. R., Mehta, S. A., & Ursenbach, M. G. (2010). Is High-Pressure Air Injection (HPAI) Simply a Flue-Gas Flood. *Journal of Canadian Petroleum Techology*, 56-63.

Moore, R. G., Belgrave, J. D., Mehta, R., Ursenbach, M., Laureshen, C. J., & Kejia, X. (1992). Some Insights Into the Low-Temperature and High-Temperature In-Situ Combustion Kinetics. *Society of Petroleum Engineers*, 179-200.

National Research Council (2013). Induced Seismicity Potential in Energy Technologies. ISBN: 978-0-309-25367-3. DOI: 10.17226/13355.

NETL. (2012). *Alkaline Flooding*. Retrieved February 14, 2012, from National energy technology Laboratory: http://www.netl.doe.gov/technologies/oil-gas/publications/eordrawings/BW/bwalkaline.PDF

Netzsch. (2009). *Leading Thermal Analysis*. Retrieved 10 2011, 2, from NETZSCH: www.netzsch-thermal-analysis.com

Nganje, T. N., Adamu, C. I., Ntekim, E. E. U., Ugbaja, A. N., Neji, P., Nfor, E. N. (2010). Influence of Mine drainage on Water quality along River Nyaba in Enugu South- Eastern Nigeria.

Niu, B., Ren, S., Liu, Y., Wang, D., Tang, L., & Chen, B. (2011). Low-Temperature Oxidation of Oil Components in an Air Injection Process for Improved Oil Recovery. *Energy and Fuels*, 4299-4304.

Nwakalor Michael (2016, September 1). What's a nickel worth: Solid mineral deposits discovered in Northern Nigeria. Ventures Africa. Retrieved from www.venturesafrica.com

Oil-Chem. (2010). *Foam Flood*. Retrieved February 20, 2012, from Oil Chem Technilogies: http://www.oil-chem.com/foamflood.htm

Oldenburg, C. M., Pruess, K., & Benson, S. M. (2001). Process Modeling of CO2 Injection into Natural Gas Reservoirs for Carbon Sequestration and Enhanced Gas Recovery. *Energy Fuels*, 293-98.

Oliver, D. S., Reynold, A. C and Liu, N. (2008). Inverse Theory for Petroleum Reservoir Characterization and History Matching. Cambridge University Pres. ISBN 978-0-521-88151-7.

Onyeobi, T. U. S., and Imeokparia, E. G (2014). Heavy Metal contamination and distribution in soils around Pb-Zn mines of Abakaliki district, South eastern Nigeria. *Frontiers in Geosciences.* Volume 2 Issue 2, 30-40.

Orr, F. M. (2007). Theory of Gas Injection Processes. Tie-Line Publications, Copenhagen, Denmark.

Pederson, K. S., and Christenson, P. L. (2007). *Phase Behaviour of Petroleum Reservoir Fluids.* Boca Raton: CRC Press.

PerkinElmer. (2006). *Differential Scanning Calorimeter*. Shelton: PerkinElmer Life and Analytical Sciences.

Pwaga, S., Iluore, C., Hundseth, O., Perales, F. J., & Idrees, M. U. (2010). *Comparative Study of Different EOR Methods.* Trondheim: NTNU, Trondheim.

Qiu, Y., & Sego, D. (2001). Laboratory properties of mine tailings. *Canadian Geotechnical Journal*, 183-190.

Ray, R. M., & Wesson, T. C. (1982). Enhanced Oil Recovery Data Base Analysis by Simplified Predictive Models. *Society of Petroleum Engineers of AIME, SPE 11259*, 63-69.

Ren, S. R., Greaves, M., & Rathbone, R. (1999, April). Air Injection LTO Process: An IOR Technique for Light-Oil Reservoirs. *Society of Petroleum Engineers*, 90-98.

Rezaei, M., Schaffie, M., & Ranjbar, M. (2013). Thermocatalytic in situ combustion: Influence of nanoparticles on crude oil pyrolysis and oxidation. *Fuel* , 516-521.

Roduit, B. (2008). *Advanced Kinetics-based simulation method for determination of the thermal aging, thermal runaway TMRad and SADT using DSC.* Siders: AKTS AG.

Sakthikumar, S., Madaoui, K., & Chastang, J. (1996). An Investigation of the Feasibility of Air Injection into a Waterflood Light Oil Reservoir. *Society of Petroleum Engineers*, 343-356.

Sarathi, P. S. (1998). *In-situ Combustion Handbook - Principles and practices.* Bartlesville, Oklahoma: BDM Petroleum Technologies.

Sarma, H., & Das, S. (2009). Air Injection Potential in kenmore Oil Field in Eromanga Basin, Australia: A Screening Study Through Thermogravimetric and calometric Analyses. *SPE International, SPE 120595*, 1-8.

Schumacher, M. M. (1980). Enhanced recovery of residual and heavy oils. Noyes Data Corp., 1980 - Technology & Engineering. 0815508166, 9780815508168.

Shahani, G. H., & Hansel, J. G. (1987). Oxygen Fireflooding: Combustion Tube Tests with Light, medium and Heavy Crude Oils. *Society of Petroleum Engineers, SPE 12726*, 583-590.

Sheng, J. J. (2013). Enhanced Oil Recovery Field Case Studies. Gulf professional publishing, USA. ISBN 978-12-386545-8.

Shokoya, O. S., Mehta, S. A., Moore, R. G., Maini, B. B., Pooladi Darvish, M., & Chaka, A. (2004). The mechanism of flue gas injection for enhanced light oil recovery. *Journal of energy resources technology* , 119-124.

Shokrlu, Y. H., Maham, Y., Tan, X., Babadagli, T., & Gray , M. (2013). Enhancement of the efficiency of in situ combustion technique for heavy-oil recovery by application of nickel ions. *Fuel*, 397-407.

Sonibare, O., Alimi, H., Jarvie, D., & Ehinola, O. A. (2008). Origin and occurrence of crude oil in the Niger delta, Nigeria. *Journal of Petroleum Science and Engineering* , 99-107.

Sola, B. S and Rashidi, F. (2008). Experimental Study of Hot Water Injection into Low-Permeability Carbonate Rocks. Energy Fuels, 2008. V.22 (4) 2353–236. DOI: 10.1021/ef800009r.

Sorbie, K. S. (1991). Polymer-Improved Oil Recovery. Springer Science and Business Media, LLC. ISBN 978-94-010-5354-9. DOI 10.1007/978-94-011-3044-8.

Standing, M. B. (1947). *A Pressure-Volume-Temperature correlation for mixtures of California Oils and Sands.* Los Angeles: General Petroleum Corporation.

Statoil. (2012, February 16). *Microbial enhanced oil recovery (MEOR)*. Retrived from Statoil: http://www.statoil.com/en/TechnologyInnovation/OptimizingReservoirRecovery/RecoveryMethods/WaterAssistedMethodsImprovedOilRecoveryIOR/Pages/MicrobialEnhancedOilRecovery(MEOR).aspx

Surguchev, L. M., Alexander, K., & Yannimaras, D. (1998). Air Injection - Cost Effective IOR Method to Improve Oil Recovery from Depleted and Waterflooded Fields. *Society of Petroleum Engineers SPE 57296*, 1-10.

Taber, J.J., Martin, F.D., and Seright, R.S. (1997). EOR Screening Criteria Revisited: Part 2—Applications and Impact of Oil Prices, SPERE.

Tarek, A. (2006). *Reservoir Engineering Handbook.* Burlington: Gulf Professional Publishing.

Tarek, A. (2007). *Equation of State and PVT Analysis: Application for Improved Reservoir Modelling.* Houston, Texas: Gulf Publishing Company.

Teodori, C., Falcone, G., & Espinel, A. (2006). *Letting Off Steam and Getting Into Hot Water – Harnessing the Geothermal.* Texas: World Energy .

Teramoto, T., Uematsu, H., Takabayashi, H., & Onishi, T. (2006). Air Injection EOR in Highly Water Saturated Water Saturated Light-Oil Rerservoir. *Society of Petroleum Engineers SPE100215*, 1-10.

Thomas, S. (2008). Enhanced Oil Recovery - An Overview. *Oil & Gas Science and Technology* , 9-19.

TOTSA (2016). Crude Assays: Africa. Total Oil Trading SA. www.totsa.com

Tiffin, D. L. and Yanimaras, D. V.: "The In-situ Combustion Performance of Light Oils as a Function of Pressure," *In Situ* (1997) **21,** No. 1, 47.

Tiorco. (2009). *Alkaline Surfactant Polymer / Surfactant Polymer Technologies*. Retrieved February 10, 2012, from TIORCO: http://www.tiorco.com/pdf/cutsheet/ASP-SP_cutsheet.pdf

Trushenski, S. P., Duaben, D. L., & Parish, D. R. (1974). Miceller Flooding - Fluid Propagation, Interaction, and Mobility. *American Institute of Mining, Metallurgical and Petroleum Engineers, SPE 4582*, 633-645.

Turta, A. T., Chattopadhyay, S. K., Bhattacharya, R. N., Condrachi, A., & Hanson, W. (2007). Current Status of Commercial In Situ Combustion Projects Worldwide. *Journal of Canadian Petroleum Technology*, 1-7.

Turta, A., & Singhal, A. (2001). Reservoir Engineering Aspects of Light-Oil Recovery by Air Injection. *SPE Reservoir Evaluation & Engineering, SPE 72503*, 336-344.

Veld, K. V., & Phillips, O. R. (2010). The Economics of Enhanced Oil Recovery: Estimation Incremental Oil Supply and CO2 demand in the Power River BAsin. *The Energy Journal*, 31-56.

Wassmuth, F. (2012). *Technology Futures: Building globally competitive commerce in Alberta*. Retrieved February 10, 2012, from Alberta Innovates Technology Future: http://www.albertatechfutures.ca/RDSupport/UnconventionalNaturalGasandLightOilRecovery/EnhancedOilRecovery/PolymerFlooding/PolymerFloodingJIPforHeavyOils.aspx

Waziri, N. M. (2014). Environmental Geochemistry of Soils and Stream Sediments from the Birnin-Gwari Artisanal Gold Mining Area, North-western Nigeria. *Universal Journal of Geoscience* 2(1): 18-27.

Worden, R. H., & Smalley, P. (1996). H2S-producing reactions in deep carbonate gas reservoirs: Khuff Formation, Abu Dhabi. *Chemical Geology*, 157-171.

Xia, T., Greaves, M., & Rathbone, R. R. (2004). *Air Injection: Maximising IOR Benefit from UKCS Light Oil Fields.* Bath: DTI Licencing.

Yannimaras, D. V., & Tiffin, D. L. (1995). Screening of Oils for In-Situ Combustion at Reservoir Conditions via Accelerating Rate Calorimetry. *SPE Reservoir Engineering*, 1-4.

Yin, D., Zhou, Y., & Peng, B. (2010). The Study Of Foam Flooding In High Water Cut Stage Using Computer Numerical Simulation. *IEEE*, 517-520.

Zhang, A., Ma, Q., Wang, K., Liu, X., Shuler, P., & Tang, Y. (2006). Naphthenic acid removal from crude oil through catalytic decarboxylation on magnesium oxide. *Applied Catalysis A: General* , 103-109.

Zhu, C., Fengshan, Z., & Zhou, J. Z. (2001). An EOR Application @ Liaohe Oil Field in China: Test of Pumping Flue Gas Into Oil Wells. *First National Conference on Carbon Sequestration*, (pp. 1-10). Washinton DC.

Zick, A. A. (1986). A Combined Condensing/Vaporizing Mechanism in the Displacement of Oil by Enriched Gases. *Society of Petrleum Engineers, SPE 15493*, 1-11.

APPENDICES

Appendix A: Mineral Liberation Analysis (MLA) of Tailings

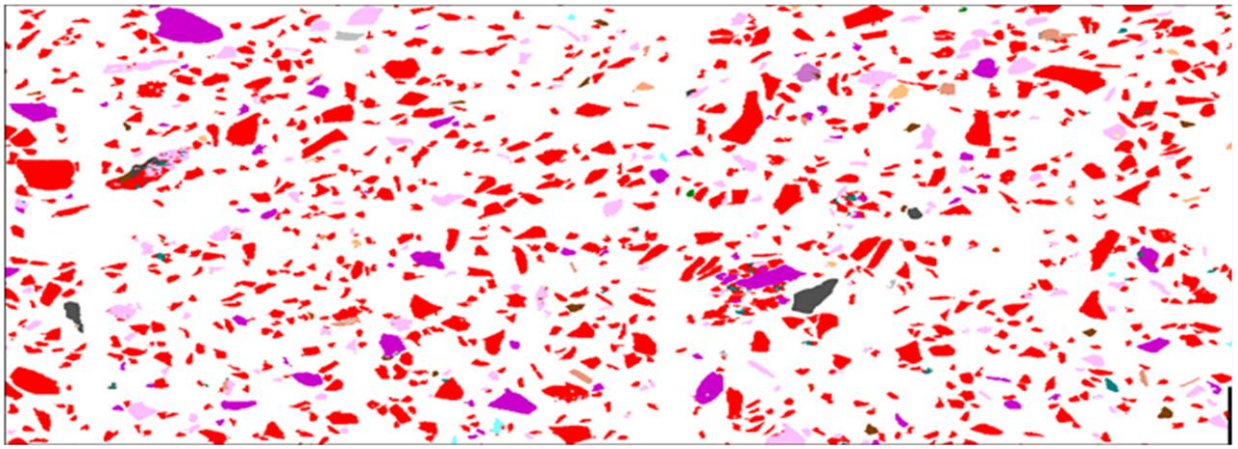


Plate A.1: Backscatter image of Tailings

Legend: Mineral Liberation Analyser color code

Name	Pixels
Pyrrhotite	7523513
Magnetite	965513
Plagioclase	753051
Amphibole	270164
Olivine	168870
Cpx	110058
Orthoclase	108573
Biotite	78373

Biotite	78373
Unknown	63996
Albite	57319
Opx	53005
Quartz	45823
Chlorite	29161
Ilmenite	21677
Pumic-glass	19803
Ti-magnetite	19001

Ti-magnetite	19001
Pentlandite	18851
Garnet	16332
Apatite	15696
Chalcopyrite	13852
Cordierite	10589
Celadonite	10192
Ferrosilite	9379
Perthite	7189
Epidote	7031

Epidote	7031
Knebelite	6823
Pyrite	3063
Spinel	2711
Muscovite	1293
Dolomite	1063
Calcite	812
Titanite	332
Tourmaline	310
Macaulayite	310
Serpentine	162
Zircon	127

Appendix B: Data from Accelerating Rate calorimetry (ARC)

Table B.1: Summary of ARC's reproducibility tests.

Tailings amount (%)	Trial	T_{onset} (°C)	T_{end} (°C)	T_{range} (°C)	P_{onset} (bar)	P_{end} (bar)	P_{range} (bar)
0.0	a	146.1	165.4	19.3	11.8	11.3	0.6
0.0	b	149.9	187.0	37.0	12.1	8.4	3.7
0.0	**Mean**	**148.0**	**176.2**	**28.2**	**11.9**	**9.8**	**2.1**
5.0	a	149.2	167.1	17.9	11.8	10.8	0.9
5.0	b	149.0	168.9	19.8	12.2	11.3	0.9
5.0	c	150.0	176.4	26.5	11.1	7.6	3.5
5.0	**Mean**	**149.4**	**170.8**	**21.4**	**11.7**	**9.9**	**1.8**
10.0	a	120.0	138.4	18.4	12.9	11.4	1.5
10.0	b	143.0	167.4	24.4	12.6	11.7	0.9
10.0	**Mean**	**131.5**	**152.9**	**21.4**	**12.7**	**11.5**	**1.2**
20.0	a	72.7	270.2	197.4	11.0	4.2	6.8
20.0	b	127.9	189.0	61.1	10.5	6.1	4.4
20.0	c	143.0	191.6	48.5	12.5	10.9	1.6
20.0	d	106.6	127.0	20.4	11.4	11.3	0.1
20.0	e	117.7	155.5	37.8	10.6	10.6	0.0
20.0	f	126.0	144.5	18.4	11.1	9.7	1.4
20.0	**Mean**	**115.7**	**179.6**	**63.9**	**11.2**	**8.8**	**2.4**
30.0	a	149.8	155.8	6.0	11.9	11.7	0.2
30.0	b	147.8	165.1	17.3	12.1	11.4	0.7
30.0	**Mean**	**148.8**	**160.4**	**11.6**	**12.0**	**11.6**	**0.4**
40.0	a	135.9	150.5	14.5	12.3	11.6	0.7
40.0	b	150.0	170.2	20.2	12.2	11.6	0.7
40.0	**Mean**	**143.0**	**160.3**	**17.4**	**12.3**	**11.6**	**0.7**

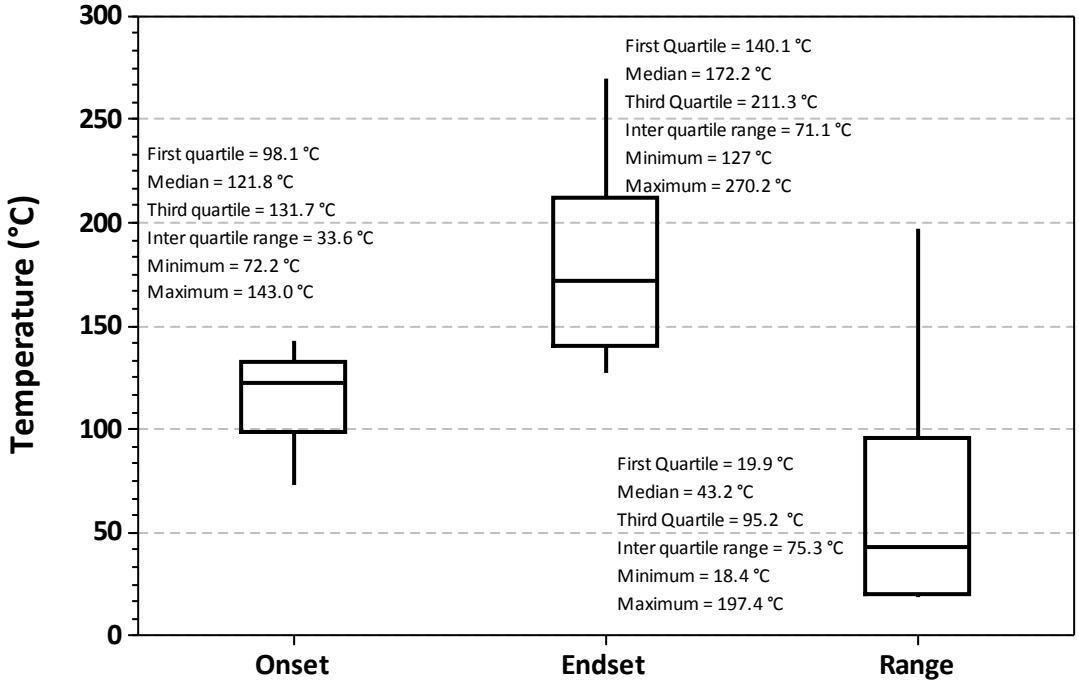


Figure B1: Box plot of the summary of ARC data on 20% tailings with oil

Appendix C: Property of Nigerian Crude oil

Compound	Reservoir fluid	Residual gas	Stock tank oil	Molecular weight (g/mol)	Density (kg/m^3)
Hydrogen sulfide	0.383	0.77	0		
Nitrogen	0.45	0.91	0		
Carbon dioxide	2.07	4.18	0		
Methane	26.576	53.74	0		
Ethane	7.894	15.66	0.29		
Propane	6.73	12.34	1.24		
i-Butane	1.485	2.31	0.68		
n-Butane	3.899	5.05	2.78		
i-Pentanes	1.937	1.72	2.15		
n-Pentane	2.505	1.61	3.39		
i-Hexanes	1.783	-	-	86.2	679.4
n-Hexane	1.568	0.96	5.7		
i-Heptanes	0.531	-	-	92.6	726.2
Benzene	0.538	-	-		
Cyclanes C7	2.229	-	-		
n-Heptane	1.013	0.7	7.84		
i-Octanes	1.215	-		108.9	750.9
Toluene	1.004	-	-		
Cyclanes C8	1.065	-	-		
n-Octane	0.849	0.05	8.13		
i-Nonanes	0.866	-	-	120.1	771.6
Aromatics C9	1.043	-		-	
Cyclanes C9	0.62	-		-	
n-Nonane	0.522	0	6		
i-Decanes	1.267	-	-	137.9	787.8
Aromatics C10	0.433	-		-	
n-Decane	0.333	0	4.02		
Undecanes	2.635	0	5.215	149	803.7
Dodecanes	2.285	0	4.523	163	815.4
Tridecanes	2.364	0	4.679	177	827
Tetradecanes	2.038	0	4.034	191	841.2
Pentadecanes	1.752	0	3.468	205	858.8
Hexadecanes	1.589	0	3.145	219	862.7
Heptadecanes	1.492	0	2.953	234	858.6
Octadecanes	1.263	0	2.5	248	864.8
Nonadecanes	0.812	0	1.607	263	877.1

Eicosanes plus	12.962	0	25.656	450	956

Table C.1: Paraffins, Napthenes and Aromatics content of the Nigerian reservoir fluid (394.25K and 145.8 bar)

Table C.2: Isothermal constant mass expansion of the Nigerian crude: T=394.25K; Psat=145.8 bar

Pressure (bar)	Relative volume	Density (kg/m3)
500.5	0.946	762.777
450.5	0.951	758.725
400	0.957	753.58
351	0.964	748.503
300.5	0.972	742.39
250.5	0.98	735.835
200	0.989	729.395
160	0.997	723.589
145.8	1	721.501
144	1.003	719.424
138	1.016	709.723
132	1.032	699.301
123	1.059	681.199
112	1.103	654.022
94	1.211	595.948
78	1.371	526.316
62	1.652	436.872
50	2.023	356.633

Table C.3: Isothermal differential vaporization test of the crude at 394.25K

Pressure (bar)	Relative volume	Density (kg/m3)	Gas to Oil Ratio	Gas compressibility
351.0000	0.9644	748.3	–	–
300.5000	0.9716	742.4	–	–
250.5000	0.98	736.2	–	–
200.0000	0.989	729.3	–	–
160.0000	0.9974	723.6	–	–
145.8000	1	721.5	0	–
114.8000	0.9638	732	20.8	0.819
86.5000	0.9282	743.8	41.4	0.836
60.0000	0.8927	757.4	60.5	0.859
34.8000	0.8565	769.8	79.8	0.886
16.0000	0.8222	780.4	97.2	0.919
1.0000	0.6852	831	132.9	1

Table C.4: First isothermal swelling tests of the crude

100*Xgas	Psat (bar)	Psat (kg/m3)	V swell
0	145.8	721.6	1
23.08	225.6	672.6	1.122
33.33	276.5	649.8	1.195
39.39	316.4	636.6	1.245
42.86	335.1	627.3	1.281

Appendix D: Characterisation of modelled crude using Soave-Redlich-Kwong (SRK) Equation of State

Table D.1: Properties of characterized crude oil using SRK Equation of State

Component	Mol %	Mol wt	Liquid Density g/cm³	Crit T °C	Crit P bara	Acentric factor -	Normal Tb °C	Wt av Mol wt
N2	0.45	28.014		-146.95	33.94	0.04	-195.75	28.014
O2	0.1	31.999		-118.55	50.46	0.021	-182.95	31.999
CO2	2.068	44.01		31.05	73.76	0.225	-78.5	44.01
H2S	0.383	34.08		100.05	89.37	0.1	-59.65	34.08
C1	26.549	16.043		-82.55	46	0.008	-161.55	16.043
C2	7.886	30.07		32.25	48.84	0.098	-88.55	30.07
C3	6.723	44.097		96.65	42.46	0.152	-42.05	44.097
iC4	1.484	58.124		134.95	36.48	0.176	-11.75	58.124
nC4	3.895	58.124		152.05	38	0.193	-0.45	58.124
iC5	1.935	72.151		187.25	33.84	0.227	27.85	72.151
nC5	2.502	72.151		196.45	33.74	0.251	36.05	72.151
C6	3.348	86.178	0.664	234.25	29.69	0.296	68.75	86.178
C7	4.307	96	0.738	262.184	31.95	0.4679	91.95	96
C8	4.129	107	0.765	282.716	29.76	0.4999	116.75	107
C9	3.048	121	0.781	304.023	26.67	0.5399	142.25	121
C10-C11	4.663	141.338	0.7943	330.863	23.16	0.5975	178.414	141.632
C12	2.283	161	0.81	354.576	21.04	0.6504	208.35	161
C13	2.362	175	0.825	371.217	20.17	0.6878	227.25	175
C14	2.036	190	0.836	387.457	19.25	0.727	246.45	190
C15	1.75	206	0.842	403.116	18.24	0.7678	265.85	206
C16	1.587	222	0.849	418.308	17.48	0.8076	282.85	222
C17	1.491	237	0.845	430.338	16.47	0.8439	299.85	237
C18	1.262	251	0.848	442.295	15.93	0.8769	312.85	251
C19-C20	13.76	274.293	0.8627	463.111	15.56	0.9301	337.115	274.322

Table D.1 Cont'd: Properties of characterized crude oil using SRK Equation of State

Component	Crit V cm³/mol	Pvap model	M & C (SRK) C1 -	M & C (SRK) C2 -	M & C (SRK) C3 -	Cpen cm³/mol	CpenT cm³/mol°C	Href J/mol
N2	89.8	Classic	0.543	-0.052	-0.338	0.92	0	8330.8
O2	73.4	Classic	0.546	-0.245	0.339	0.58	0	11103.1
CO2	94	Classic	0.865	-0.439	1.345	3.03	6.69E-03	19459.1
H2S	98.5	Classic	0.551	0.453	-0.584	1.78	0	12550.9
C1	99	Classic	0.586	-0.721	1.29	0.63	0	2.6
C2	148	Classic	0.718	-0.764	1.64	2.63	0	9761.1
C3	203	Classic	0.786	-0.746	1.845	5.06	0	19519.6
iC4	263	Classic	0.24	3.836	-8.045	7.29	0	29278.1
nC4	255	Classic	0.879	-0.94	2.267	7.86	0	29278.1
iC5	306	Classic	0.828	0	0	10.93	0	39036.6
nC5	304	Classic	1.028	-2.562	6.248	12.18	0	39036.6
C6	370	Classic	0.93	0	0	17.98	0	48795.1
C7	475.55	Classic				9.65	1.49E-02	55628.2
C8	487.84	Classic				13.9	0.01	63280.8
C9	529.18	Classic				20.99	2.15E-03	73020.6
C10-C11	605.03	Classic				31.13	-1.25E-02	87169.7
C12	675.17	Classic				37.77	-2.65E-02	100848.3
C13	724.05	Classic				39.51	-3.58E-02	110588
C14	782.99	Classic				41.41	-4.71E-02	121023.4
C15	852.15	Classic				43.98	-6.11E-02	132154.5
C16	921.41	Classic				44.91	-7.48E-02	143285.6
C17	994.43	Classic				49.11	-9.25E-02	153721
C18	1057.94	Classic				49.57	-0.11	163460.7
C19-C20	1159.54	Classic				44.2	-0.12	179665.2

Table D.1 Cont'd: Properties of characterized crude oil using SRK Equation of State

Component	1. Cp-con J/mol C	2. Cp-con J/mol C^2	3. Cp-con J/mol C^3	4. Cp-con J/mol C^4	Tf °C	Delta Tf wax °C	Hf J/mol
N2	3.11E+01	-1.36E-02	2.68E-05	-1.17E-08			
O2	2.81E+01	-3.68E-06	1.75E-05	-1.07E-08	-218.75		
CO2	1.98E+01	7.34E-02	-5.60E-05	1.72E-08			
H2S	3.19E+01	1.44E-03	2.43E-05	-1.18E-08			
C1	1.93E+01	5.21E-02	1.20E-05	-1.13E-08			
C2	5.41E+00	1.78E-01	-6.94E-05	8.71E-09			
C3	-4.22E+00	3.06E-01	-1.59E-04	3.22E-08			
iC4	-1.39E+00	3.85E-01	-1.85E-04	2.90E-08			
nC4	9.49E+00	3.31E-01	-1.11E-04	-2.82E-09			
iC5	-9.52E+00	5.07E-01	-2.73E-04	5.72E-08			
nC5	-3.63E+00	4.87E-01	-2.58E-04	5.31E-08			
C6	-4.41E+00	5.82E-01	-3.12E-04	6.49E-08			
C7	-9.59E+00	5.76E-01	-2.05E-04	0.00E+00	-106.263	0	9565.2
C8	-4.92E+00	6.13E-01	-2.35E-04	0.00E+00	-84.373	0	12059.6
C9	-1.88E+00	6.80E-01	-2.70E-04	0.00E+00	-62.194	0	15239.8
C10-C11	2.21E+00	7.91E-01	-3.19E-04	0.00E+00	-37.658	0	19939.7
C12	3.42E+00	8.98E-01	-3.64E-04	0.00E+00	-19.729	0	24359.6
C13	2.76E+00	9.72E-01	-3.96E-04	0.00E+00	-9.339	0	27563.4
C14	2.69E+00	1.06E+00	-4.31E-04	0.00E+00	0.154	0	31002.8
C15	3.65E+00	1.15E+00	-4.67E-04	0.00E+00	8.819	0	34679.3
C16	4.84E+00	1.24E+00	-5.03E-04	0.00E+00	16.295	0	38363.7
C17	8.09E+00	1.34E+00	-5.37E-04	0.00E+00	22.438	0	41825.1
C18	9.29E+00	1.42E+00	-5.69E-04	0.00E+00	27.552	0	45062.1
C19-C20	9.15E+00	1.55E+00	-6.22E-04	0.00E+00	34.977	0	50460.9

Table D.1 Cont'd: Properties of characterized crude oil using SRK Equation of State

Component	P fraction	N fraction	A fraction	Wax fraction	Asp fraction	Parachor	Forms hydrates	A I Small °C/bara
N2						41	I & II & H	5.28E-02
O2						0	I & II	1.72E-02
CO2						78	I & II	4.86E-11
H2S						80.1	I & II	9.93E-03
C1						77.3	I & II & H	4.79E-02
C2						108.9	I & II	0.00E+00
C3						151.9	II	
iC4						181.5	II	
nC4						191.7	II	
iC5						225	H	
nC5						233.9	None	
C6						271	None	
C7	0.546	0.348	0.106	0.348	0	283.9	None	
C8	0.512	0.347	0.141	0.291	0	309.7	None	
C9	0.536	0.323	0.141	0.27	0	342.4	None	
C10-C11	0.58	0.295	0.125	0.257	0	390.7	None	
C12	0.583	0.285	0.131	0.237	0	436	None	
C13	0.555	0.29	0.155	0.214	0	468.8	None	
C14	0.542	0.29	0.167	0.199	0	503.9	None	
C15	0.549	0.286	0.165	0.193	0	541.3	None	
C16	0.546	0.286	0.168	0.183	0	578.8	None	
C17	0.59	0.271	0.139	0.193	0	613.9	None	
C18	0.596	0.269	0.136	0.189	0	646.6	None	
C19-C20	0.601	0.246	0.153	0.164	0	701.2	None	

Table D.1 Cont'd: Properties of characterized crude oil using SRK Equation of State

Component	B I Small °C	A I Large °C/bara	B I Large °C	A II Small °C/bara	B II Small °C	A II Large °C/bara	B II Large °C	A H Small °C/bara
N2	659.2	3.42E-02	1966.9	7.51E-03	1730.9	9.48E-02	1322.9	1.32E-05
O2	2016.2	5.70E-02	1662.3	9.80E-02	1045.9	2.68E-03	2563.9	
CO2	7196.9	9.86E-02	2343.9	6.08E-05	3417.9	1.68E-01	2317.9	
H2S	2725.9	1.61E-02	3463.9	2.68E-04	3968.9	8.55E-01	2051.9	
C1	1320.9	1.24E-02	2678.9	2.32E-03	2503.9	1.08E+00	1049.9	2.76E-04
C2	-273.2	3.00E-03	3587.9	0.00E+00	-273.2	7.36E-03	3726.9	
C3				0.00E+00	-273.2	8.26E-03	4247.9	
iC4				0.00E+00	-273.2	8.19E-02	3739.9	
nC4				0.00E+00	-273.2	1.26E-03	4306.9	
iC5								
nC5								
C6								
C7								
C8								
C9								
C10-C11								
C12								
C13								
C14								
C15								
C16								
C17								
C18								
C19-C20								

Table D.1 Cont'd: Properties of characterized crude oil using SRK Equation of State

Component	B H Small °C	A H Huge °C/bara	B H Huge °C	Ions	Crystal Water	Crit P wax bara	Omega A	Omega B
N2	3521.9						0.42748	0.08664
O2							0.42748	0.08664
CO2							0.42748	0.08664
H2S							0.42748	0.08664
C1	3116.9						0.42748	0.08664
C2							0.42748	0.08664
C3							0.42748	0.08664
iC4							0.42748	8.66E-02
nC4							0.42748	0.08664
iC5		1.64E+04	1425.9				0.42748	0.08664
nC5							0.42748	0.08664
C6							0.42748	0.08664
C7						31.95	0.42748	8.66E-02
C8						29.76	0.42748	8.66E-02
C9						26.67	0.42748	8.66E-02
C10-C11						23.16	0.42748	8.66E-02
C12						21.04	0.42748	8.66E-02
C13						20.17	0.42748	8.66E-02
C14						19.25	0.42748	8.66E-02
C15						18.24	0.42748	8.66E-02
C16						17.48	0.42748	8.66E-02
C17						16.47	0.42748	8.66E-02
C18						15.93	0.42748	8.66E-02
C19-C20						15.56	0.42748	8.66E-02

Table D.1 Cont'd: Properties of characterized crude oil using SRK Equation of State

Component	Size PC-SAFT	Diameter PC-SAFT Angstrom	Energy PC-SAFT K	Size asp PC-SAFT	Diam asp PC-SAFT Angstrom	Energy asp PC-SAFT K	Asp fraction PC-SAFT
N2	1.21	3.31	90.96				
O2	1.12	3.21	114.96				
CO2	2.07	2.79	169.21				
H2S	1.69	3.02	226.79				
C1	1	3.7	150.03				
C2	1.61	3.52	191.42				
C3	2	3.62	208.11				
iC4	2.26	3.76	216.53				
nC4	2.33	3.71	222.88				
iC5	2.56	3.83	230.75				
nC5	2.69	3.77	231.2				
C6	3.06	3.8	236.77				
C7	3.16	3.79	254.04	3	3.69	333.79	0
C8	3.45	3.78	257.89	3.16	3.76	343.96	0
C9	3.88	3.78	258.12	3.36	3.84	355.5	0
C10-C11	4.51	3.78	256.7	3.65	3.93	369.96	0
C12	5.1	3.77	257.18	3.94	4	382.3	0
C13	5.49	3.77	259.24	4.14	4.04	390.12	0
C14	5.93	3.77	260.26	4.36	4.08	397.83	0
C15	6.42	3.77	259.91	4.59	4.12	405.42	0
C16	6.89	3.77	260.18	4.82	4.16	412.44	0
C17	7.41	3.77	257.27	5.04	4.18	418.57	0
C18	7.85	3.76	256.85	5.24	4.21	423.96	0
C19-C20	8.47	3.77	260.03	5.58	4.24	432.28	0

Table D.2: Interaction Parameters [kij(-)] of components of modelled crude

N2	N2	O2	CO2	H2S	C1	C2	C3	iC4
O2	-0.0078							
CO2	-0.0315	0						
H2S	0.1696	0	0.0989					
C1	0.0278	0	0.12	0.08				
C2	0.0407	0	0.12	0.0852	0			
C3	0.0763	0	0.12	0.0885	0	0		
iC4	0.0944	0	0.12	0.0511	0	0	0	
nC4	0.07	0	0.12	0.06	0	0	0	0
iC5	0.0867	0	0.12	0.06	0	0	0	0
nC5	0.0878	0	0.12	0.0689	0	0	0	0
C6	0.08	0	0.12	0.05	0	0	0	0
C7	0.08	0	0.1	0	0	0	0	0
C8	0.08	0	0.1	0	0	0	0	0
C9	0.08	0	0.1	0	0	0	0	0
C10-C11	0.08	0	0.1	0	0	0	0	0
C12	0.08	0	0.1	0	0	0	0	0
C13	0.08	0	0.1	0	0	0	0	0
C14	0.08	0	0.1	0	0	0	0	0
C15	0.08	0	0.1	0	0	0	0	0
C16	0.08	0	0.1	0	0	0	0	0
C17	0.08	0	0.1	0	0	0	0	0
C18	0.08	0	0.1	0	0	0	0	0
C19-C20	0.08	0	0.1	0	0	0	0	0

Table D.2 Cont'd: Interaction Parameters [kij(-)] of components of modelled crude

N2	nC4	iC5	nC5	C6	C7	C8	C9	C10-C11
O2								
CO2								
H2S								
C1								
C2								
C3								
iC4								
nC4								
iC5	0							
nC5	0	0						
C6	0	0	0					
C7	0	0	0	0				
C8	0	0	0	0	0			
C9	0	0	0	0	0	0		
C10-C11	0	0	0	0	0	0	0	
C12	0	0	0	0	0	0	0	0
C13	0	0	0	0	0	0	0	0
C14	0	0	0	0	0	0	0	0
C15	0	0	0	0	0	0	0	0
C16	0	0	0	0	0	0	0	0
C17	0	0	0	0	0	0	0	0
C18	0	0	0	0	0	0	0	0
C19-C20	0	0	0	0	0	0	0	0

Table D.2 Cont'd: Interaction Parameters [kij(-)] of components of modelled crude

N2	C12	C13	C14	C15	C16	C17	C18	C19-C20
O2								
CO2								
H2S								
C1								
C2								
C3								
iC4								
nC4								
iC5								
nC5								
C6								
C7								
C8								
C9								
C10-C11								
C12								
C13	0							
C14	0	0						
C15	0	0	0					
C16	0	0	0	0				
C17	0	0	0	0	0			
C18	0	0	0	0	0	0		
C19-C20	0	0	0	0	0	0	0	

Table D.3: Interaction Parameters [kij A (-)]of components of the modelled crude

N2	N2	O2	CO2	H2S	C1	C2	C3
O2	-0.0078						kij (-)
CO2	-0.0315	0					
H2S	0.1696	0	0.0989				
C1	0.0278	0	0.12	0.08			
C2	0.0407	0	0.12	0.0852	0		
C3	0.0763	0	0.12	0.0885	0	0	
iC4	0.0944	0	0.12	0.0511	0	0	0
nC4	0.07	0	0.12	0.06	0	0	0
iC5	0.0867	0	0.12	0.06	0	0	0
nC5	0.0878	0	0.12	0.0689	0	0	0
C6	0.08	0	0.12	0.05	0	0	0
C7	0.08	0	0.1	0	0	0	0
C8	0.08	0	0.1	0	0	0	0
C9	0.08	0	0.1	0	0	0	0
C10-C11	0.08	0	0.1	0	0	0	0
C12	0.08	0	0.1	0	0	0	0
C13	0.08	0	0.1	0	0	0	0
C14	0.08	0	0.1	0	0	0	0
C15	0.08	0	0.1	0	0	0	0
C16	0.08	0	0.1	0	0	0	0
C17	0.08	0	0.1	0	0	0	0
C18	0.08	0	0.1	0	0	0	0
C19-C20	0.08	0	0.1	0	0	0	0

Table D.4: Interaction Parameters of crude oil components based on The Huron and Vidal Mixing Rule g/R (K)

N2	N2	O2	CO2	H2S	C1	C2	C3	iC4	nC4	iC5	nC5	C6	C7
O2	-52.99		436.86	737.78	91.19	478.14	806.11	1046.86	1147.42	1407.61	1486.76	1818.53	0
CO2	-257.42	-236.92		334.8	-128.94	147.73	423.66	643.43	729.22	973.79	1045.65	1365.23	0
H2S	-236.97	-339.19	-68.39		-273.54	-54.23	200.75	362.28	450.17	687.89	768.19	1055.5	0
C1	-99.3	-66.53	387.12	645.72		331.68	629.29	855.53	949.08	1198.43	1273.69	1596.39	0
C2	-216.18	-214.24	129.14	330.37	-202.98		220.32	405.16	482.2	699.2	764.36	1057.96	0
C3	-244.82	-264.72	26.61	206.89	-283.83	-158.13		142.4	209.8	391.46	448.52	706.75	0
iC4	-247.84	-274.9	-4.55	117.49	-308.52	-224.23	-108.53		62.16	213.93	265.08	491.11	0
nC4	-276.49	-296.46	-40.89	83.26	-337.09	-269.31	-163.25	-59.96		147.5	197.31	419.32	0
iC5	-276.64	-303.87	-63.91	53.37	-355.34	-319.91	-249.19	-175.79	-120.1		44.53	235.77	0
nC5	-283.05	-312.58	-79.9	45.83	-367.93	-342.59	-279.98	-212.49	-158.14	-43.32		185.52	0
C6	-292.37	-315.66	-95.18	-1.72	-380.08	-383.85	-356.61	-321.31	-270.97	-186.93	-149.33		0
C7	0	0	0	0	0	0	0	0	0	0	0	0	

NB: Interaction parameters of the other components = 0

Table D.5: Interaction Parameters kij A (-) of the crude oil components

N2	N2	O2	CO2	H2S	C1	C2
O2	-0.0078					
CO2	-0.0315	0				
H2S	0.1696	0	0.0989			
C1	0.0278	0	0.12	0.08		
C2	0.0407	0	0.12	0.0852	0	
C3	0.0763	0	0.12	0.0885	0	0
iC4	0.0944	0	0.12	0.0511	0	0
nC4	0.07	0	0.12	0.06	0	0
iC5	0.0867	0	0.12	0.06	0	0
nC5	0.0878	0	0.12	0.0689	0	0
C6	0.08	0	0.12	0.05	0	0
C7	0.08	0	0.12	0	0.03	0
C8	0.08	0	0.12	0	0.03	0
C9	0.08	0	0.12	0	0.03	0
C10-C11	0.08	0	0.12	0	0.03	0
C12	0.08	0	0.12	0	0.03	0
C13	0.08	0	0.12	0	0.03	0
C14	0.08	0	0.12	0	0.03	0
C15	0.08	0	0.12	0	0.03	0
C16	0.08	0	0.12	0	0.03	0
C17	0.08	0	0.12	0	0.03	0
C18	0.08	0	0.12	0	0.03	0
C19-C20	0.08	0	0.12	0	0.03	0

Table D.5 Cont'd: Interaction Parameters kij A (-) of the crude oil components

N2	N2	O2	CO2	H2S	C1
O2	-0.0078				
CO2	-0.0315	0			
H2S	0.1696	0	0.0989		
C1	0.0278	0	0.12	0.08	
C2	0.0407	0	0.12	0.0852	0
C3	0.0763	0	0.12	0.0885	0
iC4	0.0944	0	0.12	0.0511	0
nC4	0.07	0	0.12	0.06	0
iC5	0.0867	0	0.12	0.06	0
nC5	0.0878	0	0.12	0.0689	0
C6	0.08	0	0.12	0.05	0
C7	0.08	0	0.1	0	0
C8	0.08	0	0.1	0	0
C9	0.08	0	0.1	0	0
C10-C11	0.08	0	0.1	0	0
C12	0.08	0	0.1	0	0
C13	0.08	0	0.1	0	0
C14	0.08	0	0.1	0	0
C15	0.08	0	0.1	0	0
C16	0.08	0	0.1	0	0
C17	0.08	0	0.1	0	0
C18	0.08	0	0.1	0	0
C19-C20	0.08	0	0.1	0	0

NB: Other parameters = 0;

Interaction parameters based on kij B (-) and kij C (-) = 0 entries, therefore table not shown.

Appendix E: Characterisation of modelled crude to 3 pseudo-components

Table E.1: Properties of Characterized oil in 3 Pseudo components

Component	Mol %	Mol wt	Liquid Density g/cm³	Crit T °C	Crit P bara	Acentric factor -	Normal Tb °C	Wt av Mol wt	Crit V cm³/mol	Pvap model
Def_1	35.368	19.563		-41.102	47.59	4.12E-02	-135.332	21.482	115.5	Classic
Def_2	21.955	59.612		157.959	38.53	0.2192	7.263	63.58	270.1	Classic
Def_3	42.677	192.327	0.8319	405.688	19.16	0.787	267.835	216.987	919.97	Classic

Component	M & C (SRK) C1	M & C (SRK) C2	M & C (SRK) C3	Cpen cm³/mol	CpenT cm³/mol°C	Href J/mol	1. Cp-con J/mol C	2. Cp-con J/mol C^2	3. Cp-con J/mol C^3
Def_1	0.629	-0.699	1.34	1.09	0	2451.5	1.50E+01	9.29E-02	-1.54E-05
Def_2	0.841	-0.463	1.236	8.81	6.30E-04	30313.2	-5.20E-01	4.07E-01	-2.05E-04
Def_3				34.31	-5.58E-02	122642.5	5.05E+00	1.22E+00	-4.90E-04

Component	4. Cp-con J/mol C^4	Tf °C	Hf J/mol	P fraction	N fraction	A fraction	Wax fraction	Asp fraction	Parachor	Forms hydrates
Def_1	-4.46E-09								87.2	None
Def_2	3.76E-08								201	None
Def_3	0.00E+00	-8.774	33706.1	0.569	0.288	0.143	0.225	0	567	None

Component	Crit P wax bara	Omega A	Omega B	Size PC-SAFT	Diameter PC-SAFT Angstrom	Energy PC-SAFT K	Size asp PC-SAFT	Diam asp PC-SAFT Angstrom	Asp fraction PC-SAFT
Def_1		0.42748	8.66E-02	1.15	3.65	158.61			
Def_2		0.42748	0.08664	2.37	3.63	216.21			
Def_3	20.42	0.42748	8.66E-02	6.03	3.77	258.34			0

Table E.2: Interaction parameters of Pseudo-components

Component	Def_1	Def_2	Def_3
Def_1	Classic		
Def_2	Classic	Classic	
Def_3			

Table E.3: Interaction parameters of Pseudo-components [kij (-)]

Component	Def_1	Def_2	Def_3
Def_1	0.023		
Def_2	0.0525	0.0259	
Def_3			

Table E.4: Interaction Parameters of pseudo-components based on The Huron and Vidal Mixing Rule HV g/R (K)

Component	Def_1	Def_2	Def_3
Def_1		849.31	0
Def_2	-285.98		0
Def_3	0	0	

Table E.5: Interaction parameters of Pseudo-components Mixing Rule kij A (-)

Component	Def_1	Def_2	Def_3
Def_1	0.023		
Def_2	0.0525	0.0259	
Def_3			

NB: Kij B = kij C = 0, therefore kij A = kij

Appendix F: Equation of State (EOS) tuning of PVT tests

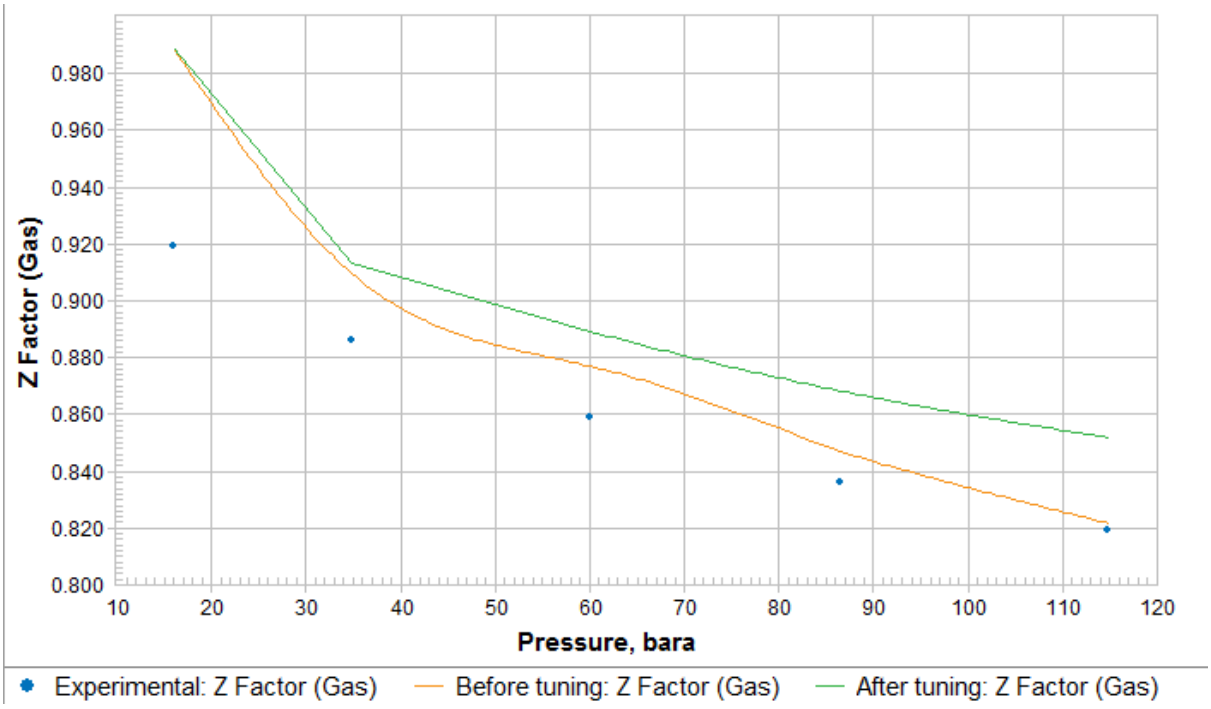


Figure F.1: Tuned Z-factor as a function of Pressure in the differential depletion experiment

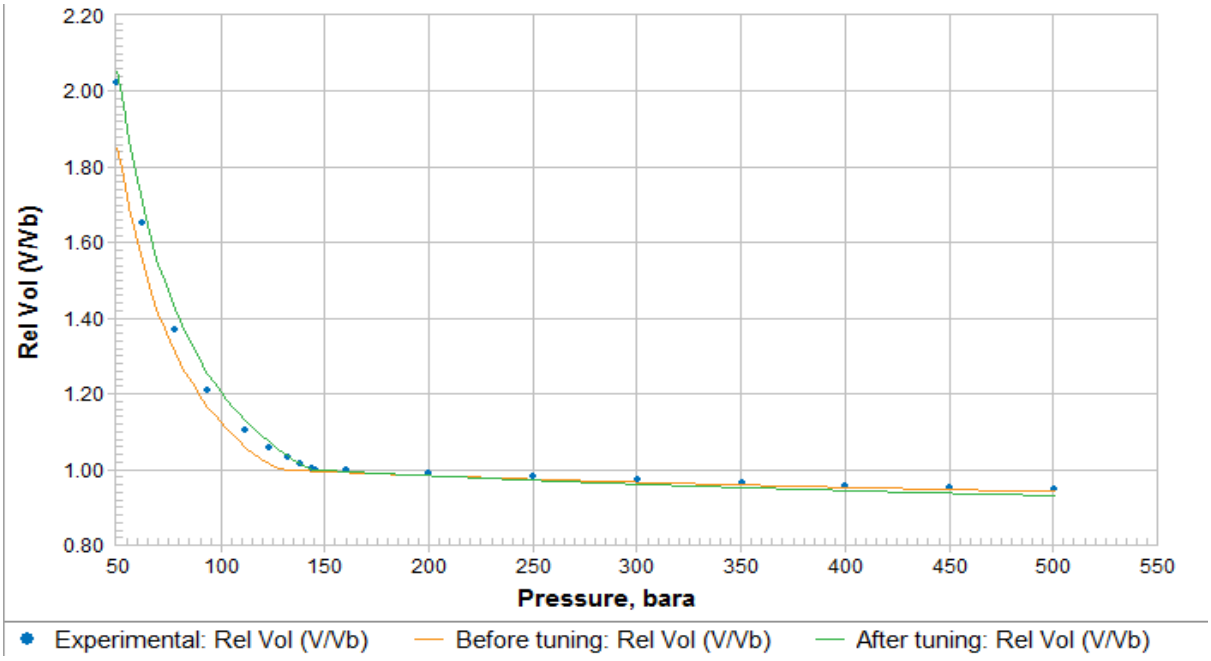


Figure F.2: Tuned Relative volume as a function of Pressure in constant mass expansion experiment

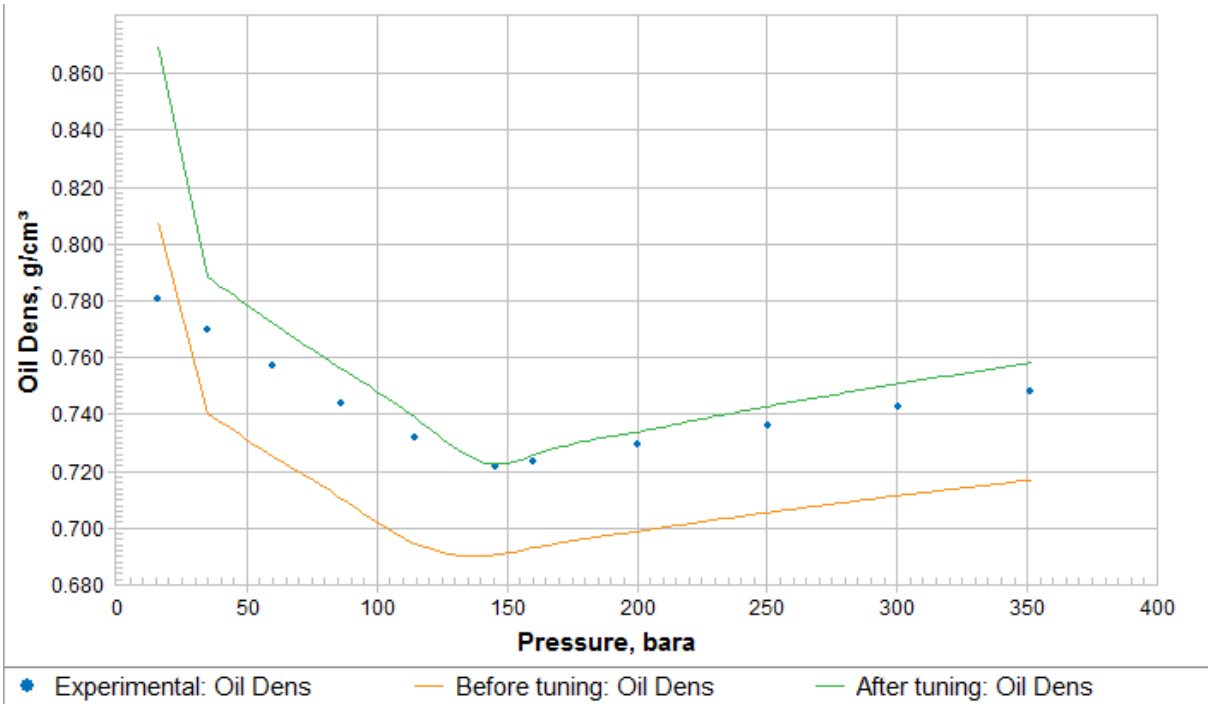


Figure F.3: Tuned Oil density as a function of Pressure in differential depletion experiment

Appendix G: Regression results of oil characterisation

Table G.1: General regression results of tuned oil properties

Objective function	**Before tuning**	**After tuning**	
	0.7458	0.5211	
Corr fac 1: Crit P (bara). Max adjustment: 20.00%.			
	Before tuning	**After tuning**	**%Adjustment**
CO2	73.7646	84.02972	13.91606
Def_1	47.59235	54.21533	13.91606
Def_2	38.53212	43.89428	13.91606
Def_3	19.16299	21.82973	13.91607
Corr fac 2: Acentric factor. Max adjustment: 20.00%.			
	Before tuning	**After tuning**	**%Adjustment**
CO2	0.225	0.27	19.99999
Def_1	0.041222	0.049467	20
Def_2	0.21915	0.262981	20
Def_3	0.786964	0.944357	20
Corr fac 3: Crit V (cm^3/mol). Max adjustment: 50.00%.			
	Before tuning	**After tuning**	**%Adjustment**
CO2	94	94	0
Def_1	115.4987	115.4987	0
Def_2	270.102	270.102	0
Def_3	919.9695	919.9695	0
Sensitivity matrix:			
Corr fac	**d(Obj)/d(Corr fac)**		
1	-1.6436		
2	-0.7309		
3	0		
1st visc correction factor (CSP)			
Before tuning	**After tuning**	**%Adjustment**	
1	1	0	
2nd visc correction factor (CSP)			
Before tuning	**After tuning**	**%Adjustment**	
1	1	0	
3rd visc correction factor (CSP)			
Before tuning	**After tuning**	**%Adjustment**	
1	1	0	
4th visc correction factor (CSP)			
Before tuning	**After tuning**	**%Adjustment**	

1	1	0	
Vc correction factor (LBC)			
Before tuning	**After tuning**	**%Adjustment**	
1	1	0	
a1 (LBC)			
Before tuning	**After tuning**	**%Adjustment**	
0.1023	0.1023	0	
a2 (LBC)			
Before tuning	**After tuning**	**%Adjustment**	
0.023364	0.023364	0	
a3 (LBC)			
Before tuning	**After tuning**	**%Adjustment**	
0.058533	0.058533	0	
a4 (LBC)			
Before tuning	**After tuning**	**%Adjustment**	
-0.04076	-0.04076	0	
a5 (LBC)			
Before tuning	**After tuning**	**%Adjustment**	
0.009332	0.009332	0	

Appendix H: Design of Experiment for oil recovery

Table H.1: Recovery response of design of experimental run

Run	Sulphur %	Temp °C	Press bar	CO2 %	Response Recovery %
1	0.2	-19.5	35	50	5.29
2	0.17	27	50	0	5.95
3	0.23	120	20	100	29.96
4	0.2	73.5	35	50	23.57
5	0.17	120	50	100	14.62
6	0.17	27	20	0	28.71
7	0.2	73.5	65	50	21.21
8	0.23	120	50	100	5.95
9	0.23	120	20	0	23.54
10	0.2	73.5	35	50	23.66
11	0.17	120	20	100	2.11
12	0.14	73.5	35	50	14.61
13	0.23	27	50	0	21.49
14	0.17	120	20	0	5.98
15	0.2	73.5	5	50	15.02
16	0.17	27	20	100	23.68
17	0.2	73.5	35	50	13.46
18	0.2	73.5	35	150	14.62
19	0.17	27	50	100	13.86
20	0.26	73.5	35	50	11.69
21	0.23	27	50	100	11.69
22	0.23	27	20	100	11.69
23	0.23	27	20	0	29.88
24	0.17	120	50	0	15.15
25	0.23	120	50	0	61.79
26	0.2	73.5	35	-50	11.7
27	0.2	73.5	35	50	11.69
28	0.2	73.5	35	50	11.69
29	0.2	73.5	35	50	84.82
30	0.2	166.5	35	50	97.09

Table H.2: ANOVA analysis of oil recovery data using response surface cubic model (Aliased)

Source	Sum of Squares	DF	Mean Square	F Value	Prob > F				
Model	13259.93	22	602.724	7.384864	0.0057	significant			
A	2743.676	1	2743.676	33.61684	0.0007				
B	895.4912	1	895.4912	10.97199	0.0129				
C	2292.773	1	2292.773	28.09216	0.0011				
D	2.864022	1	2.864022	0.035091	0.8567				
A^2	668.2554	1	668.2554	8.187786	0.0243				
B^2	130.6133	1	130.6133	1.600337	0.2463				
C^2	11.28967	1	11.28967	0.138326	0.7210				
D^2	0.813217	1	0.813217	0.009964	0.9233				
AB	1534.093	1	1534.093	18.79645	0.0034				
AC	1769.675	1	1769.675	21.6829	0.0023				
AD	49.10506	1	49.10506	0.601659	0.4633				
BC	768.537	1	768.537	9.416485	0.0181				
BD	124.9365	1	124.9365	1.530782	0.2559				
CD	0.020306	1	0.020306	0.000249	0.9879				
A^3	2891.221	1	2891.221	35.42463	0.0006				
B^3	214.8417	1	214.8417	2.632344	0.1487				
C^3	1386.643	1	1386.643	16.98981	0.0044				
D^3	38.79005	1	38.79005	0.475274	0.5128				
A^2B	0	0							
A^2C	0	0							
A^2D	0	0							
AB^2	0	0							
AC^2	0	0							
AD^2	0	0							

B^2C	0	0							
B^2D	0	0							
BC^2	0	0							
BD^2	0	0							
C2D	0	0							
CD^2	0	0							
ABC	1431.298	1	1431.298	17.53695	0.0041				
ABD	33.03376	1	33.03376	0.404745	0.5449				
ACD	17.03626	1	17.03626	0.208736	0.6616				
BCD	62.05501	1	62.05501	0.760328	0.4121				
Residual	571.3129	7	81.61613						
Lack of Fit	299.8668	2	149.9334	2.761752	0.1556	not significant			
Pure Error	271.4461	5	54.28923						
Cor Total	13831.24	29							

The Model F-value of 7.38 implies the model is significant. There is only a 0.57% chance that a "Model F-Value" this large could occur due to noise. Values of "Prob > F" less than 0.0500 indicate model terms are significant. In this case A, B, C, A++2+-, AB, AC, BC, A++3+-, C++3+-, ABC are significant model terms. Values greater than 0.1000 indicate the model terms are not significant. If there are many insignificant model terms (not counting those required to support hierarchy), model reduction may improve your model. The "Lack of Fit F-value" of 2.76 implies the Lack of Fit is not significant relative to the pure error. There is a 15.56% chance that a "Lack of Fit F-value" this large could occur due to noise. Non-significant lack of fit is good -- we want the model to fit.

Std. Dev.	9.034164		R-Squared	0.958694					
Mean	22.20567		Adj R-Squared	0.828875					
C.V.	40.68405		Pred R-Squared	-2.15024					
PRESS	43571.7		Adeq Precision	11.51794					

A negative "Pred R-Squared" implies that the overall mean is a better predictor of your response than the current model. "Adeq Precision" measures the signal to noise ratio. A ratio greater than 4 is desirable. Your ratio of 11.518 indicates an adequate signal. This model can be used to navigate the design space.

Table H.3: Desirability table on Optimised reservoir conditions for improved oil recovery

Sulphur Content (%)	Reservoir Temperature (^oC)	Reservoir Pressure (bar)	CO_2 Content (%)	Desirability
0.18	91.11	165.97	77.87	1
0.21	83.78	240.29	45.63	1
0.19	100.29	201.88	15.46	1
0.18	65.17	228.69	32.89	1
0.19	68.96	185.13	90.46	1
0.21	97.57	193.73	8.13	1
0.2	87.32	144.01	90.38	1
0.22	88.32	266.53	0.57	1
0.2	76.62	201.92	43.58	1
0.21	90.87	237.12	96.82	1 (Selected)

Table H.4: Final Equation in Terms of Actual factors Factors

Recovery	=
16.42	
18.52	* A
2.12	* B
4.57	* C
0.60	* D
5.03	* A^2
2.27	* B^2
0.26	* D^2
9.79	* A*B
-10.52	* A * C
1.75	* A * D
-6.93	*B * C
-7.76	* A^3
-2.79438	*D^3
6.35	* A^2 * B
-16.12	* A^2* C
-1.43688	* A * B * D
1.031875	* A * C * D
-1.96938	* B * C * D